PhD Thesis

The Role of Intracellular Neutral Lipid Hydrolases in Immune Cell Function

submitted by

Mag. rer. nat. Stefanie Schlager

for the Academic Degree of

Doctor of Philosophy

(PhD)

at the

Medical University of Graz

Institute of Molecular Biology and Biochemistry

under the Supervision of

Ao. Univ. Prof. Dr. Dagmar KRATKY

2015

Declaration

I hereby declare that this dissertation is my own original work and that I have fully acknowledged by name all of those individuals and organisations that have contributed to the research for this dissertation. Due acknowledgement has been made in the text to all other material used. Throughout this dissertation and in all related publications I followed the guidelines of “Good Scientific Practice”.

Graz, June 2015 ……

Stefanie Schlager

ACKNOWLEDGEMENTS

I would like to thank my supervisor Dagmar Kratky for her guidance, motivation and comprehensive support, for the trust in my ideas throughout my PhD project and for always having an open door.

I owe my gratitude to the thesis committee members Akos Heinemann, Achim Lass and Ruth Birner-Gruenberger for their critical advice and helpful comments.

My special thanks go to the colleagues at the Institute of Molecular Biology and Biochemistry for the pleasant and friendly atmosphere. In particular, I want to thank my lab colleagues, especially Silvia for always being there when a helping hand was needed, Anton for his often very helpful MacGyver skills and technical support, Nemo for fruitful discussions, Madeleine, Melly, Christina for the fun moments during lunch breaks, the hearty laughs and the cheerful company. Sascha and Eva for their valuable friendship, Christoph for the Pastaria company and for always being available if there was a need for an after-work Corona or Spritzer.

I also wish to thank my friends near and far, who were always there, available to talk, chat, cheer, for showing interest in my work and for making me forget the science world for a while. Especially, Mascha for being a friend despite the distance, Eva, Babs and Babsi for the get-away weekends to Vienna and for the hiking trips, which helped a lot to re-define true values in life again. My special thanks go to Andrea for our friendship during the last and hopefully upcoming years. Thanks for being such an unbelievable source of energy and for your infectious motivation concerning science and life overall.

It is beautiful and comforting to know, that certain things in life persist, while other things are changing. Therefore I want to thank my family for their endless support as well as the “Moimasreida Mädls” Susi, Carina and Sandra for making it so easy to always reconnect again.

Finally I would like to express my gratitude to Krisse- I am very grateful for our time together. Thanks for your patience, encouragement and moral support and for saving one or the other long working day with a warm dinner. Being with you makes all the difference.

TABLE OF CONTENTS

ABBREVIATIONS

2-AG	2-arachidonoylglycerol
AA	Arachidonic acid
ACAT	Acetyl-Coenzyme A acetyltransferase
ACC	Acetyl- Coenzyme A carboxylase
ADP	Adenosine diphosphate
ALOX	Arachidonate lipoxygenase
ATGL	Adipose triglyceride lipase
BSA	Bovine serum albumin
cAMP	Cyclic adenosine monophosphate
CBR	Cannabinoid receptor
CD36	Cluster of differentiation 36
CE	Cholesterol ester
CESD	Cholesteryl ester storage disease
CFU	Colony-forming unit
CGI-58	Comparative gene identification-58
COX	Cyclooxygenase
CPT1α	Carnitine palmitoyltransferase 1 alpha
CRP	Collagen-related peptide
CYP450	Cytochrome P450
DAGL	Diacylglycerol lipase
DG	Diacylglycerol
DGAT	Diacylglycerol acyltransferase
DHA	Docosahexaenoic acid
DHET	Dihydroxyeicosatrienoic acids
DTT	Dithiothreitol
EDTA	Ethylenediaminetetraacetic acid
EET	Epoxyeicosatrienoic acids
EPA	Eicosapentaenoic acid
ER	Endoplasmatic reticulum
FA	Fatty acid
FASN	Fatty acid synthase
FC	Free cholesterol

FCS	Fetal calf serum
FFA	Free fatty acid
fMLP	Formyl-methionyl-leucyl-phenylalanine
G0S2	G0/G1 switch gene 2
GP	Glycoprotein
GPCR	G-protein-coupled receptor
HBSS	Hank's balanced salt solution
HDL	High-density lipoprotein
HEPE	Hydroxyeicosapentaenoic acid
HETE	Hydroxyeicosatetraenoic acid
HHT	Hydroxyheptadeca-trienoic acid
HPETE	Hydroperoxyeicosatetraenoic acid
HSL	Hormone-sensitive lipase
IL	Interleukin
iNOS	Inducible nitric oxide synthase
KC	Keratinocyte-derived chemoattractant
LAL	Lysosomal acid lipase
LD	Lipid droplet
LDL	Low-density lipoprotein
LDLR	Low-density lipoprotein receptor
LOX	Lipoxygenase
LPS	Lipopolysaccharide
LT	Leukotriene
MCP-5	Monocyte chemoattractant protein-5
MG	Monoacylglycerol
MGL	Monoacylglycerol lipase
MIP	Macrophage inflammatory protein
MMP9	Matrix metallopeptidase 9
NLSD	Neutral lipid storage disease
NLSDI	Neutral lipid storage disease with ichthyosis
NLSDM	Neutral lipid storage disease with myopathy
NOXA1	NADPH oxidase activator 1
OA	Oleic acid
OCS	Open canalicular system

PA	Phosphatidic acid
PAF	Platelet-activating factor
PC	Phosphatidylcholine
PE	Phosphatidylethanolamine
PG	Prostaglandin
PI	Phosphatidylinositol
PKC	Protein kinase C
PL	Phospholipid
PLA2	Phospholipase A2
PLC	Phospholipase C
PLD	Phospholipase D
PLIN	Perilipin
PMA	Phorbol myristate acetate
PNPLA2	Patatin-like phospholipase domain containing 2
PPAR	Peroxisome proliferator-activated receptors
PRP	Platelet-rich plasma
PUFA	Polyunsaturated fatty acid
RE	Retinyl ester
ROS	Reactive oxygen species
SCD1	Stearoyl-CoA desaturase 1
SDS	Sodium dodecyl sulphate
SEM	standard error of mean
TC	Total cholesterol
TG	Triglyceride
TLC	Thin layer chromatography
TNFα	Tumor necrosis factor alpha
TxA2/B2	Thromboxane A2/B2
VLDL	Very low-density lipoprotein
vWF	von Willebrand factor
WAT	White adipose tissue

ZUSAMMENFASSUNG

Lipidtropfen (LDs) stellen wichtige intrazelluläre Organellen in Zellen des Immunsystems dar, welche maßgebend an der Entstehung von metabolischen Erkrankungen und Entzündungen beteiligt sind. Eine Akkumulierung von LDs in Makrophagen verursacht die Bildung von sogenannten „fatty streaks“ und gilt als grundlegende Erscheinung in der Entstehung von Atherosklerose. Im Rahmen einer entzündlichen Reaktion bilden auch andere Immunzellen (z.B. Leukozyten) zytosolische, Triglyzerid (TG)-reiche LDs, welche charakteristisch für die Aktivierung dieser Zellen sind. Bislang sind Enzyme, die am Metabolismus von LDs in Leukozyten beteiligt sind, großteils undefiniert.

Die vorliegende Arbeit zeigt, dass die lipolytischen Enzyme Adipose Triglyzerid Lipase (ATGL), Hormon-sensitive Lipase (HSL) und Monoazylglyzerol Lipase (MGL) den Abbau von LDs in Immunzellen regulieren und somit einen Einfluss auf die biologische Funktion dieser Zellen haben.

Mit speziellem Augenmerk auf ATGL, welches das geschwindigkeitsbestimmende Enzym in der Spaltung von TG ist, konnte ich beobachten, dass eine genetische ATGL Defizienz eine Anreicherung von intrazellulären, TG-reichen LDs in neutrophilen Granulozyten bewirkt. Diese Lipidakkumulierung zeigte sich infolge einer herbeigeführten Entzündung außerdem in Monozyten und Makrophagen, nicht jedoch in eosinophilen Granulozyten oder Lymphozyten. Funktionelle Untersuchungen von ATGL-defizienten neutrophilen Granulozyten ergaben eine erhöhte Reaktionsbereitschaft *in vitro*, welche interessanterweise eine stärkere Ausprägung in Mäusen mit globaler-, verglichen mit myeloid-spezifischer ATGL Defizienz zeigte. Des Weiteren führten sowohl eine genetische als auch pharmakologische Inhibierung von ATGL zu einer verminderten Freisetzung von Lipidmediatoren von neutrophilen Granulozyten. Diese Erkenntnisse verdeutlichen, dass die Freisetzung von Vorläufermolekülen zur Lipidmediator Synthese aus TG-reichen, zellulären Depots der enzymatischen Aktivität von ATGL bedarf.

Im zweiten Teil meiner Arbeit habe ich die Auswirkung des Fehlens der Lipasen ATGL, HSL und MGL auf die Funktion von Thrombozyten untersucht. Hierbei konnte ich beobachten, dass eine genetische Defizienz von ATGL und MGL, nicht jedoch von HSL,

eine Hemmung der Thrombenbildung *in vitro* bewirkt und somit zu einem anti-thrombotischen Phänotyp führt.

Zusammenfassend betrachtet konnte ich zeigen, dass TG-hydrolysierende Enzyme in der Regulierung des Metabolismus von LDs in Immunzellen eine wichtige Rolle spielen. Meine Erkenntnisse verdeutlichen die Beteiligung dieser Enzyme an der Regulierung von Signalwegen in Immunzellen, sowie an der Entstehung von inflammatorischen Erkrankungen. Eine Charakterisierung dieser Regulationsmechanismen könnte neue Ansatzpunkte für eine antiinflammatorische Therapie eröffnen.

ABSTRACT

Lipid droplets (LDs) are cytoplasmic organelles in immune cells with an important role in the development of metabolic diseases and inflammation. LD accumulation in macrophages is a recognized early event in atherogenesis and leads to the formation of "fatty streaks" representing initial atherosclerotic lesions. Under certain inflammatory conditions also other immune cells (e.g. leukocytes) generate cytosolic, triglyceride (TG)-rich LDs, which are considered as key markers of cellular activation. To date, the lipolytic enzymes involved in maintaining LD homeostasis in these cells have not been defined.

The first part of this thesis clearly shows that the TG-hydrolyzing enzymes adipose triglyceride lipase (ATGL), hormone-sensitive lipase (HSL), and monoacylglycerol lipase (MGL) are regulators of LD metabolism in immune cells, thereby regulating immune cell biology and function.

With specific emphasis on ATGL, which is the rate-limiting enzyme mediating TG hydrolysis, I observed an increased abundance of intracellular, TG-rich LDs in neutrophil granulocytes similar to humans with loss-of-function mutations in ATGL. In a model of inflammatory peritonitis, lipid accumulation was also observed in monocytes and macrophages but not in eosinophils or lymphocytes. Neutrophils from Atgl-/- mice showed enhanced immune responses *in vitro*, which were more prominent in cells from global compared with myeloid-specific Atgl-/- mice. Mechanistically, ATGL deficiency and pharmacological inhibition of ATGL led to an impaired release of lipid mediators from neutrophils. These findings demonstrate that the release of lipid mediators is dependent on the liberation of precursor molecules from the TG-rich pool of LDs by ATGL.

In the second part of my thesis I aimed at investigating the impact of the deficiency of the lipolytic enzymes ATGL, HSL, and MGL on platelet function. Thereby I observed that the absence of ATGL and MGL but not HSL was associated with an anti-thrombogenic phenotype, as evident by reduced *in vitro* thrombogenesis and collagen-induced platelet activation.

In summary, the present work provides profound evidence for a functional role of TG-hydrolyzing enzymes in the regulation of LD metabolism in immune cells. These observations expand the knowledge of these enzymes as signaling lipases and potent

regulators of immune cell function and inflammatory diseases. Uncovering these lipid regulatory pathways may identify new pharmacological targets to regulate the inflammatory activity of immune cells.

PART I: THE ROLE OF TG HYDROLASES IN LIPID HOMEOSTASIS AND FUNCTION OF IMMUNE CELLS

1 Introduction

1.1 Lipid homeostasis in cells of the immune system

Cellular lipids originate from *de novo* lipid biosynthesis, hydrolysis of intracellular lipid stores such as triglyceride (TG) or cholesterol ester (CE) and/or from circulating plasma lipoproteins. Complex lipids are the major components of cell membranes, and their function is critically modulated by the fatty acid (FA) composition, which determines membrane fluidity and permeability, alters its microdomain organization and other physical properties, such as cell signaling (reviewed in (1)). Phospholipids, sphingolipids, FAs and their breakdown and oxidation products are involved in controlling important cellular processes of immune cells, including cell proliferation, apoptosis, metabolism, and migration (reviewed in (2)).

The most abundant sterol, cholesterol, constitutes an important membrane component required for cell proliferation and migration, membrane expansion and remodeling. Distinct cholesterol-rich lipid domains in the plasma membranes, termed lipid rafts and caveolae, play a pivotal role in immune cell function (3). These microdomains contain proteins integral to signaling, e.g. G-protein-coupled receptors (GPCRs) and hence, are considered as critical signaling platforms to mediate cellular activation. Cholesterol depletion from these domains was shown to be associated with the down regulation of various cellular functions, including the activation, adhesion, and migration of neutrophils (4).

High levels of unesterified, free cholesterol (FC) or free fatty acids (FFAs) are lipotoxic. Thus, the control of their intracellular levels is tightly regulated. As a protective mechanism excess lipid molecules are stored in intracellular lipid droplets (LDs) and can be mobilized through a process termed lipolysis. The thereby released FAs participate in many intracellular signaling pathways and are involved in the modulation of immune function. In contrast to many other cell types and tissues, in which lipolysis represents an important biochemical mechanism to generate FAs as energy substrates, most myeloid

and lymphoid cells derive their energy mostly from glycolysis, have few mitochondria, and produce little energy from respiration (reviewed in (5)). Under specific circumstances, such as transitions between resting and activating states as well as between various differentiation states, immune cells can undergo metabolic changes using other sources as energy fuel. For example, memory T cells, Treg cells and alternatively activated M2 macrophages shift to FA β-oxidation to provide energy for cellular functions (5). These observations indicate that the metabolic pathways are regulated according to the immune cell function and fate. How the changes in metabolic profile are mediated is not fully understood and subject for further clarification.

1.2 Lipid droplets in immune cells

LDs are organelles found in the cytoplasm of a variety of cells, including cells of the immune system. Since their discovery in the 19th century, LDs have been referred to as adiposomes, oil bodies, liposomes, and lipid bodies and the latter term is still commonly used in the context of inflammatory cells. The presence of LDs in macrophages and mast cells was for the first time described in 1983 in comprehensive electron microscopy studies (6). Further studies followed, reporting the presence of LDs in other cells such as eosinophilic, basophilic and neutrophilic granulocytes (reviewed in (7)). In the past, LDs were largely associated with lipid storage but current research suggests LDs as functional and dynamic organelles beyond lipid storage and their presence in immune cells is considered as a key marker of cellular activation (reviewed in (8)).

1.2.1 LD biogenesis

In response to extracellular cues or in case of excess intracellular lipids, LDs are *de novo* synthesized and expand in number and size. Resting immune cells contain only few LDs but their number can be rapidly induced (within 15-60 min) in response to inflammatory stimuli (9-11). LD biogenesis is a highly regulated phenomenon that is stimulus- and cell-specific and can be triggered *in vivo* and *in vitro* in leukocytes and other inflammation-related cell types including endothelial and epithelial cells.

According to current knowledge, LDs are either generated *de novo* or from existing LDs by fusion or fission (12, 13). *De novo* generated LDs originate from the endoplasmic

reticulum (ER), where neutral lipid synthesis takes place. The pathway of *de novo* LD formation, however, is not fully understood since techniques for direct visualization of the initial process of LD generation are lacking. Neutral lipids are synthesized by ER-resident anabolic enzymes and accumulate within the bilayer of the ER membrane. After reaching a critical concentration, the nascent LD buds into the cytoplasm surrounded by a phospholipid monolayer derived from the cytoplasmic leaflets of ER membranes (14). Whether LDs remain associated with the ER or separate immediately after their formation and whether LD biogenesis occurs at specific ER regions remains to be defined.

Other models propose that LDs can form by fusion of smaller into larger droplets (reviewed in (15)), a process that occurs rather rarely and only under specific conditions or by fission of pre-existing LDs (13). Evidence for the latter model is derived from studies in yeast, however, the exact molecular mechanism as well as a translation of this observation into mammalian systems are still elusive.

Enzymes involved in neutral lipid synthesis, such as acetyl-Coenzyme A acetyltransferases (ACATs) and diacylglycerol acyltransferases (DGATs) are primarily located in the ER. Some enzymes such as glycerol-3-phosphate O-acyltransferase (GPAT4) and DGAT2 localize to both, the ER and LDs (12, 16, 17). Hence, TG biosynthesis is believed to take place in the immediate vicinity of the LD - either at the ER-LD interface or ER-independently through local lipid synthesis at the LD as purified LDs have been shown to possess TG biosynthetic activity (16, 18). The number of determining factors, which are involved in the LD formation process, is increasing and are reviewed in (19, 20).

1.2.2 Induction of LD generation

Leukocyte LD biogenesis is a process that happens *in vitro* and *in vivo* during inflammatory reactions. Experimental and clinical infections with different pathogens including bacteria, parasites, and viruses induce intracellular LD generation in various leukocyte types (21). LD formation has been linked also to non-infectious diseases such as inflammatory arthritis, acute respiratory distress syndrome, atherosclerosis, obesity, and cancer (reviewed in (22)).

In vitro treatment with specific unsaturated FAs but not saturated FAs accelerated the formation of LDs in eosinophils, basophils, monocytes, and mast cells (23, 24).

Interestingly, leukocyte LD formation is triggered *in vitro* even in the absence of exogenous lipids, indicating that the underlying mechanism requires more than the simple availability of lipid sources. LD biogenesis is driven by specific signaling pathways and cell-dependent mechanisms. Leukocyte activation triggered by lipids, lipid-derived molecules or protein agonists, such as cytokines and chemokines, leads to LD formation by a receptor-mediated process. As an example, platelet activating factor (PAF) and prostaglandin D2 (PGD2) initiate intracellular signaling act via GPCRs resulting in protein kinase C (PKC) and phospholipase C (PLC) activation and LD induction. IL-5, Rantes and Eotaxin act via the CC chemokine receptor 3 (CCR3) to initiate LD generation in eosinophils and basophils but not neutrophils demonstrating a stimulus specificity according to the cell type (8).

Another family of receptors, the peroxisome proliferator-activated receptors (PPARs), has been implicated to have as important in regulating intracellular LD accumulation. PPAR signaling was shown to modulate the gene transcription of perilipin 2 (PLIN2), a LD-associated protein, which promotes LD accumulation. In addition, PLIN2 amplifies the capacity of LD formation in response to other potent LD inducers such as oxidized low-density lipoprotein (LDL), PAF-like agonists, and granulocyte colony-stimulating factor (G-CSF) (reviewed in (22)). Pathogen recognition receptors play a major role in the process of LD formation, since pathogen-derived molecules such as lipopolysaccharide failed to induced LDs in leukocytes from TLR4 mutated mice (25). A list of stimuli that induce LD biogenesis in different immune cells is shown in Table 1.

Table 1: Lipid droplet formation in immune cells

	Eosinophils	Macrophages	Neutrophils	Basophils
Unstimulated	+	+	+	+
Lipoproteins				
ac-, ox-LDL but not native LDL	**n.d.**	+	–	**n.d.**
Fatty acids				
Unsaturated fatty acids	+	+	+	**n.d.**
Saturated fatty acids	–	–	–	**n.d.**
Phospholipids				
PAF	+	+	+	+
Lyso-PAF	–	**n.d.**	–	**n.d.**
Eicosanoids				
5-HETE	+	**n.d.**	+	**n.d.**
PGD2	+	–	–	**n.d.**
LTB4	–	**n.d.**	–	**n.d.**
Hormones				
Leptin	–	+	–	**n.d.**
Resistin	–	+	–	**n.d.**
Cytokines				
Eotaxin	+	**n.d.**	+	+
Rantes	+	**n.d.**	+	+
IL-8	–	**n.d.**	–	–
IL-5	+	**n.d.**	–	**n.d.**
IL-16	+	**n.d.**	–	**n.d.**
MIF	+	**n.d.**	**n.d.**	**n.d.**
MCP-I/CCL2	**n.d.**	+	**n.d.**	**n.d.**
GM-CSF	+	**n.d.**	**n.d.**	**n.d.**
IL-3+IL-5	+	**n.d.**	**n.d.**	**n.d.**
IFN-γ	+	**n.d.**	**n.d.**	**n.d.**
TNF-α	+	**n.d.**	**n.d.**	**n.d.**
Bacteria and derivatives				
Bacillus subtilis	–	–	–	**n.d.**
Mycobacterium smegmatis	–	–	–	**n.d.**
Chlamydia pneumoniae	**n.d.**	+	**n.d.**	**n.d.**
Mycobacterium bovis BCG	+	+	+	**n.d.**
Mycobacterium leprae	**n.d.**	+	**n.d.**	**n.d.**
Mycobacterium tuberculosis	**n.d.**	+	**n.d.**	**n.d.**
LPS/LAM	+	+	+	**n.d.**
Parasites				
Trypanosoma cruzi	**n.d.**	+	**n.d.**	**n.d.**
Toxoplasma gondii	**n.d.**	**n.d.**	**n.d.**	**n.d.**
Plasmodium falciparum	**n.d.**	**n.d.**	**n.d.**	**n.d.**
Schistosoma mansoni	+	**n.d.**	**n.d.**	**n.d.**
Leishmania amazonensis	**n.d.**	+	**n.d.**	**n.d.**
Fungi				
Histoplasma capsulatum	**n.d.**	+	**n.d.**	**n.d.**
Virus				
Dengue virus	**n.d.**	+	**n.d.**	**n.d.**
Hepatitis C virus	**n.d.**	**n.d.**	**n.d.**	**n.d.**

+ induced; - not induced; n.d. not determined

PAF, platelet activating factor; 5-HETE, 5-hydroxyeicosatetraenoic acid; PG, prostaglandin; LT, leukotriene; IL, interleukin; MIF, migration inhibitory factor; MCP-I/CCL2, monocytes chemoattractant protein; GM-CSF, granulocyte-macrophage colony-stimulating factor; IFN-γ, interferon-gamma; TNFα, tumor necrosis factor alpha; BCG, bacillus Calmette-Guérin; LPS, lipopolysaccharide; LAM, lipoarabinomannan (7, 22, 24, 26, 27).

1.2.3 Composition of LDs

LDs are highly conserved organelles that can be found in many different organisms including bacteria, yeast, plants, insects, and mammals. LDs are dynamic in number and size depending on the metabolic state of the cell. In mammals, most studies have been performed in adipocytes, which contain a single large LD (> 100 µm), and also in macrophages/foam cells with small LDs (0.1-5 µm) in their cytoplasm. Irrespective of the cell type, the overall architecture of LDs appears to be common consisting of a core of lipid esters and a surface phospholipid (PL) monolayer harboring various specific proteins (Fig. 1).

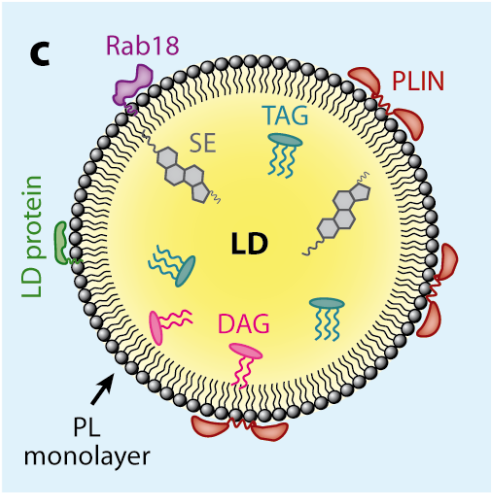

Figure 1: The architecture of LDs

LDs consist of a lipophilic core comprising neutral lipids, mainly triacylglycerol (TAG) and sterol ester (SE) that is surrounded by a monolayer of phospholipid (PL) with a distinct array of structural and functional proteins. (28)

Similar as in adipocytes, the LD core of cells of the myeloblastic lineage, e.g. neutrophils, eosinophils, basophils and mast cells contains mostly TGs (6, 29, 30), whereas macrophage foam cells and steroidogenic cells consist of CE. Depending on the cell type, diacylglycerol (DG), retinyl ester (RE), and ether lipids may be also found in the LD core (31, 32). This core of neutral lipids is surrounded by a PL monolayer comprising phosphatidylcholine (PC), phosphatidylethanolamine (PE), and small amounts of phosphatidylinositol (PI) and lysophospholipids. FC and DG can also be found to some extent in the LD monolayer, whereas sphingomyelin, phosphatidylserine (PS), and

phosphatidic acid (PA) are absent (32, 33). Whereas the LD core shows some heterogeneity, the composition of PLs appears to be similar in different cell types under different conditions (32).

An important hallmark of leukocyte LDs is their high prevalence for the 20-carbon FA arachidonic acid (AA), which acts as an important intracellular second messenger and as substrate for the enzymatic conversion into bioactive lipid mediators, also termed eicosanoids. AA is predominantly esterified at the sn-2 position of membrane PLs. However, a substantial amount of AA can be also found in the neutral lipid pool of LDs (34). Depending on the cell type and the environment (peripheral blood or tissue), the amount of AA associated with neutral lipids varies. As an example, the content of neutral lipid-associated AA in human peripheral blood neutrophils is rather low with 3%, which increases up to 25% upon migration into tissues, e.g. the lung. Peripheral blood eosinophils store 30% and tissue mast cells almost half of their cellular AA in neutral lipids, predominantly (up to 80%) in TGs (34). Based on this characteristic, leukocyte LDs are recognized as potent sites for the generation of eicosanoids.

The LD proteome is highly diverse and shows variations according to the function and the metabolic status of the cell. Evidence exists that even within the same cell LDs exhibit a distinct array of associated proteins, as they undergo cellular differentiation and maturation (35). Multiple proteomics studies in the past years revealed an ever growing number of newly described regulatory proteins many of which are involved in stabilization, synthesis, and metabolism of LDs. Among the first identified and best characterized LD-associated proteins are the PAT family of proteins. This family includes 5 PLINs: PLIN1-5 (reviewed in (36)). PLIN1 regulates the lipolytic activity in adipocytes and PLIN5 in oxidative cells (e.g. muscle cells) by regulating TG-hydrolyzing enzymes (37, 38). PLIN2, an ubiquitously expressed protein, promotes TG and cholesterol storage and reduces cholesterol efflux in human monocyte-derived macrophages (39), whereas PLIN3 as well as PLIN4 are implicated as binding and transport proteins of FFAs from the cytoplasm to LDs (35, 40).

In the last years, substantial progress how proteins target and traffic to LDs has been made. Currently suggested mechanisms of protein-LD interaction include the binding via

i) a hydrophobic domain, ii) amphipathic helices, iii) a lipid anchor, iv) protein-protein interactions or v) a combined mechanism (41). A hydrophobic targeting signal was identified in LD-associated proteins, which mediate specific binding of proteins to LDs (42). Notably, LD-associated proteins are not restricted to the surface, but can also be found in the lumen of LDs. Freeze-fracture electron microscopy revealed the presence of PAT proteins in the core of macrophage LDs (43, 44). The existence of these hydrophilic proteins inside the organelle's lipid-rich core may be explained by membranous structures of ER or ribosomal origin harboring these integral membrane proteins found in the core of LDs (45).

More than 200 LD-associated proteins have been identified that may vary according to cell type and cellular activation state and might be critical to mediate different cellular functions for this organelle. These proteins include lipogenic and lipolytic enzymes, membrane trafficking proteins, vesicle transport-related proteins, signaling proteins, cytoskeletal proteins, lysozyme proteins, chaperones, and proteins from the ER, Golgi, and mitochondria (46).

In cells of the immune system, predominantly macrophages, neutrophils and eosinophils, various enzymes involved in AA mobilization and eicosanoid biosynthesis have been found in association with LDs. These include the cytoplasmic phospholipase cPLA2 and its activating mitogen-activated protein (MAP) kinases ERK1, ERK2, p85 and p38. Moreover, enzymes for the conversion of AA into eicosanoids including cyclooxygenases (COX), 5- and 15-lipoxygenase (5-LOX, 15-LOX), and leukotriene C4 (LTC4)- synthases are present within LDs from activated immune cells (reviewed in (47)).

1.2.4 Catabolism of LDs

1.2.4.1 Lipolysis

TGs have been identified as the major lipid species being stored in the core of LDs of immune cells, such as eosinophils, basophils, neutrophils, mast cells, and macrophages (6, 29, 30). The efficient utilization of these TG-rich LDs requires the activity of specific lipases and other metabolic enzymes and is termed lipolysis. Adipocytes are cells with a high rate of lipolytic activity and have been studied extensively to reveal the molecular mechanism

of lipolysis and its regulation, which is mediated by hormones and the availability of nutrients (for further reading (37)). A scheme of lipolysis is depicted in Fig. 2.

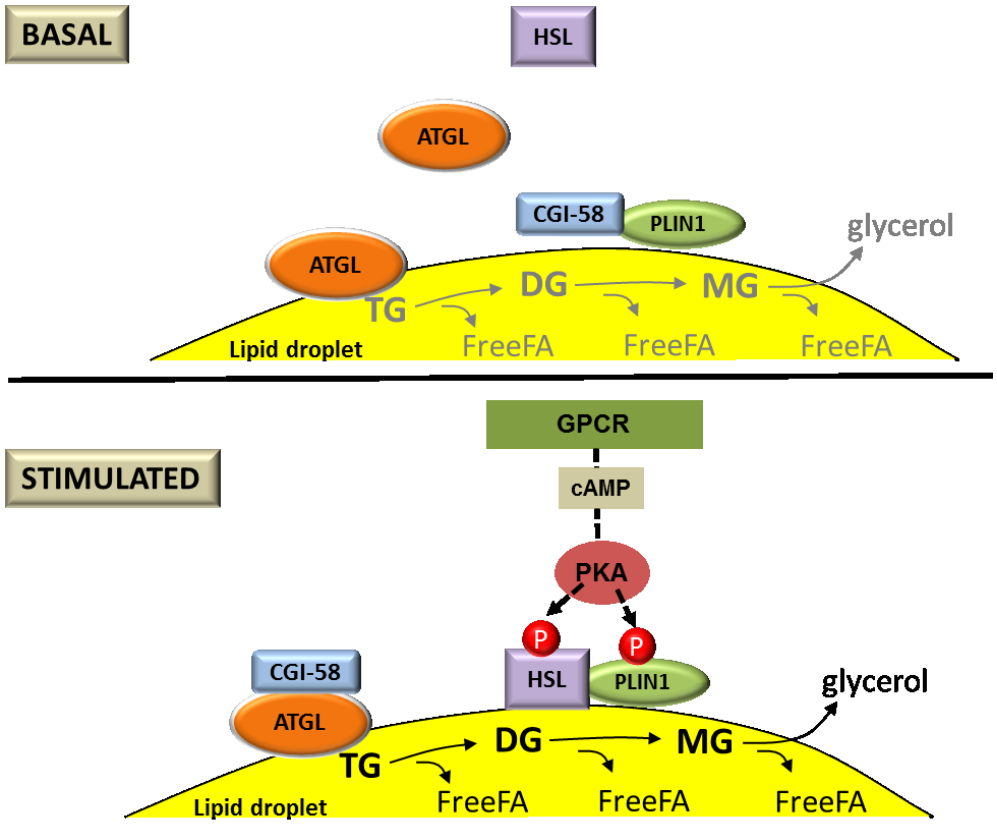

Figure 2: Basal and stimulated lipolysis in adipocytes

Lipolysis is mediated by a highly regulated multi-enzyme complex at the LD that drives the catabolism of cellular TG stores. Three lipases are needed for sequential hydrolysis of TG: ATGL, HSL, and MGL. *Basal lipolysis:* PLIN1 and CGI-58 form a complex on the LD. ATGL is localized partially to the LD and HSL mostly in the cytoplasm. The rate of lipolysis (i.e. the production of FA and glycerol) is very low under these conditions. *Stimulated lipolysis:* GPCR-generated signals induces cAMP generation, which results in protein kinase A (PKA) activation. PKA phosphorylates HSL and PLIN1, thereby CGI-58 gets released and binds ATGL to initiate lipolysis and the breakdown of TG. HSL translocates to the LD, associates with phosphorylated PLIN1, and degrades DG. MGL cleaves the final FA to produce glycerol.

The lipolytic cascade to hydrolyze TGs consists of the three lipases adipose triglyceride lipase (ATGL), hormone-sensitive lipase (HSL) and monoacylglycerol lipase (MGL). Several other regulatory proteins such as the ATGL-co activator comparative gene identification-58 (CGI-58; also termed ABHD5) and its endogenous inhibitor G0S2 as well as proteins

from the PAT family have been implicated as critical regulators of lipolysis. During lipolysis, ATGL (also termed desnutrin or PNPLA2) selectively performs the initial step resulting in the formation of DG and FFA. HSL further degrades DG to release the second FA and MG. Finally, MG is hydrolyzed by MGL to release another FA and glycerol.

The functional role of lipolytic enzymes has been reported for macrophages, which have an enormous capacity to store lipids in form of LDs. ATGL and HSL were shown to be expressed in macrophages and foam cells (48, 49). Genetic lack of ATGL in macrophages resulted, similar to other cells and tissues, in decreased TG hydrolase activity and, concomitantly, in intracellular TG accumulation (48). Hsl-/- macrophages exhibited comparable CE and FC concentrations to wild-type (wt) macrophages, despite decreased CE hydrolase activities *in vitro,* indicating that another enzyme is compensating its function *in vivo* (50). In general, HSL exhibits a wide substrate specificity including TG, DG, MG, CE and RE (51, 52).

Human monocyte-derived macrophages were shown to express MGL (53). The physiological relevance of MGL became evident when it was found to be the major enzyme in the brain for the catabolism of 2-arachidonyl glycerol (2-AG), the most abundant endocannabinoid in mammals, which regulates a number of physiological processes (54). The role of MGL in endocannabinoid signaling in macrophages is currently under investigation.

1.2.4.2 Autophagy of LDs

Another mechanism to break down TGs into FAs is the autophagic degradation of LDs, a process termed lipophagy (55). During lipophagy, cytoplasmic LDs are engulfed by a growing membrane that eventually encloses the entire LD and thereby forms an autophagosome. After the fusion with the lysosome, the lipid cargo is degraded by the action of the enzyme lysosomal acid lipase (LAL). A simplified scheme of autophagy-mediated LD degradation is shown in Fig. 3. The role of autophagy in lipid metabolism is considered to be highly tissue- and condition-dependent. Lipophagy has been reported for tissues such as the liver (56) and adipose tissue (57), although a growing number of cell types, including fibroblasts, neurons, stellate cells, and macrophages are reported to utilize this pathway (58, 59). The way in which lipophagy is regulated and connected to

other cellular processes, such as lipoprotein uptake, lipolysis or ß-oxidation in mitochondria is subject of current investigations (60).

In immune cells, the process of autophagy to eliminate damaged organelles and invading microorganisms constitutes a critical housekeeping function and is important for the differentiation, survival, and activation of myeloid and lymphoid cells (61). In a recent publication it was shown that LD catabolism by autophagy contributes to the intracellular breakdown of CE in macrophage-derived foam cells and thereby promotes cholesterol efflux from these cells (62). Whether increased lipophagy results in atheroprotective effects *in vivo*, however, remains to be determined. A recent study from our group revealed that in macrophages with defective lipolysis (due to the combined lack of ATGL and HSL) lipophagy is likely not a compensatory mechanism for generating FAs as energy substrate (63). In immune cells other than macrophages, the relative contribution of LD degradation by autophagy in comparison to intracellular lipolysis is largely unexplored.

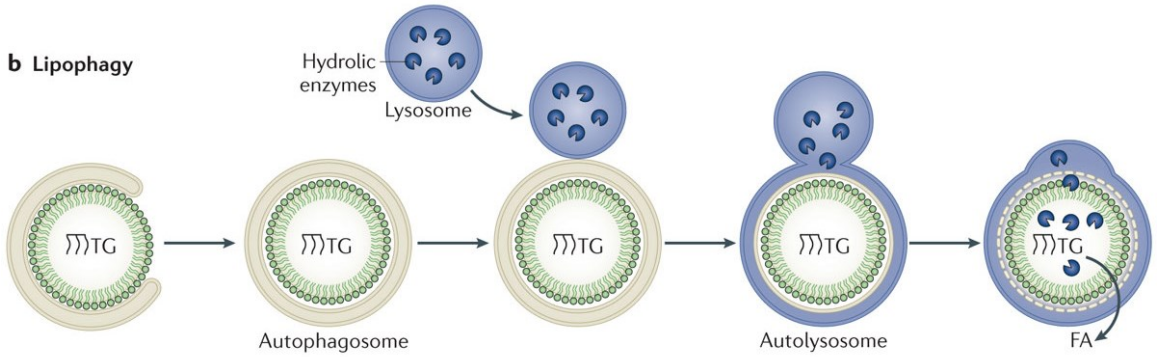

Figure 3: LD degradation via autophagy

Lipophagy is a dynamic cellular process that proceeds through multiple steps starting with the formation of phagophores that engulf the LD. Phagophores mature to autophagosomes, which are then converted into autolysosomes via fusion with lysosomes. Finally, the sequestered LD and the inner membranes of autolysosome are broken down to FAs by hydrolytic enzymes from lysosomes and the resulting FAs are released into the cytosol. (64)

1.2.4.3 The fate of hydrolyzed lipids

Lipolysis liberates lipid molecules, which may either directly or indirectly (through their derivatives and metabolites) regulate cellular structure and function (Fig. 4). FFAs can act as cell signaling molecules, e.g. as ligands for nuclear transcription factors, thereby modulating gene transcription, or they can be re-esterified to TGs or exported from the cell. The liberated FAs may also be transported to mitochondria, where they are

used as energy substrates for FA β-oxidation. Further, FAs are important precursors for the synthesis of membrane lipids and biologically active lipid mediators (e.g. prostaglandins or leukotrienes). FAs can also be used for post-translational protein modification such as acylation or acetylation, thereby influencing protein interactions, activity and localization (65, 66).

The biological activities of DG and MG for lipid synthesis and signaling crucially depend on their stereochemical structure. For example, only the sn-1,2 DAG isoform activates PKC and can directly enter phospholipid synthesis. Since ATGL was shown to specifically generate sn-1,3 and (in the presence of its co-activator CGI-58) sn-1,3 and sn-2,3 DG (67), DG isoforms derived from ATGL/CGI-58 mediated lipolysis cannot directly enter phospholipid synthesis or activate PKC. MGs (e.g. 2-AG) act as ligands for endocannabinoid signaling. The end product arising from hydrolysis of TG is glycerol, which is converted to the glycolytic intermediate dihydroxyacetone phosphate (DHAP) or phosphorylated by glycerol kinase to glycerol-3-phosphate for reuse in TG synthesis.

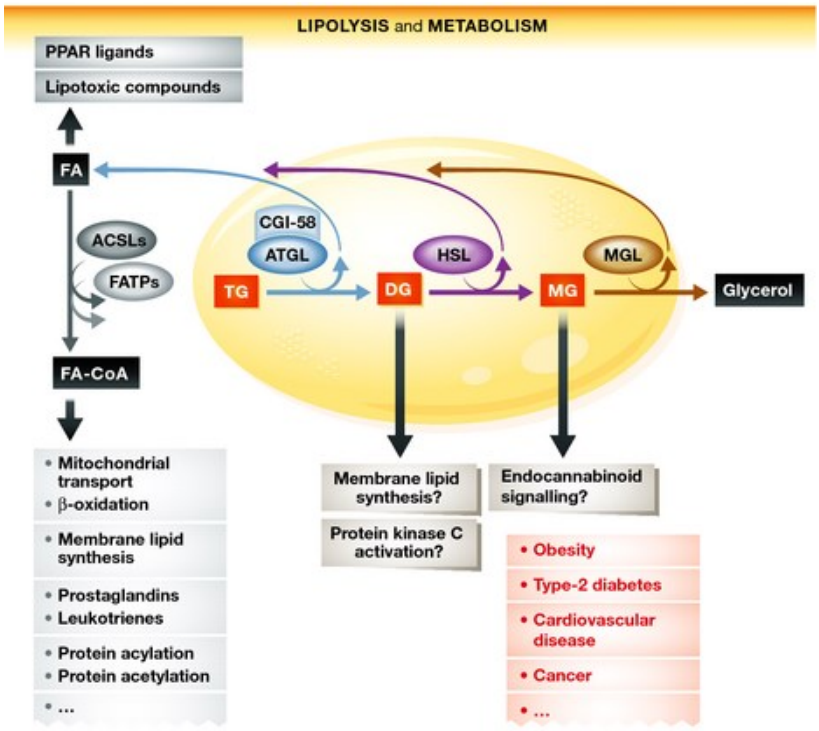

Figure 4: Lipids generated by TG hydrolysis

Lipolysis products including FA, DG and MG as well as their derivatives and metabolites are implicated in several cellular signaling pathways. (68)

1.2.5 Physiological function of LDs

Besides the classical function of LDs, i.e. the storage of lipids, LDs have been linked to a variety of biological functions, many of which have only been recently identified. These include the cellular regulation of lipid homeostasis and signaling, protein folding, storage and degradation, infection, and immunity (reviewed in (28, 69, 70)). Further, LDs represent an organelle for the storage of bulk lipids, which protects against lipotoxicity. Electron and light microscopic studies revealed that LDs are localized in close proximity to other cellular organelles, such as the ER, mitochondria, peroxisomes, endosomes, and lysosomes, which likely reflects close functional interactions and an active involvement of LDs in a diversity of cellular processes (18) . A close LD-cytoskeleton interaction has been reported, possibly mediating motility, relocation as well as LD fusion and growth (22).

Significant inflammation-relevant functions that have been described for LDs include the regulation of host/pathogen interactions (71), virus assembly (72), nutrient source for intracellular pathogens (73), and functions in antigen cross-presentation (74). Numerous studies have provided substantial evidence that LDs serve as major organelles for the generation of AA-derived lipid mediators (reviewed in (75)).

1.2.6 Pathologies associated with increased LD generation in immune cells

1.2.6.1 Inflammatory and infectious diseases

Emerging functions in cell signaling have placed LDs as key organelles to regulate inflammatory processes and an involvement of LDs in several immunopathologies has been established. The prime example is atherosclerosis, a chronic, multifactorial lipid-driven inflammatory disease of the arteries. A hallmark of early atherosclerotic lesions is macrophage foam cell formation, which is the result of an uncontrolled lipoprotein uptake causing a massive accumulation of CE-rich intracellular LDs.

The generation of LDs in various types of leukocytes has been observed also in other human inflammatory diseases e.g. rheumatoid arthritis, asthma and respiratory distress syndrome (22). Furthermore, leukocytes generate LDs in response to infection with pathogens, including bacteria, parasites, and viruses (21). Growing evidence indicates an important role of LDs in neoplastic cells and in cancer pathogenesis (76). In malignant

cells, such as breast, prostate, cervical, liver, and colon cancer cells LD size and number are elevated suggesting that LD-associated lipids may play a critical role in tumor cell growth (reviewed in (77)).

1.2.6.2 Neutral lipid storage disease

Neutral lipid storage disease (NLSD) describes a group of rare autosomal-recessive disorders of lipid metabolism with systemic deposition of neutral lipids in multiple tissues, including skin, skeletal muscle, heart, liver, the CNS, and peripheral blood leukocytes. The disease was initially discovered in 1953 by Jordans (78), who reported a case with progressive muscular dystrophy accompanied by fat-containing vacuoles in leukocytes, which since then was termed Jordans' anomaly.

Two forms of NLSD are distinguished clinically: NLSD with ichthyosis (NLSDI) caused by a mutation in CGI-58 (79) and NLSD with myopathy (NLSDM) caused by a loss of function mutation in the gene encoding ATGL (80). NLSD patients display a great variability of clinical involvement including variable degrees of ichthyosis, liver steatosis, hepatosplenomegaly, skeletal and cardiac myopathy, growth retardation, hearing loss as well as mental retardation (81). Due to the high heterogeneity of clinical phenotypes, Jordans' anomaly of polymorphnuclear leukocytes, which was consistently observed in all reported cases of NLSD, was postulated as a major hallmark criterion for the diagnosis of NLSD (82). To date, the functional consequence of Jordans' anomaly in these patients remains elusive.

1.2.6.3 Wolman disease and Cholesteryl ester storage disease

LAL is the enzyme responsible for the hydrolysis of lipoprotein-derived CE and TG taken up by receptor-mediated endocytosis as well as for the lysosomal degradation of intracellular LDs during the process of lipophagy. In humans, LAL deficiency causes a severe lysosomal storage disorder characterized by the increased storage of lipids in various organs, including liver, spleen, adrenals, bone marrow, lymph nodes, and macrophages (reviewed in (83)). Based on the disease severity, two clinical forms of the disease are distinguished: Wolman disease and Cholesteryl ester storage disease (CESD). Wolman disease is characterized by a neonatal-onset with hepatosplenomegaly, adrenal calcification, severe malabsorption, and cachexia leading to death before one year of life.

In CESD, the clinical outcome is less severe with a later-onset and a progressive lysosomal CE and TG accumulation, predominantly in the liver. Humans with CESD have elevated LDL-cholesterol, low HDL-cholesterol levels and develop premature atherosclerosis, indicating a critical role for LAL in cellular lipoprotein and lipid metabolism (83, 84).

1.3 LDs as eicosanoid-generating organelles

The fact that leukocyte LDs have a high capacity to store the eicosanoid precursor AA together with the observations that eicosanoid-forming enzymes localize to LDs have implicated this organelle as an important intracellular domain for the generation of eicosanoids. Other subcellular compartments for the metabolism of arachidonyl lipids into eicosanoids are the nuclear membrane, phagosomes, lysosomes, and the ER (75). The relative contribution of each of these compartments remains to be determined. However, the finding that the presence of LDs increases the potential to generate eicosanoids implicates a key role for LDs as eicosanoid-generating organelles in inflammatory cells (25, 85).

1.3.1 AA biosynthesis, cellular storage and remodeling

AA is an ω-6 essential FA obtained from the diet or synthesized *in vivo* after stepwise desaturation and elongation of linoleic acid, a process mainly occurring in the liver. AA is a highly bioactive molecule by exerting directly potent biological functions such as inducing apoptosis (86) or by acting as a source for a variety of eicosanoids with important regulatory function, particularly during inflammation. Hence, intracellular free concentrations of AA and its mobilization are tightly controlled.

Within the cell, AA is incorporated into neutral lipids as well as different PL classes. The incorporation into distinct lipid classes appears to be cell-dependent. Results from radiolabeling studies demonstrated that eosinophils contain most of their cellular AA in PLs (87), whereas arachidonate was esterified predominantly into neutral lipids of monocytes and macrophages (34, 88). Once taken up by the cell, a dynamic deacylation/reacylation process of AA occurs, which results in a remodeling of AA between different lipid classes (89). Upon cellular activation, such as receptor-mediated

activation of leukocytes, the deacylation process dominates resulting in the increased release of AA, which can be subsequently used for eicosanoid generation.

1.3.2 Lipid mediator generation

Lipid mediators constitute a large and expanding family of lipid signaling molecules derived from the ω-3 FA eicosapentaenoic acid (EPA), docosahexaenoic acid (DHA), and the ω-6 FA AA. AA-derived mediators (also termed eicosanoids) are widely appreciated for their pro-inflammatory activities and are key players during inflammation, whereas EPA- and DHA-derived anti-inflammatory mediators, such as protectins, maresins and resolvins, exhibit anti-inflammatory and pro-resolving properties (90). Inflammatory cells typically contain a high proportion of AA and low proportions of other polyunsaturated fatty acids (PUFAs) (such as EPA or DHA).

Once liberated from cellular pools, free AA can be metabolized into eicosanoids through four different pathways: the COX, LOX, cytochrome P450 (CYP450), and the non-enzymatic oxidation pathway (Fig. 5). COX isozymes (constitutive COX-1 and inducible COX-2) catalyze the formation of PGH2, which is converted by cell-specific PG synthases to biologically active products, including PGD2, PGE2, PGF2α, PGI2, and TxA2, known collectively as prostanoids. The LOX pathway catalyzes the formation of leukotrienes (LTs), hydroxyeicosatetraenoic acids (HETEs), and diverse hydroperoxyeicosatetraenoic acids (HPETEs). This pathway involves several enzymes with 5-LOX, 12-LOX, and 15-LOX being the most abundant. The pathway of CYP450 leads to the formation of HETEs and epoxyeicosatrienoic acids (EETs). By binding to distinct receptors, eicosanoids act in an autocrine or paracrine manner, thereby modulating the intensity and duration of inflammatory responses.

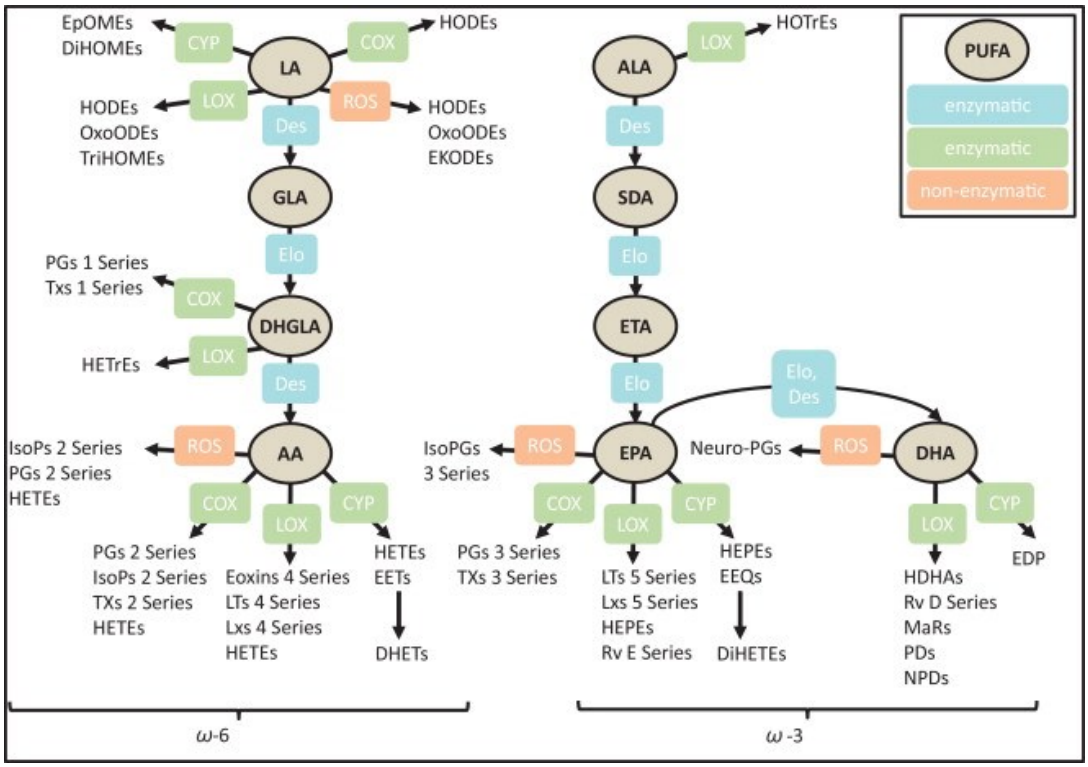

Figure 5: Overview of synthesis pathways for ω-6 and ω-3 FA-derived lipid mediators. (91)

1.3.3 Putative lipid sources of AA for eicosanoid biosynthesis

The current knowledge implicates that there are two distinct lipid species within LDs, which can act as a source of AA for eicosanoid production: PLs, which constitute the surface layer of LDs, and TGs stored in the neutral lipid core.

1.3.3.1 Phospholipids

In immune cells, AA is mainly found in the sn-2 position of PLs, such as PC, PE, and PI (92). An active remodeling process of AA between these lipid species, mainly between PC and PE, has been reported (reviewed in (93)). This appears to be important to maintain membrane homeostasis as well as an appropriate response upon cell activation. Of the more than 30 enzymes possessing PLA2 activity described so far, the cytosolic PLA2α (cPLA2α), also known as group IVA PLA2, has been studied most extensively and was ascribed a central role in stimulus-dependent AA mobilization in immune cells. cPLA2 liberates AA from the ER, phagosomal, nuclear and LD-membranes but not from the

plasma membrane (75). Under certain stimulatory conditions, soluble PLA2 (sPLA2) may also be involved by amplifying the cPLA2α-mediated response (94).

1.3.3.2 Neutral lipids

A large amount of AA is also incorporated into neutral lipids, predominantly TGs of immune cells. This was shown by electron microscopic autoradiography studies, where exogenous AA was predominantly incorporated to neutral lipids of LDs of eosinophils, neutrophils, mast cells, macrophages, and epithelial cells (reviewed in (95)). Further, compositional analysis of human leukocytes revealed that immune cells derived from inflammatory tissues, e.g. lung macrophages and mast cells, contain a large amount of AA stored in the TG pool (34). Since then, speculations that AA-containing TGs might serve as a source of AA for the generation of eicosanoids have been made (96, 97). However, the mechanism of AA liberation from this TG pool remained unsolved. Owing to the increased knowledge that has been gained on TG-hydrolyzing enzymes since the initial investigations, ATGL, the rate-limiting enzyme in TG degradation, was recently identified as critical player to liberate AA for eicosanoid generation in human mast cells (98). Based on these observations, three possible pathways are suggested for the liberation of AA from LDs (Fig. 6). In addition to the well-established pathway of a direct release from PL via the action of PLA2, AA can also be released directly or indirectly (via re-acylation into PLs) from TGs via ATGL. The physiological importance of each of these pathways remains to be investigated.

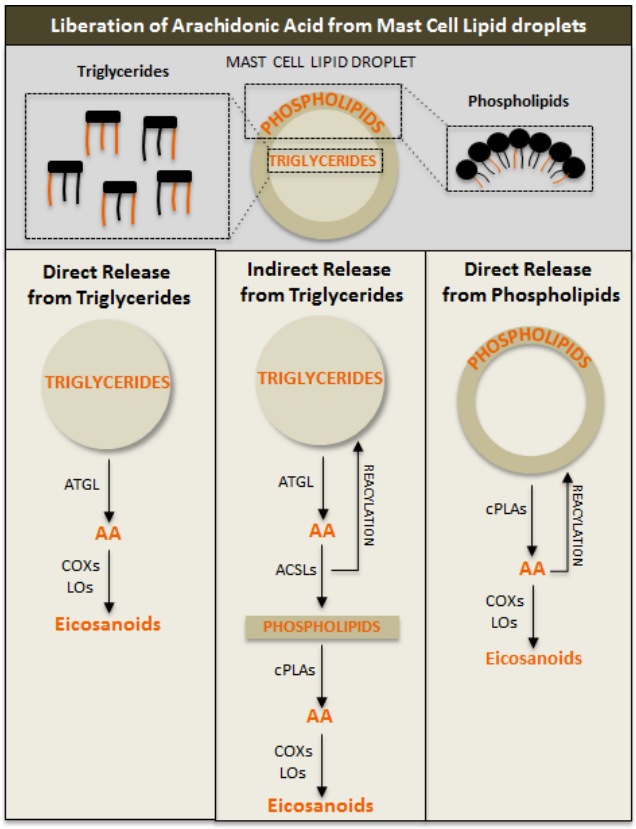

Figure 6: Model of different pathways of AA liberation for eicosanoid biosynthesis in human mast cells. Upon mast cell activation, AA can be liberated from LDs via three putative pathways: AA is directly released from the TG or PL pool via the action of ATGL and cPLA2, respectively. Alternatively, AA is liberated from LD-associated TGs by ATGL and then re-esterified into PLs, from where it is finally released by cPLA2 for the generation of eicosanoids. (99)

1.4 Aims

Lipolysis occurs in essentially all tissues and cell types. This process is most abundant in adipose tissue, where it has a major role to provide FAs as metabolic fuel. Studies in other cells than adipocytes provide substantial evidence that the lipolytic pathway as well as its intermediate and end products, either directly or indirectly, regulate cellular signaling pathways (reviewed in (100)). Hence, lipolysis is considered to be critically involved in the modulation of immune responses, inflammation, and atherosclerosis (101).

TG-rich LDs have been reported in various leukocyte types, including eosinophils, neutrophils, and basophils. However, the role of distinct lipolytic enzymes in these cells is largely unexplored. The major aims of this work were (i) to analyze the spectrum of TG-hydrolyzing enzymes as well as other regulatory proteins involved in lipolysis in mouse leukocytes, (ii) to identify their roles in lipid homeostasis under resting and immunologically active conditions, (iii) to determine the consequences of Jordans' anomaly caused by ATGL deficiency on neutrophil function, and (iv) to analyze the production and release of lipid mediators from neutrophils upon activation.

2 Materials and Methods

2.1 Buffers, solutions, and equipment

3% Thioglycolate medium

0.7 g agar, 6 g glucose, 17 g peptone 140, 3 g peptone 110, 2.5 g NaCl, 0.1 g Na_2SO_3, 0.5 g sodium thioglycolate, and 1000 ml ddH_2O were mixed, boiled, cooled down to RT, and stored at -20°C.

SDS-Gel

Stacking gel (4%)

Reagents (1 gel)	Volume (µl)
Acrylamide solution	250
0.5 M Tris-HCl pH 6.8	385
ddH_20	885
TEMED	3.8
10% APS	38
Total Volume	1561.8

Separating gel (10%)

Reagents (1 gel)	Volume (µl)
Acrylamide solution	2867
1.5 MTris-HCl, 10%SDS pH 8.8	2170
ddH_20	213
TEMED	4.4
10% APS	76
Total Volume	5330.4

Acrylamide solution
29.2% Acrylamide
0.8% N,N´-methylenebisacrylamide

RIPA buffer
50 mM Tris-HCl pH 8.0
150 mM NaCl
1% Triton X-100
0.5% SDS

SDS sample buffer
2.3 g SDS
0.6 g Tris
25 ml H_2O
pH 6.8 with HCl
10 ml Glycerol
25 mM DTT
add H_2O to 45 ml
one drop of bromphenolblue

Ponceau S
0.2% Ponceau S
3% Trichloracetic acid
diluted in 1 x PBS

10x Electrophoresis buffer
250 mM Tris
1.92 M Glycine
1% SDS

10x Blotting buffer
100 mM Tris
0.38 M Glycine

10x TBS-T (washing buffer)
100 mM Tris-HCl pH 7.4
1.5 M NaCl
1% Tween 20

10x PBS pH 7.4
1.4 M NaCl
25 mM KCl
81 mM Na_2HPO_4
15 mM KH_2PO_4

Oil red O (ORO) staining solution
2.8 g Oil red O
400 ml Propylene glycol

10x HBSS pH 7.4
53.33 mM KCl
4.4 mM KH_2PO_4
1.4 M NaCl
3.36 mM Na_2HPO_4
55.56 mM Glucose

HEPES buffer pH 7.2
140 mM NaCl
10 mM Hepes
5 mM KCl
1 mM $MgCl_2$

ACK lysis buffer pH 7.2
150 mM NH_4Cl
10 mM $KHCO_3$
1 mM Na_2EDTA

Ca-flux Assay buffer pH 7.4
10 mM Hepes
10 mM Glucose
0.1% BSA

Equipment	**Company**
Centrifuge 5471R	Eppendorf
Power supply Power Pac 300	Bio-Rad
LightCycler 480	Roche
Sonicator	B.Braun
Nano Drop Spectrophotometer	Peqlab
Thermal cycler C1000	Biorad
Anthos 2000	Anthos
Guava Easy Cyte 8	Merck Millipore
LSR II	BD Biosciences
FACSAria III Cellsorter	BD Biosciences

Reagents	
Name	**Company**
Peptone 140	Gerbu
Peptone 110	
Proteinase K	Roth
Chloroform	
Isopropanol	
Ethanol	
Formaldehyde	
Tris	
EDTA	
Glycine	
Methanol	
Ponceau S	
TCA	
Hepes	
$CaCl_2$	
Tween 20	Merck
NaCl	
KCl	
Na_2HPO_4	
Na_2SO_3	
KH_2PO_4	
K_2HPO_4	
NH_4Cl	
$KHCO_3$	
Triton X-100	
$MgCl_2$	
DMSO	
NaN_3	
Glycerol	
Agarose	Sigma
Sodium thioglycolate	
APS	
DTT	
Protease-Inhibitor	
BSA	
Mayer’s Hematoxylin	
Oil red O	
Propylene glycol	
ß-Mercaptoethanol	
Glucose	
Percoll	
Acrylamide	Bio-Rad
TEMED	
SDS	Serva
Triglyceride FS	DiaSys
Total Cholesterol FS	
Free Cholesterol FS	
Nefa C	Wako
Cellfix	BD Biosciences
DMEM	Gibco, Invitrogen
Pen/Strep	

2.2 Animals

Global Atgl-/- mice were generated as described elsewhere (102). Mice carrying a LoxP-modified Atgl allele (B6.129- Pnpla2^{tm1Eek} mice; backcrossed onto C57BL/6 x N3; herein designated as Atgl^{flox} mice) were generated as described (103). Cgi-58$^{flox/flox}$ were generated as described (104) and were kindly provided by Dr. Guenter Haemmerle, University of Graz, Austria. Mice with a targeted deletion of Atgl or Cgi-58 in myeloid cells were obtained by crossing Atgl$^{flox/flox}$ or Cgi-58$^{flox/flox}$ mice with transgenic mice that express Cre recombinase under the control of the murine M lysozyme promoter (LysMCre, C57BL/6 background; provided by Dr. Thomas Ruelicke, University of Veterinary Medicine Vienna, Austria). Atgl$^{flox/flox}$ and Cgi-58$^{flox/flox}$ mice were used as controls. Hsl-/-, Mgl-/-, and Lal-/- were generated as described elsewhere (105-107). Mice were kept on a standard chow diet (4% fat and 19% protein; Altromin Spezialfutter GmbH & Co, Lage, Germany) and water ad libidum on a regular light-dark cycle (12 h light, 12 h dark). Animal protocols were approved by the Austrian Federal Ministry of Science, Research and Economy, Division of Genetic Engineering and Animal Experiments, Vienna, Austria.

2.3 Genotyping

At the age of ~4 weeks, animals were genotyped. A two mm piece of ear punch was collected and digested in lysis buffer (Peqlab, Erlangen, Germany) and Proteinase K (0.7 mg/ml) for 1-2 h at 56°C under vigorous shaking. Then, samples were incubated for 45 min at 85°C to inactivate Proteinase K. The reaction mix contained ~200 ng of the template DNA, 2.5 mM $MgCl_2$, 0.4 mM of each dNTP, 0.1 µM of each primer, 4% DMSO, 2.5 U Hot Firepol DNA Polymerase I (Solis BioDyne OU, Tartu, Estonia) and the reaction buffer system of DyNAzyme™ DNA Polymerase (Finnzymes, Espoo, Finland).

For genotyping, primers listed in Table 2 were used.

Table 2: Primer sequences for genotyping of mice

Gene	Primer sequence (5'-3')
Atgl-fwd	AGAGAGAGAAGCTGAAGCCT
Atgl-rev	GCCAGCGAATGAGATGTTCC
$Atgl^{flox/flox}$-fwd	CGGTGAGGGTGGGGAACGGA
$Atgl^{flox/flox}$-rev	CAGGGGGCCAGGCGGTCAGA
Cgi-58-fwd	GTCATGGTTGTGGGGAAATC
Cgi-58-rev	GACTGGAAGGATTTGAGGGG
Cre-mut	CCCAGAA ATGCCAGATTACG
Cre-comm	CTTGGGCTGCCAGAATTTCTC
Cre-wt	TTACAGTCGGCCAGGCTGAC
Hsl-fwd	CATGCACCTAGTGCCATCCTT
Hsl-rev	CTCACTGAGGCCTGTCTCGTT
Hsl-neo-rev	TACCGAGCCATCTTCCTAGTCC
Mgl-fwd	TTGCAGCTGGAGTCTGTGTC
Mgl-rev	GTCAGTCGAGGCTGGAAGAG
Mgl-ko-fwd	GAGAGTAGAGGCAGCACTGA
Lal-fwd	CTGCATGGAGACTCACAAAGG
Lal-rev	AAGTCTTCCCTGTTCCCATGG
Lal-neo-fwd	CGTCGTGATTAGCGATGATGA
Lal-neo-rev	TCCAGCAGGTCAGCAAAGAA

The following cycle conditions were used for the amplification of the specific DNA-products:

Table 3: PCR programs for genotyping of mice

	Atgl/Cgi-58-flox		**Atgl-flox**		**Cre**	
Initial	95°C 15 min		95°C 15 min		95°C 15 min	
Denaturation	95°C 30 sec	35x	95°C 30 sec	35x	95°C 60 sec	40x
Annealing	62°C 30 sec		55°C 60 sec		60°C 60 sec	
Elongation	72°C 60 sec		72°C 60 sec		72°C 90 sec	
Final elongation	72°C 10 min		72°C 10 min		72°C 10 min	
Cool down	4°C ∞		4°C ∞		4°C ∞	

	Hsl		**Mgl**		**Lal**	
Initial	95°C 15 min		95°C 15 min		95°C 15 min	
Denaturation	95°C 30 sec	35x	95°C 30 sec	35x	95°C 60 sec	35x
Annealing	64°C 60 sec		66°C 60 sec		60°C 60 sec	
Elongation	72°C 60 sec		72°C 60 sec		72°C 90 sec	
Final elongation	72°C 10 min		72°C 10 min		72°C 10 min	
Cool down	4°C ∞		4°C ∞		4°C ∞	

2.4 Isolation of neutrophils

Neutrophils were isolated from either peritoneal exudate or bone marrow. Cells of peritoneal exudate were collected one day after intraperitoneal injection of 2.5 ml 3% thioglycolate by rinsing the peritoneum with 10 ml Hank's balanced salt solution (HBSS) containing 1 mM EDTA. For bone marrow isolation, tibia and femur from both hind legs were collected, flushed with HBSS-EDTA and pushed through a cell strainer to disperse cell clumps. The cell suspension was centrifuged (400 x *g*, 10 min, 4°C) and neutrophils were purified by using a Percoll gradient as described (108). Briefly, cell suspensions were layered on top of a three-layer Percoll gradient of 78%, 69% and 52% and centrifuged (1500 x *g*, 30 min, RT) with brakes off. Neutrophils from the 69% - 78% interphase were harvested and counted. After washing with HBSS-EDTA containing 1% BSA, cells were suspended in HEPES buffer plus 9 mM glucose and immediately used for further experiments.

2.5 Sorting of inflammatory cells

Cells were flow-sorted using a BD FACSAria III Cellsorter (BD Biosciences, San Jose, CA). Peritoneal lavages from wt mice two days after thioglycolate injection were used to sort eosinophils, neutrophils, monocytes, and macrophages. B- and T-lymphocytes were sorted from peripheral blood after red blood cell lysis in ammonium-chloride-potassium (ACK) lysis buffer.

2.6 RNA isolation and quantitative real-time PCR

Total RNA from sorted cells was extracted using TriFast reagent according to the manufacturer's protocol (Peqlab). One µg of total RNA was reverse transcribed using the High Capacity cDNA Reverse Transcription Kit (Applied Biosystems, Carlsbad, CA).

Table 4: Mastermix for reverse transcription

Component	Volume
10x RT buffer	2
25x dNTP mix (100 mM)	0.8
10x RT random primers	2

Multiscribe reverse transcriptase	1
RNase inhibitor	0.7
Nuclease-free H_2O	3.5
1µg RNA/10µl H_2O	10
Total volume	**20**

Table 5: Thermal cycling conditions for reverse transcription

	Step 1	**Step 2**	**Step 3**	**Step 4**
Temperature	25°C	37°C	85°C	4°C
Time	10 min	120 min	5 sec	∞

Quantitative real-time PCR was performed on a LightCycler 480 (Roche Diagnostics, Rotkreuz, Switzerland) using the QuantifastTM SYBR® Green PCR kit (Qiagen, Hilden, Germany). For data normalization, Gapdh was used endogenous control and the relative units for gene expression were calculated by using the $2^{-\Delta\Delta ct}$ method.

Table 6: Real-time PCR program

	Temperature	**Time**	**Cycles**
Initial denaturation	95°C	5 min	1
Denaturation and amplification	95°C	10 sec	40
	40°C	30 sec	1
Melting curve	95°C	10 sec	1
	60°C	20 sec	1
	95°C	∞	
Cool down	4°C	20 sec	1

Table 7: Primer sequences for real-time PCR

Gene	**Forward primer (5`-3`)**	**Reverse primer (5`-3`)**
Gapdh	AGGTCGGTGTGAACGGATTTG	GGGGTCGTTGATGGCAACA
Atgl	GCCACTCACATCTACGGAGC	GACAGCCACGGATGGTGTTC
Hsl	GCTGGTGACACTCGCAGAAG	TGGCTGGTGTCTCTGTGTCC
Mgl	GCCACTCACATCTACGGAGC	GACAGCCACGGATGGTGTTC
Lal	CGGCTTGCTGGCAGATTCTA	GTGCAGCCTTGAGAATGACC
Cgi-58	GACAGCCACGGATGGTGTTC	CAGCGTCCATATTCTGTTTCCA
G0S2	GTGAAGCTATACGTGCTGGG	CCGTCTCAACTAGGCCGAG
Cd36	GCAGGTCTATCTACGCTGTG	GGTTGTCTGGATTCTGGAGG
Acc	GGACTTGGAGCAGAGAACCTTCG	CAAGCTGGTTGTTGGAGGTGTA
Fasn	GAAGCCGAACACCTCTGTGCAGT	GCTCCTTGCTGCCATCTGTATTG

Scd1	CCGGAGACCCCTTAGATCGA	TAGCCTGTAAAAGATTTCTGCAAACC
Cpt1α	CTCCGCCTGAGCCATGAAG	CACCAGTGATGATGCCATTCT
Dgat1	GTGCACAAGTGGTGCATCAG	CAGTGGGATCTGAGCCATCA
Dgat2	CAGCAAGAAGTTTCCTGGCAT	CCTCCCACCACGATGATGAT
iNOS	GTTCTCAGCCCAACAATACAAGA	GTGGACGGGTCGATGTCAC
Mmp9	GGACCCGAAGCGGACATTG	CGTCGTCGAAATGGGCATCT
Noxa1	CGAGCCCTGGCCTATATGATA	GGTCCTTTGTAGCTGCTCC
cPla2	TGGTGGGATTCTCTGGTGTGA	GGAAAATCGGGGTGAGAGTACA
Cox1	ATGAGTCGAAGGAGTCTCTCG	GCACGGATAGTAACAACAGGGA
Cox2	TTCAACACACTCTATCACTGGC	AGAAGCGTTTGCGGTACTCAT
Alox5	ACTACATCTACCTCAGCCTCATT	GGTGACATCGTAGGAGTCCAC
Alox12	TCCCTCAACCTAGTGCGTTTG	GTTGCAGCTCCAGTTTCGC
Alox15	GGCTCCAACAACGAGGTCTAC	AGGTATTCTGACACATCCACCTT
Cyp2j	TCTGGGAAGCACTCCATCTCA	CCCTGGTGGGTAGTTTTTGG

2.7 Immunophenotyping of peripheral blood, peritoneal, and bone marrow cells

Peripheral blood cells were collected by retrobulbar puncture from isoflurane anesthetized mice. Peritoneal lavage cells were collected as mentioned above. After red blood cell lysis, remaining cells were fixed with 10% methanol-free formalin for 10 min at 4°C and blocked with PBS containing 10% FCS for 10 min at 4°C. After incubation, cells were stained in PBS containing 3% FCS for 20 min at 4°C with the following antibodies against surface markers: CD11b-Alexa Fluor647, SiglecF-PE, Gr-1-APC-Cy7 (all purchased from BD Biosciences), CD115-PE-Cy7, CD19-eFluor605, CD3-eFluor450 antibodies (all purchased from eBioscience Inc, San Diego, CA) for peripheral blood cells, and F4/80-eFluor450 (eBioscience), SiglecF-PE, Gr-1-PerCP-Cy5.5, CD19-PE-Cy7, and CD3-APC antibodies (all purchased from BD Biosciences) for peritoneal cells. All antibodies were titrated prior to use. The frequencies of specific cell types were calculated as the percentage of living cells. Intracellular LDs were quantified by staining with the fluorescent dye BODIPY493/503 (1 µg/ml; Life Technologies, Carlsbad, CA). After 10 min of incubation at 4°C, cells were washed, resuspended in PBS, and analyzed (1 x 10^5 cells/measurement) using an LSR II flow cytometer (BD Biosciences). Data were acquired using DIVA 6.1.2 software (BD Biosciences) and the analysis was performed using FlowJo (Treestar Inc., San Carlos, CA).

For bone marrow analysis, femurs and tibias were collected and the marrow was flushed out of the bones with HBSS-EDTA. Cell pellets were resuspended in 200 µl of antibody

cocktail and incubated at RT for 10 min. For LD staining, BODIPY493/503 was added to the cells for another 10 min. Finally, cells were washed in buffer (PBS, 0.5% BSA, 0.025% NaN_3) and analyzed immediately. A forward-side scatter gate excluded cell debris and remaining red blood cells, and dead cells were excluded by 7-aminoactinomycin D (7-AAD; BD Biosciences) uptake. LSK populations were defined as $Lin^-Sca\text{-}1^+c\text{-}Kit^+$, granulocyte/monocyte progenitors (GMP) were defined as $Lin^-c\text{-}Kit^+CD34^+Fc\gamma RII/III^+$, monocyte/dendritic cell progenitors (MDP) as $Lin^-c\text{-}Kit^{+/Int}CD115^+Flt3^+$, and common lymphoid progenitors (CLP) were identified as $Lin^-c\text{-}Kit^{lo}Sca\text{-}1^{lo}IL7R\alpha^+$. CD115-PE, CD117(c-Kit)-PE-Cy7, CD16/32(FcγRII/III)-eFluor450, and Ly-6A/E(Sca-1)-PE-Cy7 antibodies were purchased from eBioscience. IL7Rα(CD127)-brilliant violet and Flt3(CD135)-APC antibodies were purchased from BioLegend (San Diego, CA) and CD117(c-Kit)-APC from BD Biosciences. The lineage antibody cocktail encompassed anti-Gr-1, anti-CD11b, anti-Ter119, anti-B220, and anti-CD3e (BD Biosciences). The gating strategies to define various cell populations in blood, peritoneal lavage and bone marrow are shown in Appendix (Fig. S1-5).

2.8 Oil red O (ORO) staining

Cells from the peritoneal lavage were sedimented by cytocentrifugation (Shandon Southern Instruments Ltd., Camberley, United Kingdom) onto glass slides (2 x 10^4 cells/slide) and fixed with 10% neutral-buffered formalin. Cells were stained with ORO for 30 min and counterstained with Mayer's Hematoxylin. Coverslips were mounted with Aquamount (DAKO, Glostrup, Denmark) to retain ORO staining. Microscopic images were taken using a Nikon Eclipse E600 equipped with a Nikon Digital Sight DS-U1 unit (Spach Optics Inc., New York, NY).

2.9 Transmission electron microscopy

Bone marrow cells were fixed in 2.5% glutaraldehyde (w/vol) and 5% methanol-free formalin in 0.1 M phosphate buffer (pH 7.4) for 2 h at RT, postfixed in 2% osmium tetroxide (w/vol) for 2 h, dehydrated in graded series of ethanol, and embedded in a TAAB epoxy resin. Ultrathin sections (75 nm) were cut with a Leica UC 6 Ultramicrotome (Leica Microsystems, Wetzlar, Germany) and stained with lead citrate (5 min) and with

uranyl acetate (15 min). Images were taken using a FEI Tecnai G2 20 transmission electron microscope (FEI Corporation, Eindhoven, Netherlands) with a Gatan ultrascan 1000 CCD camera. Acceleration voltage was 120 kV. Electron microscopy was performed by Dr. Dagmar Kolb.

2.10 Western blot analysis

Protein concentrations from cell lysates were determined by the Bio-Rad DC protein assay (Bio-Rad Laboratories, Hercules, CA). Proteins were separated by SDS-PAGE under reducing conditions (25 mM DTT) and then transferred onto a nitrocellulose membrane (Hybond-C Extra; Amersham Biosciences, Piscataway, NJ). Non-specific binding sites were blocked by incubating the membrane with 5% non-fat dry milk in 1x TBS-T buffer for 1 h at RT. Immunodetection was performed using mouse anti-ATGL (1:200), mouse anti-HSL (1:800), anti-COX-2 (1:1000) (Cell Signaling Technology, Danvers, MA), rabbit anti-MGL (1:1000, kindly provided by Dr. Robert Zimmermann, University of Graz, Austria), and anti-mouse beta-ACTIN (1:10000) antibodies (Sigma-Aldrich, Steinheim, Germany). The horseradish peroxidase-conjugated goat anti-rabbit (1:5000) and rabbit anti-mouse antibodies (1:1000) (Dako, Glostrup, Denmark) were visualized by enhanced chemiluminescence detection (ECL Plus; Thermo Scientific, Rockford, IL) using a ChemiDoc^{TM} MP Imaging System (Bio-Rad).

2.11 Lipid analysis of peritoneal lavage

Peritoneal lavages were harvested from mice one day after intraperitoneal thioglycolate injection. Cellular lipids from peritoneal exudates were extracted using the Folch method. After evaporation under constant nitrogen flow, 100 µl 1% Triton X-100 (dissolved in chloroform) were added, and lipids were dried again under a stream of nitrogen. Thereafter, samples were dissolved in 100 µl ddH_2O for 15 min at 37°C. Aliquots were used for enzymatic measurements of TG, total cholesterol (TC), and free cholesterol (FC) using kits according to manufacturer's protocols (DiaSys, Holzheim, Germany). The readings were normalized to protein concentrations. To determine the composition of TG, PC and PE species, extracted lipids were dissolved in 2-propanol:chloroform:methanol

(7:2:1, v:v:v) and analyzed by LC/ESI-MS as described (109). Lipid analysis was performed in collaboration with Dr. Thomas Eichmann.

2.12 Calcium flux and chemotaxis assays

Free intracellular Ca^{2+} levels $[Ca^{2+}]_i$ of bone marrow-derived neutrophils were analyzed in response to formyl-methionyl-leucyl-phenylalanine (fMLP) (Sigma-Aldrich) and keratinocyte-derived chemoattractant (KC) (PeproTech Inc., Rocky Hill, NJ). Changes in $[Ca^{2+}]_i$ were detected by flow cytometry as an increase in fluorescence intensity of the Ca^{2+}-sensitive dye Fluo-3 in the FL-1 channel. Cells (1×10^7) were incubated with 500 µl assay buffer containing 2 µM Fluo-3 acetoxymethylester (AM) (Life Technologies) and 0.02% pluronic F-127 (Sigma-Aldrich) in the absence of Ca^{2+} and Mg^{2+} for 1 h at RT. Cells were washed with assay buffer and resuspended in assay buffer containing Ca^{2+} and Mg^{2+} to a final concentration of $0.3\text{-}0.5 \times 10^6$ neutrophils/ml. Aliquots of 500 µl were used for each condition. Maximal Ca^{2+} responses were determined after adding various concentrations of fMLP and KC. Kinetics of Ca^{2+} flux were analyzed using FlowJo software (Treestar).

For chemotaxis assays, bone marrow-derived neutrophils were suspended in assay buffer containing Ca^{2+} and Mg^{2+} (2×10^6 cells/ml). Fifty µl cell suspension per well were placed onto the top plate of an AP48 microBoyden chemotaxis chamber with a 5 µm pore-size polycarbonate filter (Neuro Probe, Gaithersburg, MD). Cells were allowed to migrate towards 30 µl of fMLP and KC in the bottom wells of the plate for 1 h at 37°C. The membrane was carefully removed and migrated cells were enumerated by flow cytometric counting.

2.13 Measurement of CD11b cell surface expression

Isolated neutrophils were pre-incubated with anti-CD11b-Alexa Fluor647 (BD Biosciences) for 10 min at RT in the dark and then stimulated with various concentrations of fMLP, KC, and phorbol myristate acetate (PMA) (Sigma-Aldrich) for 30 min at 37°C. Cells were resuspended in Cellfix and analyzed by flow cytometry.

2.14 Fatty acid uptake

Peritoneal neutrophils (one day after thioglycolate injection) were resuspended in HBSS containing Ca^{2+}, Mg^{2+}, and 0.1% FA-free BSA. After 15 min incubation in culture medium (DMEM, 10% lipoprotein-deficient serum, 1% penicillin/streptomycin), 5 µM BODIPY 500/510 C1, C12 (Life Technologies) was added for 10 min. Thereafter, cells were fixed with 10% methanol-free formalin for 10 min at 4°C, washed two times with HBSS-EDTA, stained with a neutrophil-specific marker (Ly6G-PE; BD Biosciences), and analyzed by flow cytometry.

2.15 Phagocytosis and ROS measurement

Neutrophils were isolated from peritoneal lavages one day after thioglycolate injection. After 1 h of pre-incubation in culture medium in the absence of glucose, neutrophils (1 x 10^6) were incubated with 100 µl of fluorescein-labeled *E.coli* particles (Vybrant™ Phagocytosis Assay, Molecular Probes®, Life Technologies, Carlsbad, CA) for 1 h at 37°C in the dark under gentle rotation. The suspension was removed and 100 µl trypan blue were added for 1 min to quench extracellular fluorescein-labeled bacteria. Cells were washed with cold HBSS-EDTA, stained with a neutrophil-specific marker (Ly6G-PE; BD Biosciences) and the amount of phagocytosed *E.coli* was measured by flow cytometry. Intracellular reactive oxygen species (ROS) generation during phagocytosis and after a 20 min exposure to KC (20 ng/ml) and fMLP (1 µM) were measured according to the manufacturer's protocol (Life Technologies).

2.16 Apoptosis assay

Neutrophils from bone marrow were isolated by gradient centrifugation as described (108) and cultured at a density of 1 x 10^7 in culture medium containing 25 mM glucose for 6 and 18 h. Two hundred µl cells were stained with annexin V and propidium iodide according to manufacturer's protocols (Annexin V-FITC apoptosis detection kit I; BD Biosciences). Cells were immediately analyzed by flow cytometry.

2.17 Plasma cytokine array

Plasma cytokine levels of wt, Atgl-/-, Atgl flox, and myeloid Atgl-/- mice were determined using a mouse cytokine array (RayBiotech, Norcross, GA). The arrays were performed according to the manufacturer's instructions. Membranes spotted in duplicate with antibodies against 32 cytokines were incubated with plasma (pooled in an equal amount from 6 individual mice of each group) and then developed by chemiluminescence. The intensity of each spot on the arrays was quantified by densitometry using ImageJ.

2.18 Pharmacological inhibition of ATGL *in vitro*

Peritoneal neutrophils were cultivated in culture medium containing 25 mM glucose supplemented with either 300 µM OA or AA (Sigma-Aldrich) complexed to BSA (OA-BSA, AA-BSA). Fatty acid:BSA complexes were prepared as described (23). After an incubation period of 6 h in the absence or presence of the ATGL inhibitor Atglistatin (40 µM) and the HSL inhibitor Hi 76-0079 (25 µM) (kindly provided by Dr. Martina Schweiger, University of Graz, Austria), the medium was replaced by serum-free DMEM containing Atglistatin or Atglistatin/Hi. After 4 h and 6 h of incubation, LDs were quantified by flow cytometry as described above.

To study cytokine-induced LD formation, wt neutrophils collected from peritoneal lavages one day post thioglycolate injection were pre-incubated in culture medium for 2 h in the absence or presence of 40 µM Atglistatin, after which recombinant MIP-1 and MIP-2 (100 ng/ml; PeproTech) were added. After 5 h of incubation, LDs were quantified by flow cytometry.

2.19 Quantification of PUFAs and lipid mediators

Peritoneal neutrophils were pre-incubated in culture medium (containing 25 mM glucose) with or without 40 µM Atglistatin for 6 h. Thereafter, the medium was replaced by HBSS containing Ca^{2+} and Mg^{2+} in the absence or presence of the Ca^{2+} ionophore A23187 (0.5 µM) (Sigma-Aldrich) for 1 h. Then, cells were placed on ice, transferred into tubes, and centrifuged at 400 x *g* for 10 min at 4°C. Supernatants were immediately frozen in liquid N_2 and stored at -80°C (max. one week) until analysis. To determine PUFA and lipid mediator concentrations in peritoneal lavage fluid one day after thioglycolate injection,

the peritoneum was rinsed with 3 ml HBSS-EDTA. The cell-free exudate was snap-frozen in liquid N_2 and stored at -80°C. An AB Sciex 5500 QTrap mass spectrometer (Darmstadt, Germany) operating in negative electrospray ionization mode was applied for LC-MS/MS analysis, using 200 µl of cell supernatant or peritoneal lavage fluid as previously described (110). Eicosanoid analysis was performed in collaboration with Dr. Uta Ceglarek and Juliane Dorow.

2.20 Bacterial peritonitis model

Mice were injected intraperitoneally with a sublethal dose of live *E. coli* (serotype O18:K1; 2×10^4 CFU in 200 µl of sterile saline). After 18 h, blood was collected by retrobulbar puncture from isoflurane anesthetized mice. Then, mice were sacrificed by dislodging the cervical vertebrae. Livers were surgically removed and homogenized in 4 ml sterile PBS. Peritoneal lavages were collected as described earlier. *E. coli* CFUs were calculated from the colony numbers on the Luria-Bertoni (LB) agar plates after overnight culture with serial 10-fold dilutions. This experimental model was performed in collaboration with Dr. Birgit Strobl (University of Veterinary Medicine in Vienna).

2.21 Statistical analysis

Statistical analyses were performed using GraphPad Prism 5.0 software. Significance was calculated by Student's *t*-test or ANOVA, followed by Bonferroni correction. Data are shown as means + SEM. For statistical analysis of PUFAs and lipid mediators, non-parametric Wilcoxon signed-rank tests and Mann-Whitney U tests were used. Data are expressed as median with minimum and maximum range. The following levels of statistical significance were used: $*p < 0.05$, $** p \leq 0.01$, $*** p \leq 0.001$.

3 Results and Discussion

3.1 Impact of the deficiency of TG hydrolases on lipid homeostasis in immune cells

3.1.1 Expression of TG hydrolases in immune cells

With the exception of macrophages, the knowledge about enzymes hydrolyzing TGs in cells of the innate or adaptive immune system is scarce and the enzyme expression profiles are largely unexplored. Hence, I have used a fluorescence-activated cell sorting (FACS) approach to sort various murine immune cells including neutrophils, monocytes, macrophages (derived from thioglycolate-elicited lavage) and B- and T-lymphocytes (derived from peripheral blood). From these flow-sorted cells I examined the expression of Atgl, Hsl, Mgl, and Lal as well as the regulators of lipolysis Cgi-58 and G0S2 by quantitative real-time PCR (Fig. 7).

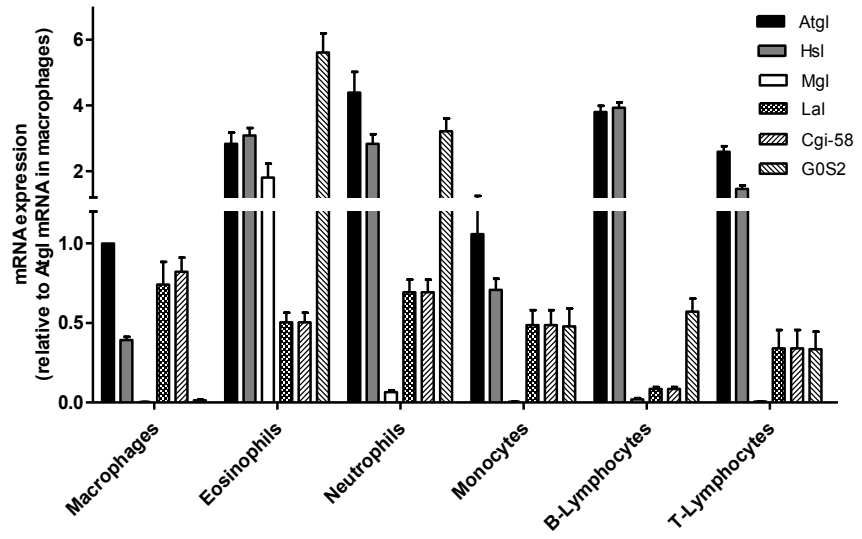

Figure 7: Lipase expression in immune cells

Total RNA of flow-sorted immune cells was isolated and analyzed for mRNA expression of Atgl, Hsl, Mgl, Lal, Cgi-58 and G0S2 by quantitative real-time PCR. For data normalization, Gaph was used as reference gene. Transcript expression levels are shown as -fold change relative to Atgl mRNA levels in macrophages and represent means + SEM (n=4).

mRNA expression of Atgl was highest in neutrophils, followed by B-lymphocytes, eosinophils, T-lymphocytes, monocytes, and macrophages. Hsl was highly expressed in B-lymphocytes and in comparable amounts in eosinophils and neutrophils. T-lymphocytes, monocytes, and macrophages showed the lowest levels of Hsl mRNA. Mgl was most abundant in eosinophils, whereas all other cell types showed little expression. Lal showed similar expression levels in macrophages, eosinophils, neutrophils, monocytes and only low expression in B- and T-lymphocytes. The expression of the Atgl co-activator Cgi-58 was similar in granulocytes and T-lymphocytes and lowest in B-lymphocytes. The endogenous inhibitor G0S2 was expressed very heterogeneously in the different cells types with peak expression levels in eosinophils and neutrophils. Summarized, from these mRNA expression profiles I conclude that neutral lipases are expressed in immune cells.

To get an insight into their functional role in the regulation of LD homeostasis in immune cells, I used the respective genetic knock-out (-/-) mouse models and monitored the LD content, under both, resting and inflammatory conditions. For these studies I have included global Atgl-/-, Hsl-/-, Mgl-/-, Lal-/- mice as well as myeloid-specific Atgl-/- and CGI-58-/- mice. The results from these analyses will be described in the next paragraphs.

3.1.2 LD homeostasis in immune cells of Atgl-/- mice

Immunophenotyping of peripheral blood by flow cytometry revealed comparable relative blood counts between wt and Atgl-/- mice (Fig. 8A). By using BODIPY493/503 as a neutral lipid dye, I observed increased fluorescence intensity exclusively in neutrophils of Atgl-/- mice (Fig. 8B). To gain insight into the ultrastructural morphology of the cells, we performed transmission electron microscopy of wt and Atgl-/- bone marrow cells. As shown in Fig. 8C, intracellular LDs were present in the cytoplasm of Atgl-/- bone marrow cells as electron-lucent round-shaped structures, whereas no LDs were visible in wt cells. Since a morphological evaluation between differentiated and precursor cells appeared difficult and to obtain quantitative insight into LD distribution, I analyzed bone marrow cells by flow cytometry. Relative populations of bone marrow cells were comparable between wt and Atgl-/- mice (Fig. 8D). I observed an increased amount of LDs exclusively in mature Gr-1^{+} neutrophils of Atgl-/- mice but not in hematopoietic stem cells such as $Lin^{-}Sca\text{-}1^{+}cKit^{+}$ cells (LSK) or any of the investigated precursor cells such as common

lymphoid progenitors (CLP), monocyte-dendritic cell progenitors (MDP), and granulocyte-monocyte progenitors (GMP) (Fig. 8E).

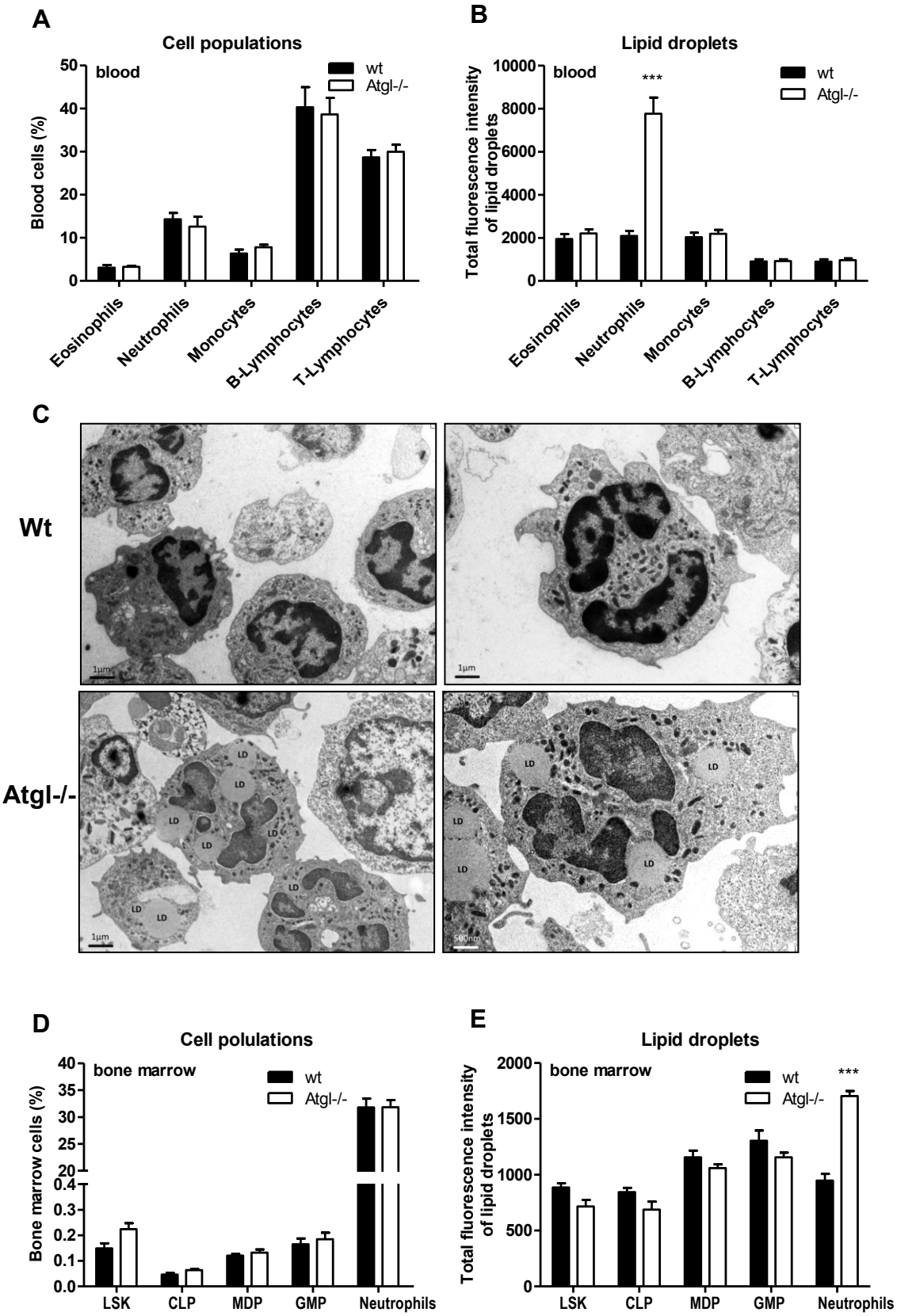

Figure 8: Atgl-/- mice accumulate LDs in neutrophils of peripheral blood and bone marrow

(A) Relative counts of peripheral blood cells from wt and Atgl-/- mice were determined by immunophenotyping using flow cytometry. (B) LDs in peripheral blood cells were quantified by using BODIPY493/503 as neutral lipid stain. Wt and Atgl-/- bone marrow were analyzed by (C) transmission electron microscopy and (D,E) flow cytometry. LSK: hematopoietic precursors, CLP: common lymphoid progenitors, MDP: monocyte-dendritic cell progenitors, GMP: granulocyte-monocyte progenitors. Data are shown as geometric means of fluorescence intensity + SEM (n=5). ***$p \leq 0.001$

To elucidate the effect of ATGL deficiency under inflammation-driven conditions, I used a murine thioglycolate-induced peritonitis model. This model is commonly used to obtain a large number of immune cells and to study inflammatory events. Thioglycolate induces an acute inflammatory response, which is typically characterized by early neutrophil recruitment between 4 and 24 hours, followed by an influx of monocytes that develop into inflammatory macrophages reaching peak levels at 3 to 4 days.

First I analyzed naive peritoneal lavages from wt and Atgl-/- mice, which consisted predominantly of macrophages, lymphocytes, and small numbers of granulocytes and monocytes (Fig. 9A). Similar to the findings in peripheral blood, I observed a selective LD accumulation in neutrophils of naive lavages from Atgl-/- mice (Fig. 9B). After thioglycolate-induced inflammation, the cellular infiltration into the peritoneum was unchanged between wt and Atgl-/- mice both one day (Fig. 9C) and three days (Fig. 9E) post injection. An increased LD abundance in neutrophils and monocytes was observed on day one (Fig. 9D) and in neutrophils, monocytes and macrophages on day three post injection (Fig. 9F) in peritoneal lavages from Atgl-/- mice.

ORO stainings of sedimented peritoneal cells one day (Fig. 9G,H) and three days (Fig. 9I,J) after thioglycolate administration confirmed the data from flow cytometry showing an increased abundance of LDs in cells from Atgl-/- mice (Fig. 9H,J), whereas in wt cells only few LDs were detectable (Fig. 9G,I).

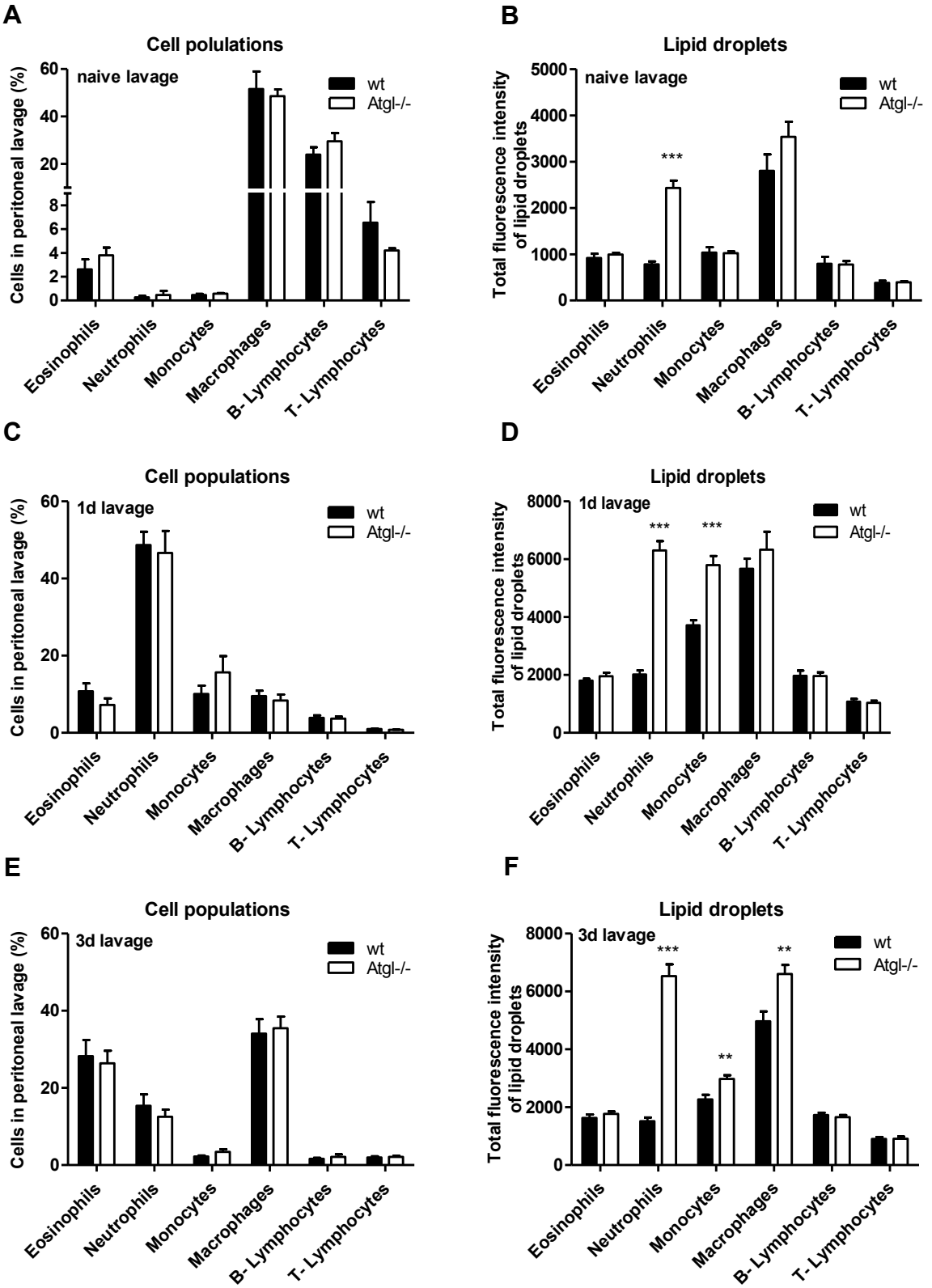
A
Cell polulations
naive lavage
Cells in peritoneal lavage (%)
wt
Atgl-/-
Eosinophils
Neutrophils
Monocytes
Macrophages
B- Lymphocytes
T- Lymphocytes
B
Lipid droplets
naive lavage
Total fluorescence intensity of lipid droplets
***
C
Cell populations
1d lavage
D
Lipid droplets
1d lavage
***
***
E
Cell populations
3d lavage
F
Lipid droplets
3d lavage
***
**
**

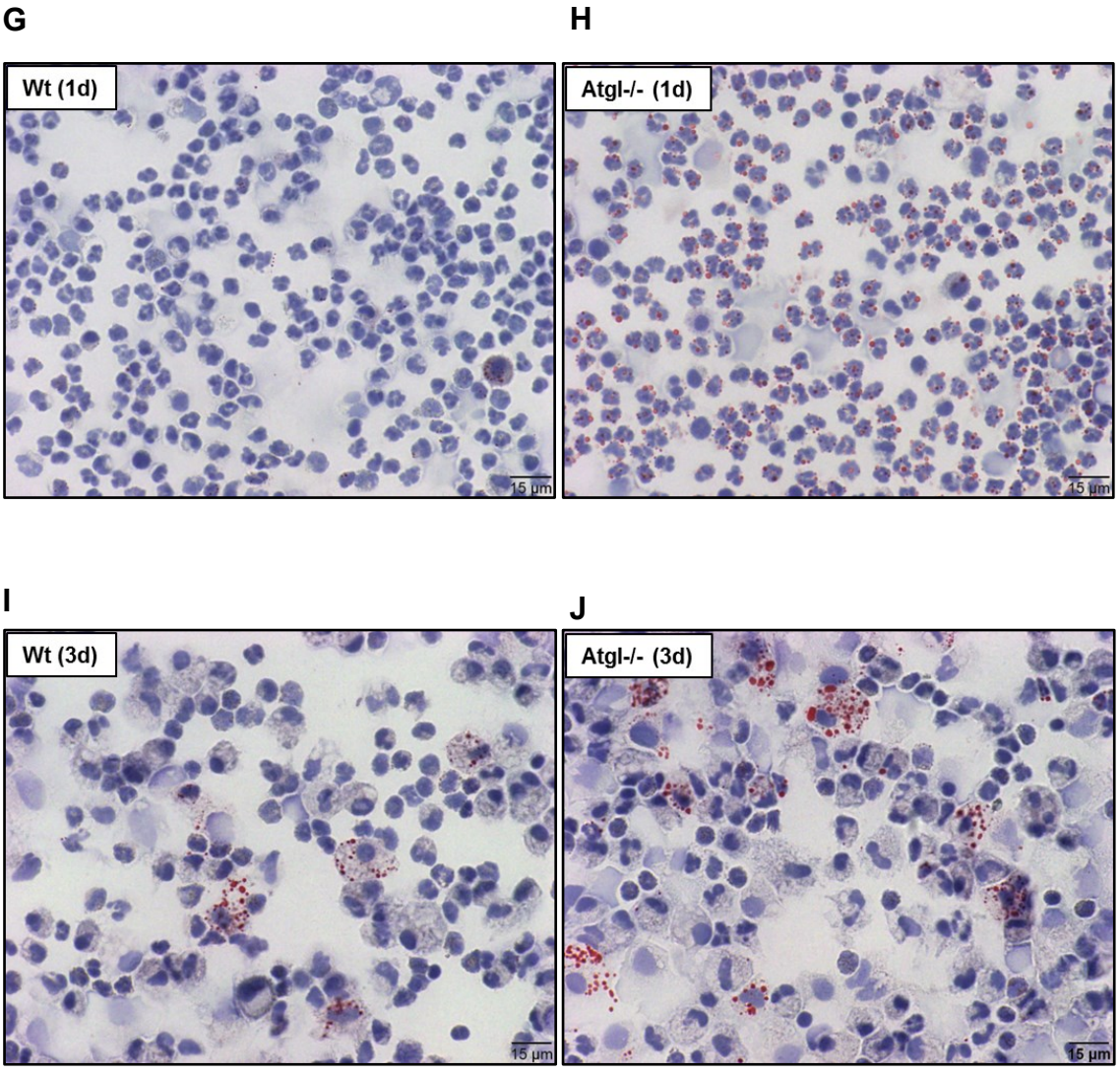

Figure 9: Pronounced accumulation of LDs in Atgl-/- cells under inflammatory conditions

Peritoneal lavage of (A,B) naive, (C,D) one day and (E,F) three day thioglycolate-injected wt and Atgl-/- mice were collected and immunophenotyped using BODIPY493/503 as neutral lipid stain. Data are shown as geometric means of fluorescence intensity + SEM (n=5). **p ≤ 0.01; ***p ≤ 0.001. Intracellular neutral lipids of wt and Atgl-/- peritoneal cells (G,H) one day and (I,J) three days post thioglycolate injection were visualized by ORO/Hematoxylin staining. Representative images of cells are shown. Scale bar: 15 µm.

3.1.3 LD homeostasis in immune cells of myeloid-specific Atgl-/- mice

To elucidate whether the LD accumulation in immune cells of global Atgl-/- mice is caused by cell-specific or systemic lack of ATGL, I also characterized mice with targeted deletion of Atgl in myeloid cells (myeloid Atgl-/-). Compared to Atgl flox mice, myeloid-specific Atgl-/- mice did not show alterations in peripheral blood counts (Fig. 10A). Similar to observations from global Atgl-/- mice with a 3.7-fold increase in LD abundance in peripheral blood neutrophils, myeloid-specific Atgl-/- mice showed a 1.7-fold increase in neutrophil LDs (Fig. 10B).

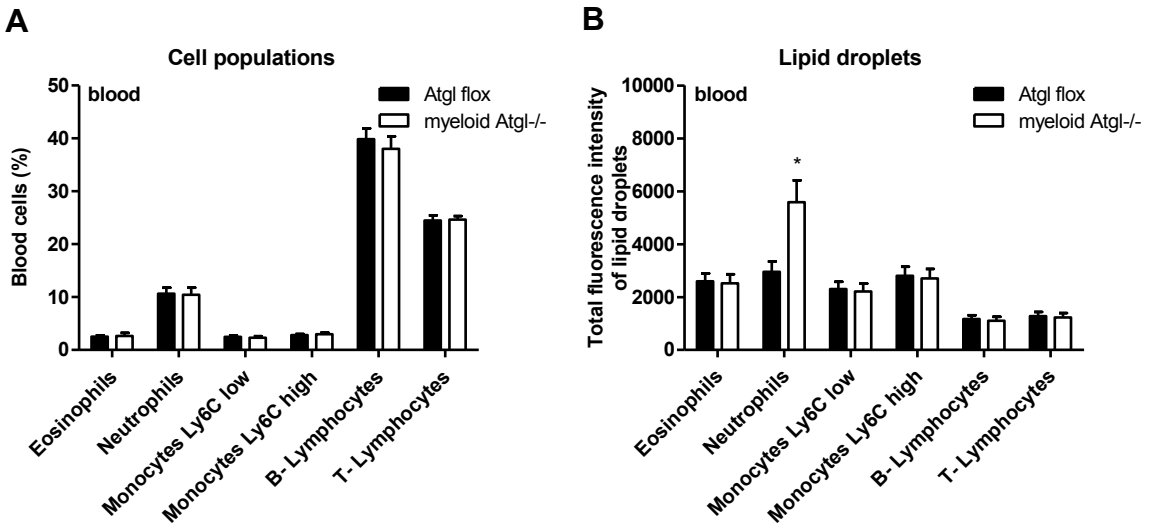

Figure 10: Myeloid-specific Atgl-/- mice accumulate LDs in neutrophils of peripheral blood

(A) Relative counts of peripheral blood cells from Atgl flox and myeloid Atgl-/- mice were determined by immunophenotyping using flow cytometry. (B) LDs in peripheral blood cells were quantified by using BODIPY493/503 as neutral lipid stain. Data are shown as geometric means of fluorescence intensity + SEM (n=5). *$p < 0.05$

Under inflammatory conditions, Atgl flox and myeloid-specific Atgl-/- mice showed an unchanged cellular composition of peritoneal lavages, which were collected three days after thioglycolate injection (Fig. 11A). Cellular LD staining revealed an increased LD abundance exclusively in neutrophils (Fig. 11B), which was of lower magnitude as compared with global Atgl-/- mice (2.2-fold in myeloid Atgl-/- vs. 3.1-fold in global Atgl-/-

mice). In analogy, ORO stainings showed an increased presence of LDs selectively in polymorphnuclear cells (=neutrophils) from myeloid Atgl-/- mice (Fig. 11D), whereas in cells from Atgl flox mice ORO-positive LDs were scarce in all cells (Fig. 11C).

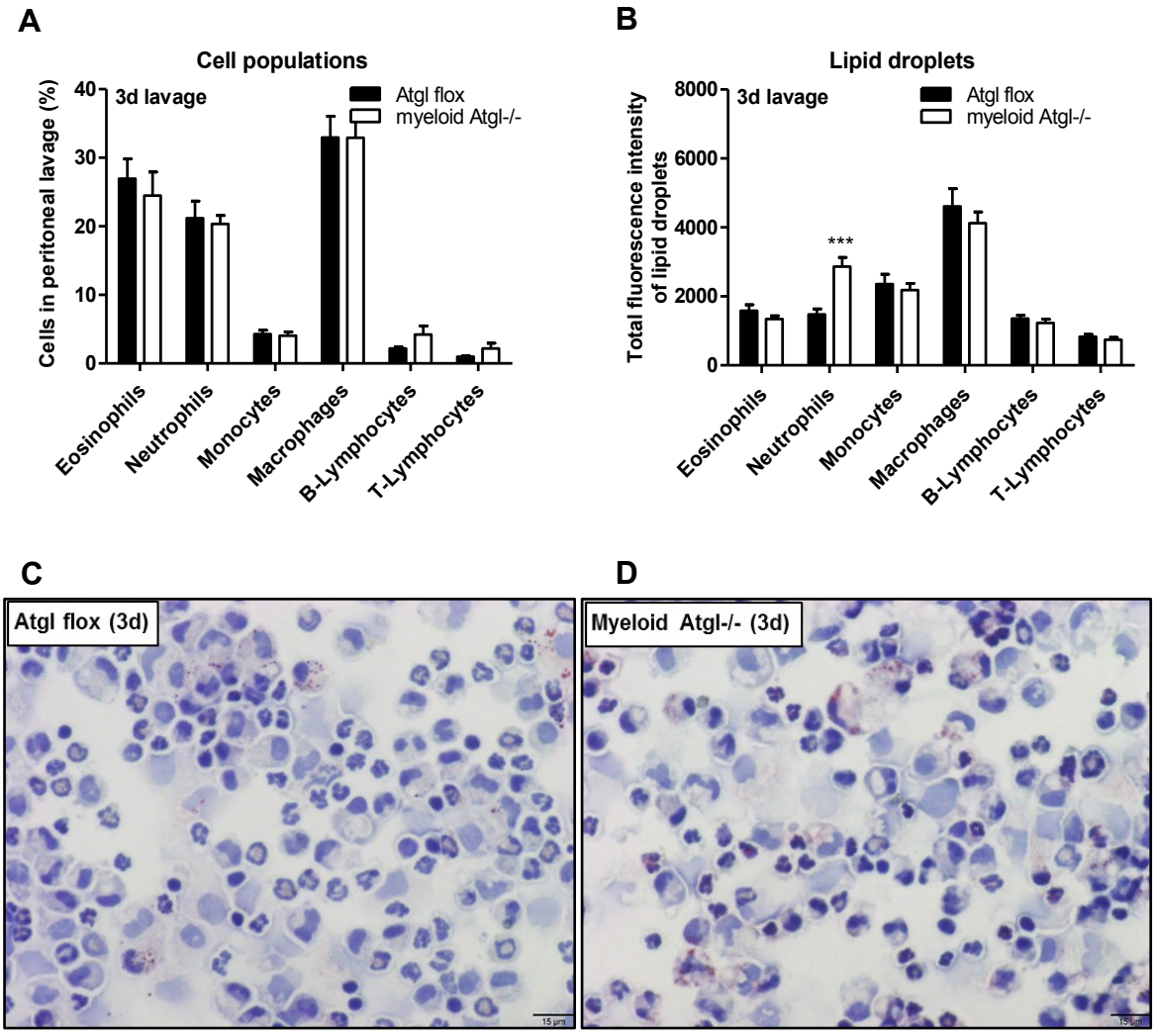

Figure 11: Selective LD accumulation in neutrophils from myeloid Atgl-/- mice under inflammatory conditions

(A,B) Peritoneal lavage of three day thioglycolate-injected Atgl flox and myeloid Atgl-/- mice were collected and immunophenotyped using BODIPY493/503 as neutral lipid stain. Data are shown as geometric means of fluorescence intensity + SEM (n=5). ***p ≤ 0.001. Intracellular neutral lipids of (C) Atgl flox and (D) myeloid Atgl-/- peritoneal cells were visualized by ORO/Hematoxylin staining. Representative images of cells are shown. Scale bar: 15 µm.

3.1.4 LD homeostasis in immune cells of myeloid-specific CGI-58-/- mice

Immunophenotyping of peripheral blood from mice with targeted deletion of CGI-58 in myeloid cells revealed an unchanged blood count (Fig. 12A) and an increased abundance of LDs in peripheral blood neutrophils when compared with CGI-58 flox mice (Fig. 12B).

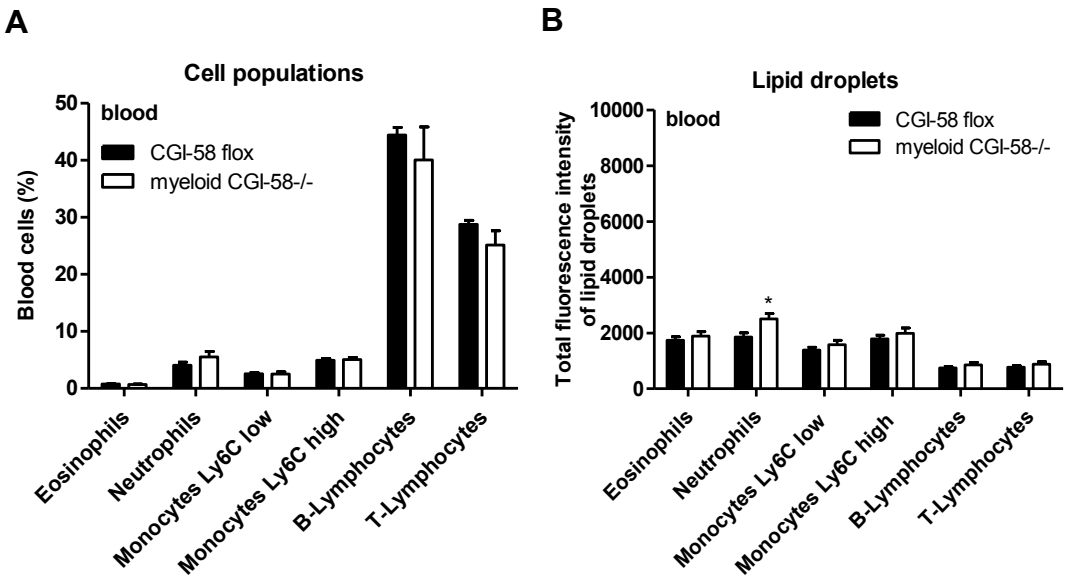

Figure 12: Myeloid-specific CGI-58-/- mice accumulate LDs in neutrophils of peripheral blood

(A) Relative counts of peripheral blood cells from CGI-58 flox and myeloid CGI-58-/- mice were determined by immunophenotyping using flow cytometry. (B) LDs in peripheral blood cells were quantified by using BODIPY493/503 as neutral lipid stain. Data are shown as geometric means of fluorescence intensity + SEM (n=5). *$p < 0.05$

Similar observations were made during the analysis of thioglycolate-induced peritoneal lavages, which were characterized by an unaltered cellular composition (Fig. 13A) and an increased presence of LDs selectively in neutrophils. This was evident by increased fluorescence intensities after BODIPY staining (Fig. 13B) and an increased presence ORO-positive staining in sedimented cells from myeloid-specific CGI-58-/- mice (Fig. 13D) when compared with CGI-58 flox cells (Fig. 13C).

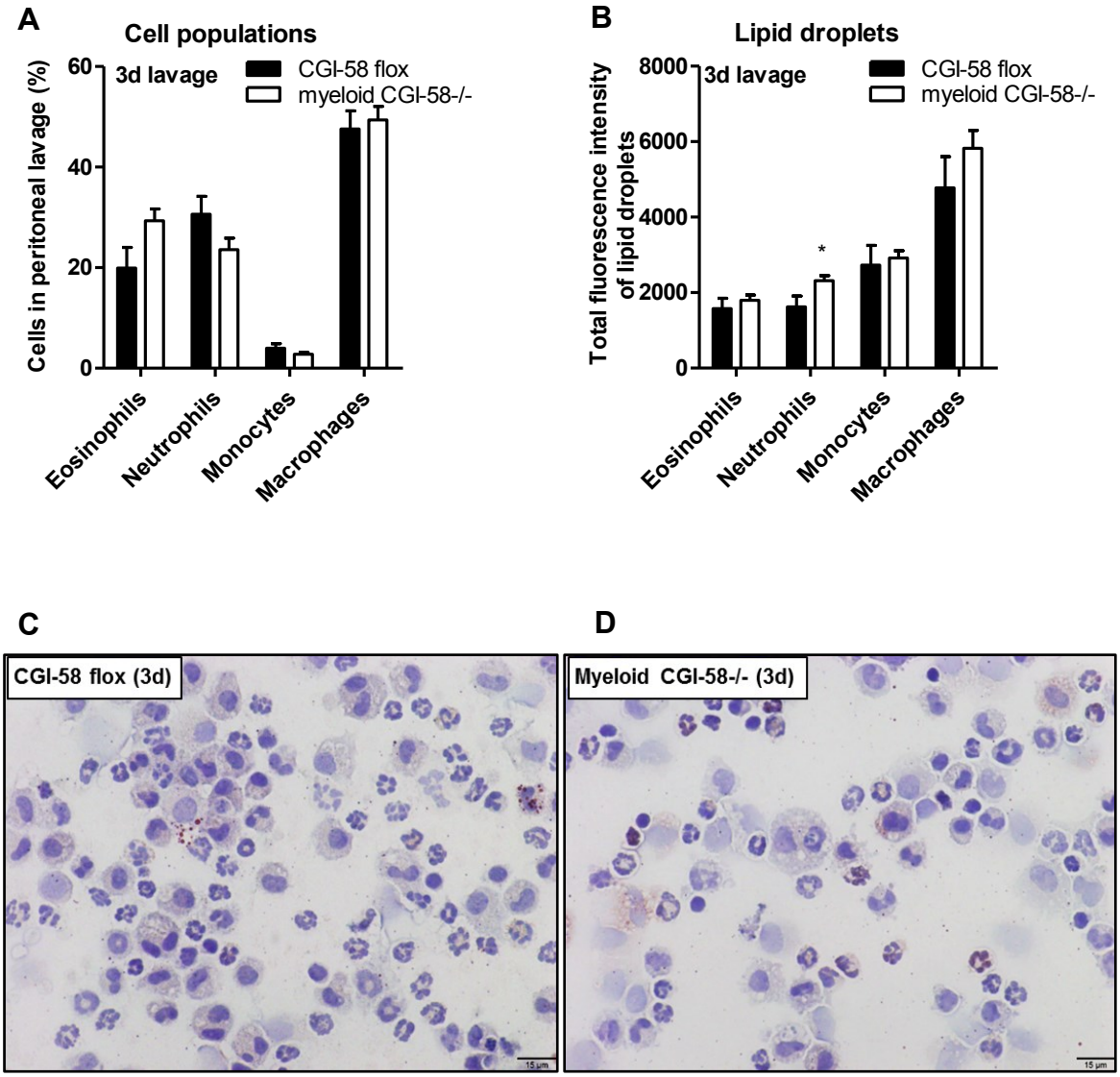

Figure 13: Selective LD accumulation in neutrophils from myeloid CGI-58-/- mice under inflammatory conditions

(A,B) Peritoneal lavage of three day thioglycolate-injected CGI-58 flox and myeloid CGI-58-/- mice were collected and immunophenotyped using BODIPY493/503 as neutral lipid stain. Data are shown as geometric means of fluorescence intensity + SEM (n=5). *$p < 0.05$. Intracellular neutral lipids of (C) CGI-58 flox and (D) myeloid CGI-58-/- peritoneal cells were visualized by ORO/Hematoxylin staining. Representative images of cells are shown. Scale bar: 15 µm.

3.1.5 LD homeostasis in immune cells of Hsl-/- mice

The peripheral blood composition was comparable between wt and Hsl-/- mice (Fig. 14A). Also with respect to LD content in various immune cell populations, I did not observed any differences between cells from wt and Hsl-/- mice (Fig. 14B).

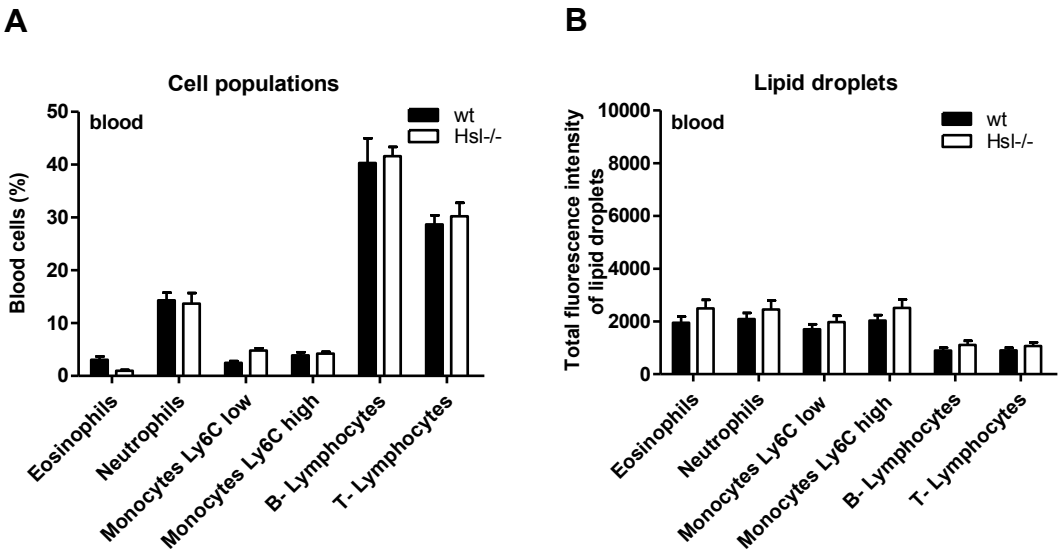

Figure 14: Hsl-/- mice show unaltered LD contents in immune cells from peripheral blood

(A) Relative counts of peripheral blood cells from wt and Hsl-/- mice were determined by immunophenotyping using flow cytometry. (B) LDs in peripheral blood cells were quantified by using BODIPY493/503 as neutral lipid stain. Data are shown as geometric means of fluorescence intensity + SEM (n=5).

Immunophenotyping of peritoneal lavages three days after thioglycolate injection revealed further similarities between wt and Hsl-/- mice, both in terms of cellular composition (Fig. 15A) and LD content (Fig. 15B-D).

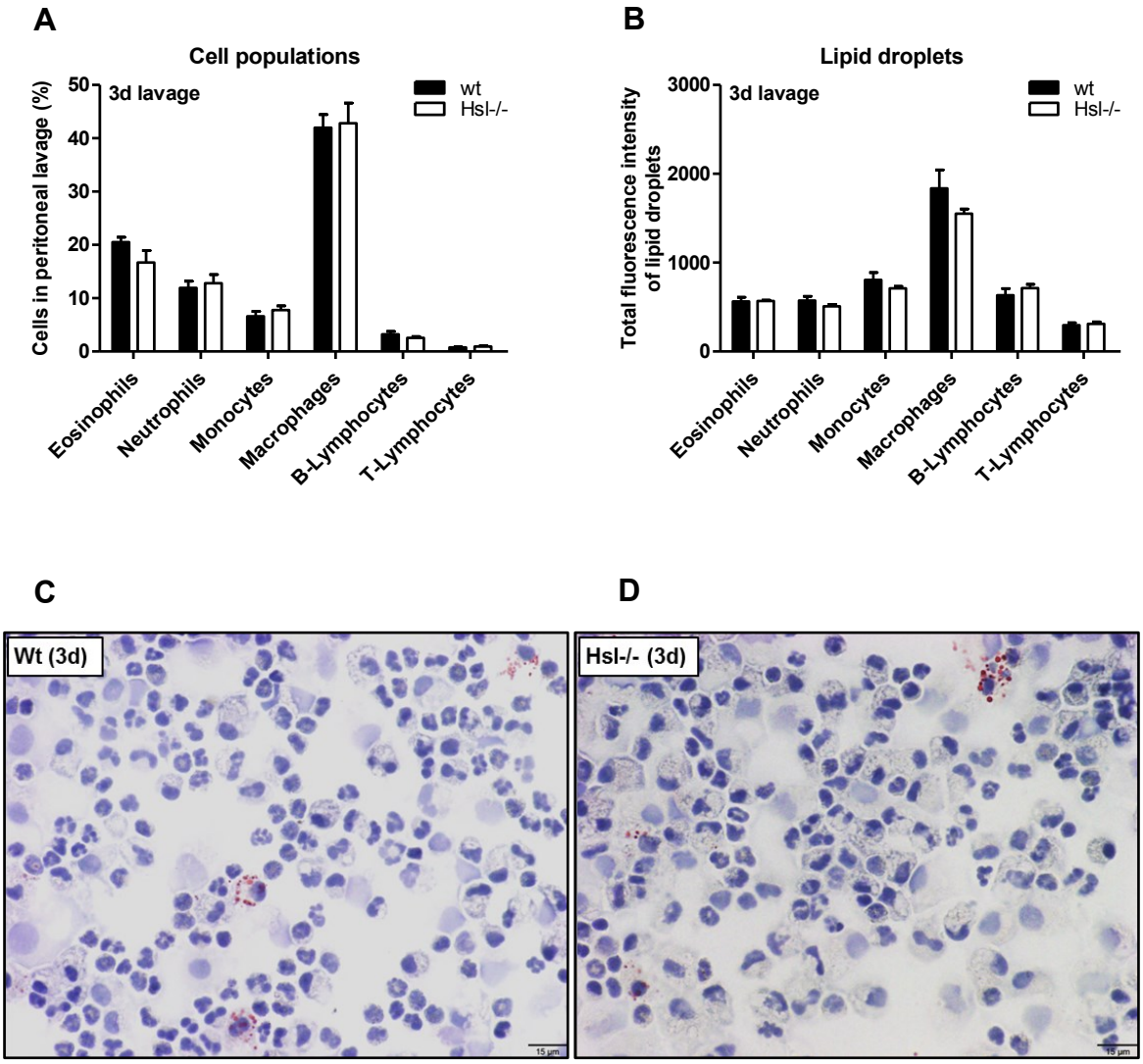

Figure 15: Unaltered LD homeostasis between wt and Hsl-/- mice under inflammatory conditions

(A,B) Peritoneal lavage of three day thioglycolate-injected wt and Hsl-/- mice were collected and immunophenotyped using BODIPY493/503 as neutral lipid stain. Data are shown as geometric means of fluorescence intensity + SEM (n=5). Intracellular neutral lipids of (C) wt and (D) Hsl-/- peritoneal cells were visualized by ORO/Hematoxylin staining. Representative images of cells are shown. Scale bar: 15 µm.

3.1.6 LD homeostasis in immune cells of Mgl-/- mice

In Mgl-/- mice, immunophenotyping of peripheral blood cells revealed no alterations neither in relative composition (Fig. 16A) nor in LD content of the distinct peripheral blood cells investigated (Fig. 16B).

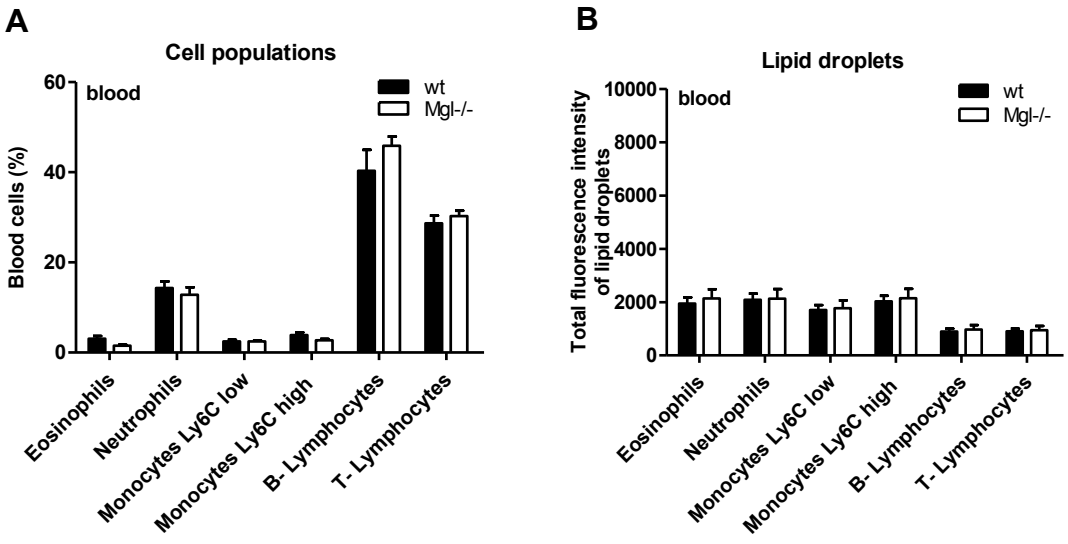

Figure 16: Mgl-/- mice show unaltered LD contents in immune cells from peripheral blood

(A) Relative counts of peripheral blood cells from wt and Mgl-/- mice were determined by immunophenotyping using flow cytometry. (B) LDs in peripheral blood cells were quantified by using BODIPY493/503 as neutral lipid stain. Data are shown as geometric means of fluorescence intensity + SEM (n=5).

Thioglycolate-elicited peritoneal lavages of Mgl-/- mice showed an increased relative abundance of macrophages with a concomitant reduced number of eosinophils (Fig. 17A). Determination of intracellular LD content by flow cytometry (Fig. 17B) or ORO staining (Fig. 17C,D) did not reveal any differences between immune cells of wt and Mgl-/- mice.

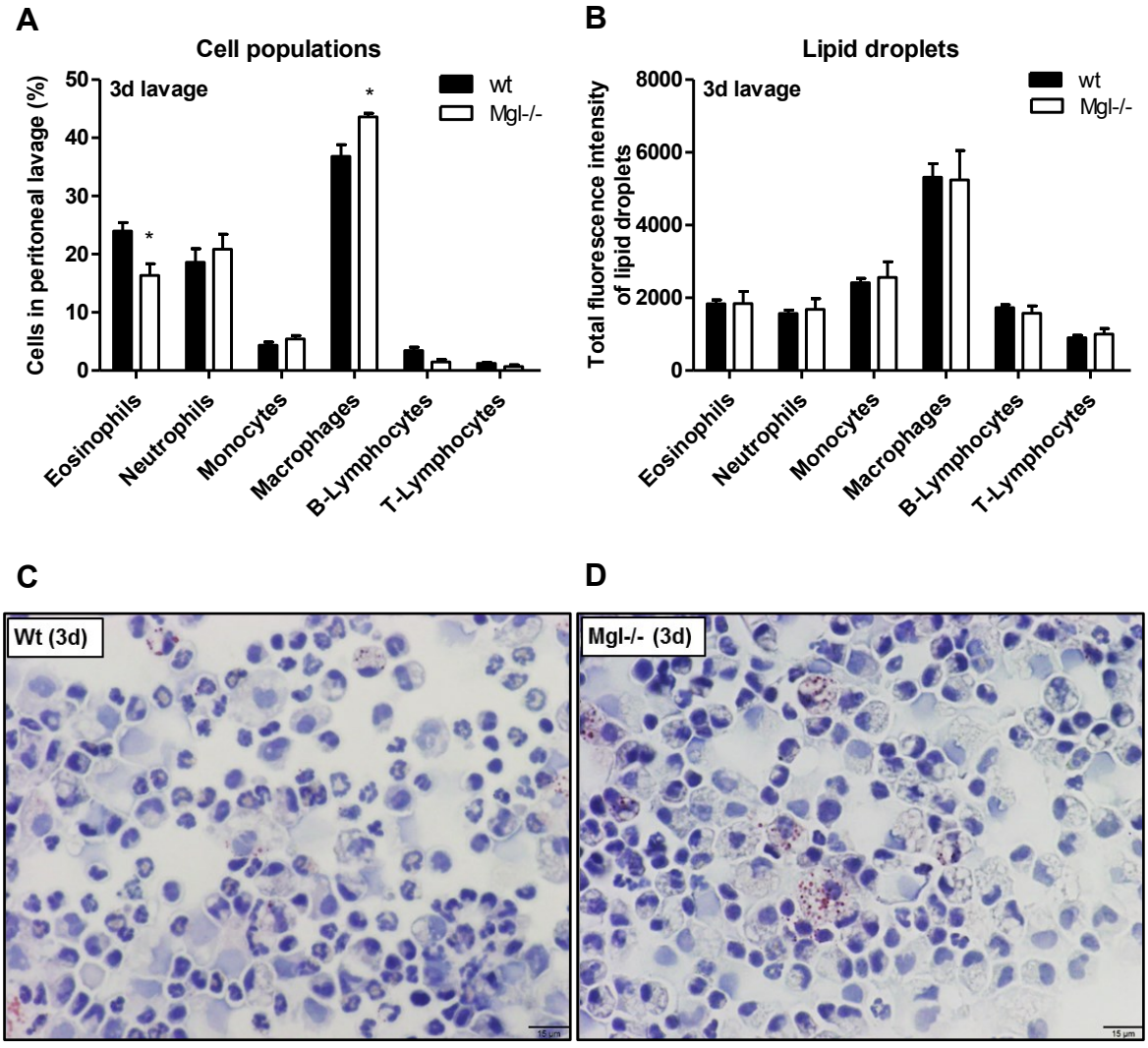

Figure 17: Unaltered LD homeostasis between wt and Mgl-/- mice under inflammatory conditions

(A,B) Peritoneal lavage of three day thioglycolate-injected wt and Mgl-/- mice were collected and immunophenotyped using BODIPY493/503 as neutral lipid stain. Data are shown as geometric means of fluorescence intensity + SEM (n=5). *$p < 0.05$. Intracellular neutral lipids of (C) wt and (D) Mgl-/- peritoneal cells were visualized by ORO/Hematoxylin staining. Representative images of cells are shown. Scale bar: 15 µm.

3.1.7 LD homeostasis in immune cells of Lal-/- mice

In Lal-/- mice, immunophenotyping demonstrated substantial differences in the blood composition with a highly increased abundance of neutrophils and monocytes and reduced numbers of B- and T-lymphocytes compared to wt mice (Fig. 18A). Peripheral blood monocytes, particularly subsets with a low expression profile of Ly6C (Ly6C low) but not of the Ly6C high subset, showed an increased amount of LDs in Lal-/- mice (Fig. 18B).

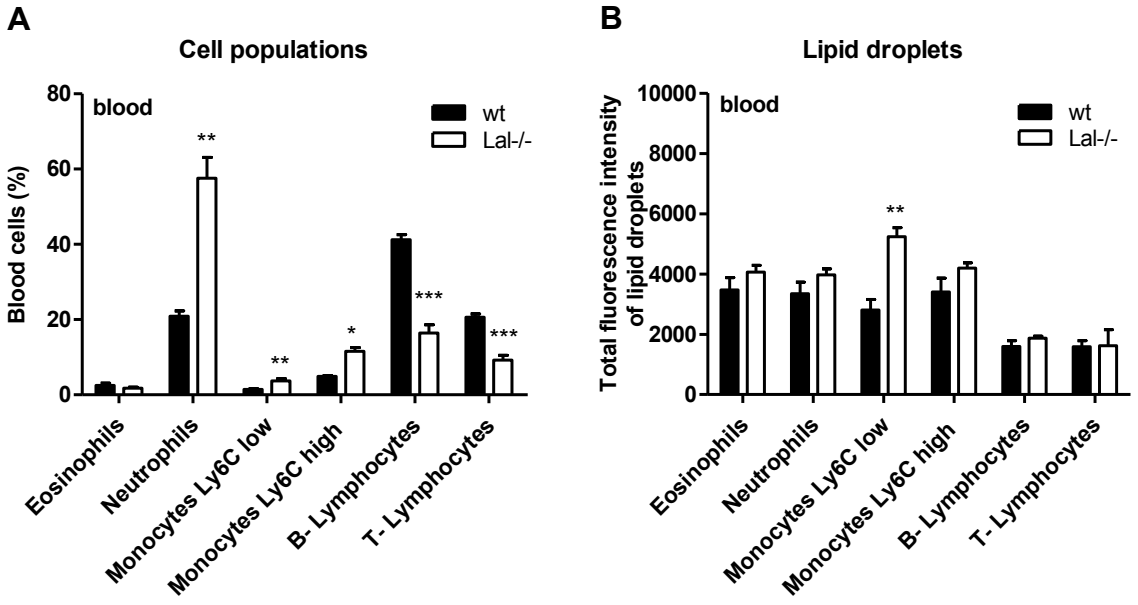

Figure 18: Altered peripheral blood counts and LD accumulation in monocytes from Lal-/- mice

(A) Relative counts of peripheral blood cells from wt and Lal-/- mice were determined by immunophenotyping using flow cytometry. (B) LDs in peripheral blood cells were quantified by using BODIPY493/503 as neutral lipid stain. Data are shown as geometric means of fluorescence intensity + SEM (n=4). *$p < 0.05$; **$p \leq 0.01$; ***$p \leq 0.001$

In response to thioglycolate stimulation, peritoneal lavages showed increased levels of neutrophils and T-lymphocytes in the absence of LAL (Fig. 19A). LD stainings with BODIPY (Fig. 19B) and ORO (Fig. 19C,D) indicated an increased abundance of LDs in macrophages from Lal-/- mice.

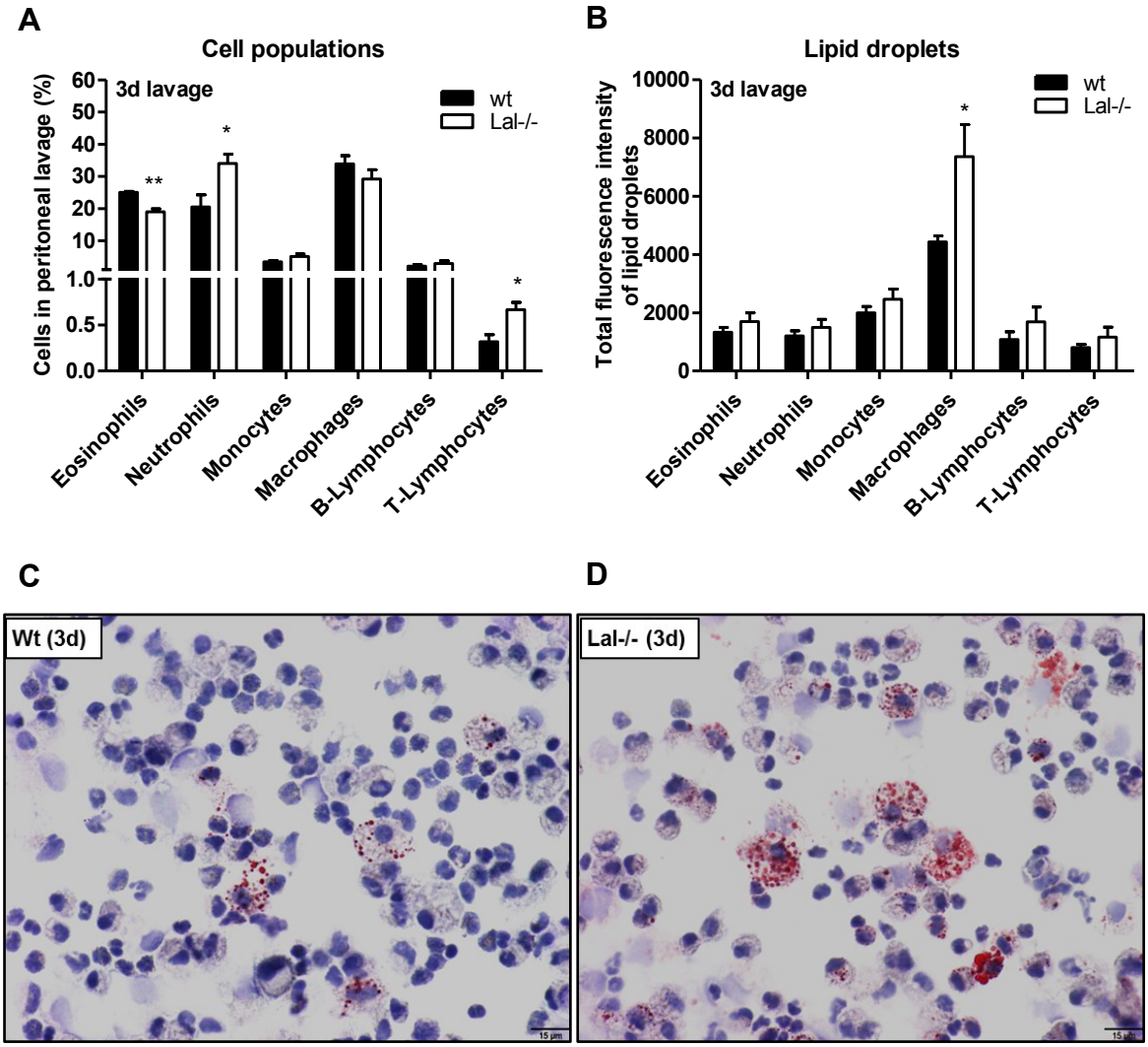

Figure 19: Altered cellular composition and LD content in peritoneal lavages from Lal-/- mice under inflammatory conditions

(A,B) Peritoneal lavage of three day thioglycolate-injected wt and Lal-/- mice were collected and immunophenotyped using BODIPY493/503 as neutral lipid stain. Data are shown as geometric means of fluorescence intensity + SEM (n=3). *$p < 0.05$; **$p \leq 0.01$. Intracellular neutral lipids of (C) wt and (D) Lal-/- peritoneal cells were visualized by ORO/Hematoxylin staining. Representative images of cells are shown. Scale bar: 15 µm.

3.1.8 Discussion

Cytoplasmic and lysosomal hydrolysis of CE and TG require the activity of enzymes such as ATGL, CGI-58, HSL, MGL, and LAL in order to liberate FA for cellular usage. Apart from macrophages with its well described capacity to store high amounts of lipids, also other inflammatory cells, predominantly granulocytes, have been reported to contain intracellular pools of neutral lipids (7). To date, the role of TG-hydrolyzing enzymes in these cells is largely unexplored. By using mouse models with genetic deletions of lipases, either systemic or myeloid-specific, I investigated the functional role of the respective lipases in LD homeostasis of immune cells.

My results show for the first time that thioglycolate-elicited inflammation triggers LD formation in all investigated immune cells. This is evident by an increased amount of LDs in cells from thioglycolate-injected (Fig. 9D,F) as compared with naive lavages (Fig. 9B). Glycosylated proteins in the thioglycolate medium activate receptors for advanced glycation end products (RAGE), which further induce pro-inflammatory responses through NFκB-mediated secretion of cytokines and inflammatory factors (111). This suggests that RAGE-mediated signaling, either directly or indirectly by inducing the generation of pro-inflammatory factors, induces LD generation in leukocytes.

Further, I observed that the systemic loss of ATGL in mice results in an increased abundance of TG-rich LDs specifically in neutrophil granulocytes from bone marrow, peripheral blood and peritoneal lavage under basal conditions. Under inflammatory conditions, lipid accumulation was also observed in monocytes and macrophages but not in eosinophils or lymphocytes. This finding is somehow surprising considering that all immune cells investigated expressed ATGL. Whether eosinophils and lymphocytes require other stimuli to trigger ATGL-mediated functions remains to be investigated.

In contrast to global Atgl-/- mice, mice with targeted deletion of ATGL in myeloid cells show LD accumulation exclusively in neutrophils, both under basal and inflammatory conditions. These findings indicate that lipid accumulation in monocytes and macrophages of global Atgl-/- mice is likely triggered by secondary effects due to systemic ATGL deficiency.

Mice lacking the ATGL co-factor CGI-58 in myeloid cells show a similar phenotype as myeloid-specific Atgl-/- mice with a selective LD accumulation in neutrophils, both from blood and thioglycolate-elicited lavages.

Clinical reports from patients with mutations in ATGL describe an analogous phenotype to global Atgl-/- mice: they suffer from massive TG accumulation in multiple tissues and develop severe myopathy resulting in cardiac insufficiency and premature death in Atgl-/- mice starting with the age of ~12 weeks and cardiac transplantation in humans (112). Patients with defective CGI-58 develop ichthyosis, a skin barrier defect that is also observed in global CGI-58-/- mice. In mice, the skin defect is even more severe and causes premature death soon after birth. A common manifestation in patients with mutations in either ATGL or CGI-58 is Jordans' anomaly, which has been described to affect various immune cells, such as neutrophils, eosinophils, monocytes and lymphocytes (113, 114). In accordance, I observed that Atgl-/- and CGI-58-/- mice exhibit Jordans' anomaly in certain cell types, which can be triggered e.g. by inflammation. This indicates that ATGL-mediated lipolysis in immune cells is not only highly cell-specific but also a condition-dependent process.

The findings that HSL and MGL deficiency did not affect LD homeostasis argue for a minor role of these lipases in immune cells under the experimental conditions investigated. HSL was previously shown to hydrolyze various substrates, including TG, DG, MG, CE, and RE (51, 52), whereas MGL predominantly cleaves MGs (115). Whether a deficiency of these lipases in immune cells causes an accumulation of the respective substrate lipid species was not investigated here and requires a more sensitive lipid analysis, e.g. lipid mass spectrometry.

LAL was shown to be a highly abundant enzyme in macrophages, fibroblasts, lymphocytes, and hepatocytes (116). A major manifestation in Lal-/- mice is the increased lysosomal TG and CE accumulation in macrophages within multiple organs, including Kupffer cells, bronchoalveolar macrophages, and intestinal macrophages (117). In patients with LAL deficiency, the presence of lipid-loaded macrophages in the bone marrow and vacuolated peripheral blood lymphocytes were reported (118). In this study I revealed an increased abundance of LDs in peripheral blood monocytes in Lal-/- mice, mainly in Ly6C low monocytes. Further, these mice suffered from neutrophilia and highly

reduced peripheral lymphocyte levels. This observation is in agreement with extensive studies from Hong Du et al., showing that LAL is critical for lymphoid and myeloid progenitor development and function (119). Peritoneal thioglycolate-induced lavages showed an altered cellular composition with an increase in neutrophils and T-lymphocytes. Macrophage numbers were unaltered under these conditions but showed an elevated accumulation of LDs. Unlike Atgl-/- mice, where LD accumulation is observed in the cytoplasm of cells, Lal-/- macrophages, due to their inability to hydrolyze lysosomal lipids, accumulate lipids derived from endocytosis of lipoproteins within lysosomes. Together, these findings implicate an important role for LAL-mediated lysosomal degradation, which, among various immune cells, seems to be an active process predominantly in macrophages. However, it remains elusive whether lipophagy is active in immune cells and if to which extent LAL deficiency has an impact on lysosomal degradation of LDs in these cells.

In conclusion, cytosolic and lysosomal TG hydrolases are expressed in immune cells and play an important role in maintaining lipid homeostasis in these cells. Our observations obtained from mouse models with genetic ablation of lipases show a lipid accumulation phenotype in distinct immune cell types with cells from the myeloid lineage being mostly affected. These findings argue that the functional role of TG hydrolases may be highly cell type- and condition-dependent. By controlling the release of lipid molecules and their metabolic derivatives in immune cells, I suggest that TG hydrolases have immunoregulatory functions.

3.2 Functional consequences of ATGL deficiency in neutrophils

3.2.1 Increased FA uptake in neutrophils lacking ATGL

To assess whether the observed increased presence of LDs due to ATGL deficiency is caused solely by the lipolytic defect or whether also an increased cellular uptake or synthesis of lipids contribute to this phenotype, I investigated the sensitivity of wt, global, and myeloid-specific Atgl-/- neutrophils to extracellular FAs (Fig. 20A,B). After 10 min exposure to fluorescently-labeled FAs, Atgl-/- neutrophils (from global and myeloid-specific Atgl-/- mice) showed a ~ 3-fold increased uptake of FAs compared to control cells as measured by flow cytometry.

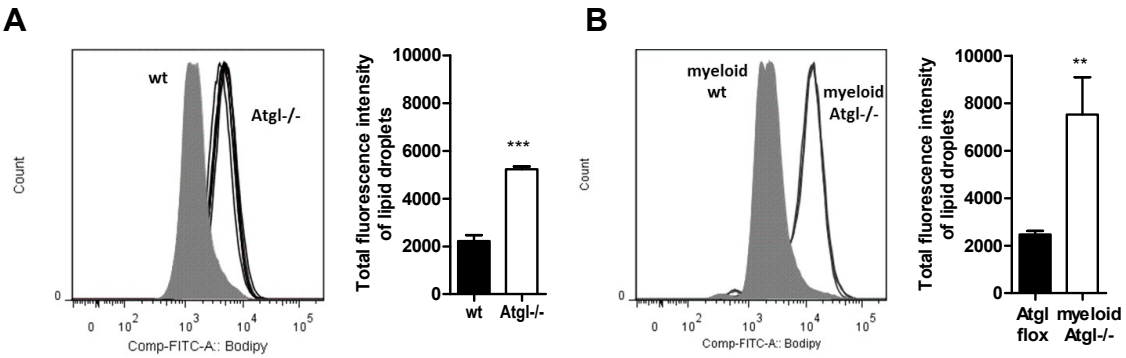

Figure 20: Increased FA uptake in neutrophils lacking ATGL

Uptake of BODIPY-labeled FAs by neutrophils from (A) wt and Atgl-/- and (B) Atgl flox and myeloid Atgl-/- was determined as total fluorescence intensities by flow cytometry and is expressed as means + SEM (n=6). **p ≤ 0.01; ***p ≤ 0.001

To further elucidate the mechanism(s) accounting for LD accumulation in Atgl-/- neutrophils, key enzymes involved in FA uptake (Cd36), synthesis (Acc, Fasn, Scd1) and FA β-oxidation (Cpt1α) were determined by quantitative PCR (Fig. 21A). Relative mRNA levels of Cd36 and Cpt1α were unchanged, whereas Acc, Fasn, and Scd1 showed reduced transcript levels in neutrophils from global Atgl-/- mice. Further, I explored whether the expression of other lipases and proteins regulating lipolysis are altered in neutrophils lacking ATGL. These analyses revealed absent mRNA levels of Atgl, reduced expression of Hsl, and unchanged mRNA expression of Mgl, G0S2, and CGI-58 in neutrophils from Atgl-

/- compared to wt mice (Fig. 21B). ATGL deficiency was shown to modulate PPARα target gene expression in liver and heart (120, 121). I therefore determined the expression of various PPAR target genes, including Dgat1, Dgat2, iNos, Mmp9 and Noxa1, which showed comparable expression levels between neutrophils from wt and Atgl-/- mice (Fig. 21C).

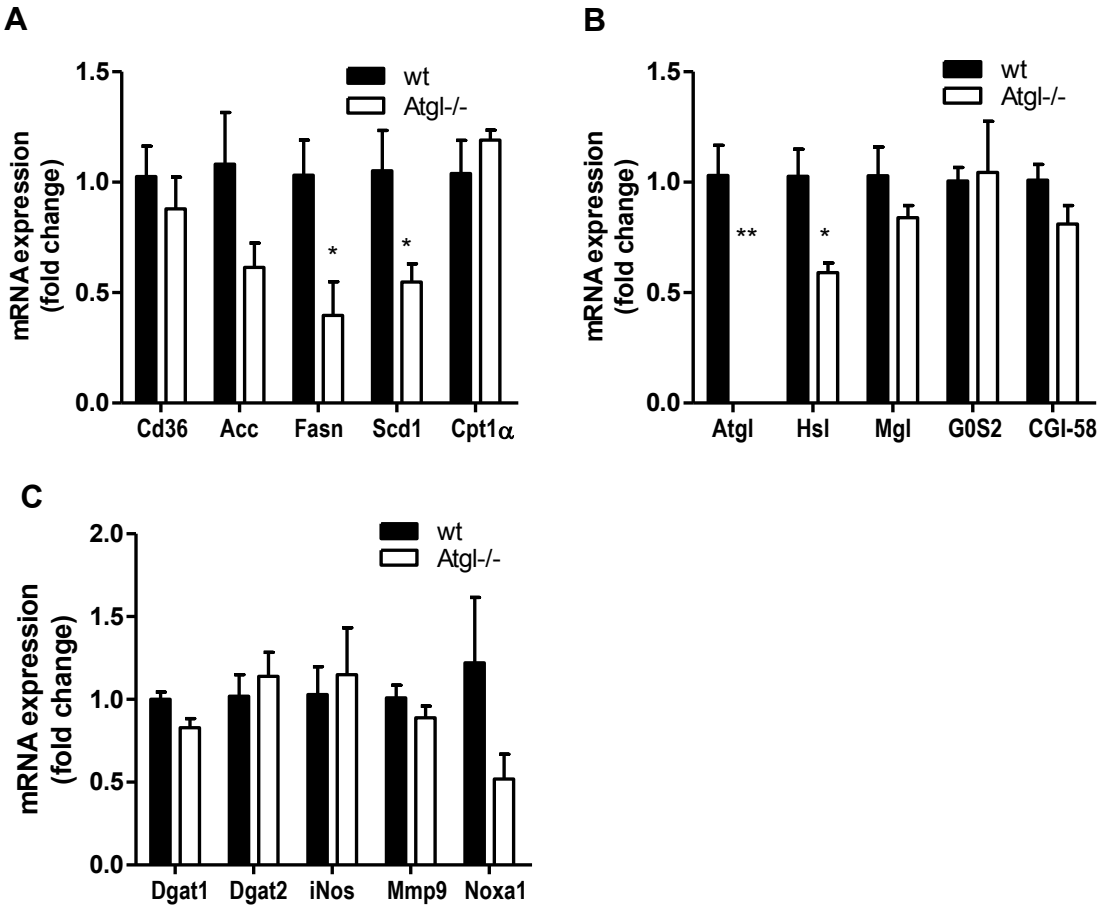

Figure 21: Gene expression in purified neutrophils from wt and Atgl-/- mice

mRNA expression of (A) FA uptake and synthesis genes, (B) lipases and lipolysis-regulating genes, and (C) PPAR target genes were determined in flow-sorted neutrophils from wt and Atgl-/- mice by real-time PCR, including normalization to Gapdh. Data are presented as mean values (n=4) performed in duplicate + SEM. *$p < 0.05$; **$p \leq 0.01$

Summarized, these gene expression data suggest that ATGL deficiency in neutrophils is accompanied with reduced Hsl expression, possibly due to the lack of substrates generated by ATGL. Further, the reduced expression of Acc, Fasn, Scd1 and the

unchanged expression of Dgat enzymes indicate that the LD accumulation in Atgl-/- neutrophils is not caused by an increased FA or TG synthesis but results from an increased FA uptake from extracellular sources. The mechanism of cellular FA uptake is likely not Cd36-mediated as gene expression levels of Cd36 are unchanged in Atgl-/- neutrophils. Finally, unlike in other cells and tissues, PPAR signaling, at least under the tested conditions here, is not affected in neutrophils lacking ATGL.

3.2.2 Agonist-induced Ca^{2+} flux and chemotaxis are increased in Atgl-/- neutrophils

Of particular interest was to examine the functionality of LD-rich Atgl-/- neutrophils. Therefore, I determined agonist-induced intracellular Ca^{2+} flux and chemotaxis. As agonists, I used the bacterial peptide fMLP and the neutrophil-specific chemoattractant KC (also known as Gro-α or CXCL1). Compared with wt cells, which reached a maximal Ca^{2+} response of ~230% over baseline, I observed an enhanced mobilization of intracellular Ca^{2+} by > 300% in Atgl-/- neutrophils with fMLP concentrations ranging from 1-5 µM (Fig. 22A). KC (5 and 50 µM) induced an even higher response in Atgl-/- cells with peak values of 369% and 447% over baseline in wt and Atgl-/- neutrophils, respectively (Fig. 22A). Next, we examined the cellular phenotype of Atgl-/- cells by measuring *in vitro* migration. These studies revealed that neutrophils from Atgl-/- mice possessed increased chemotactic properties towards both tested agonists compared with wt neutrophils (Fig. 22B). As another marker for neutrophil activation, agonist-induced CD11b expression was determined by flow cytometry. fMLP- and KC-mediated stimulation showed a slight, yet non-significant trend for an increased activation in Atgl-/- neutrophils (Fig. 22C). By using PMA to achieve a maximal and robust activation of neutrophils I found an increased responsiveness in Atgl-/- compared with wt cells (Fig. 22C).

Next, I addressed whether the lack of ATGL affects phagocytosis and ROS production of neutrophils. *In vitro* phagocytosis assays revealed comparable phagocytosis rates between neutrophils from wt and Atgl-/- mice (Fig. 22D). Simultaneously, I measured intracellular ROS formation following synchronized phagocytosis of *E.coli* particles as well as ROS production in response to KC and fMLP. All conditions tested showed comparable fluorescence intensities, indicating unchanged ROS concentrations (Fig. 22E). Moreover, I assessed apoptosis under various conditions (after 6 and 18 h of cultivation), which was

unaltered between wt and Atgl-/- neutrophils as annexinV/propidium iodide staining revealed the same amount of alive, early and late apoptotic as well as necrotic cells (Fig. 22F).

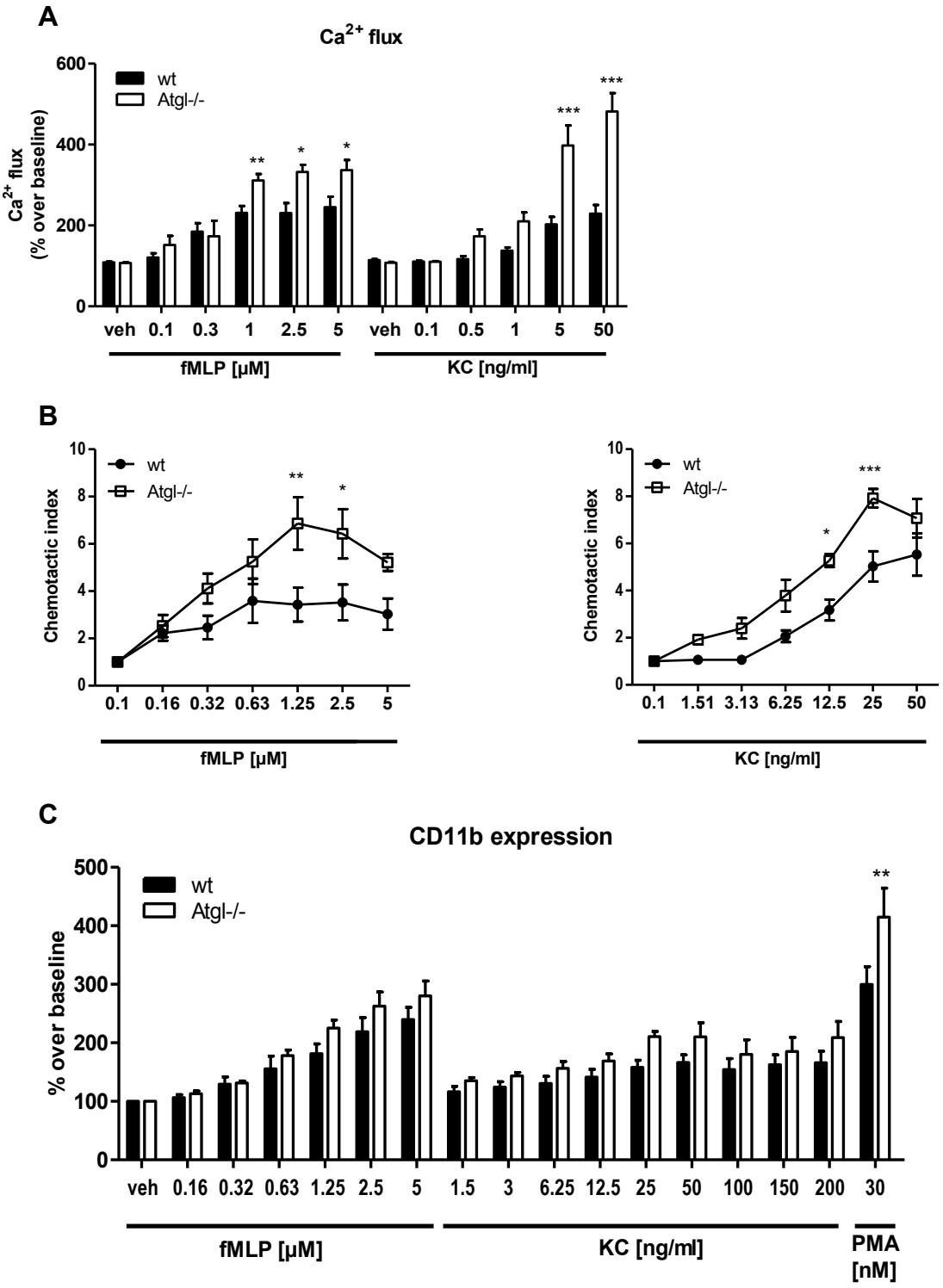

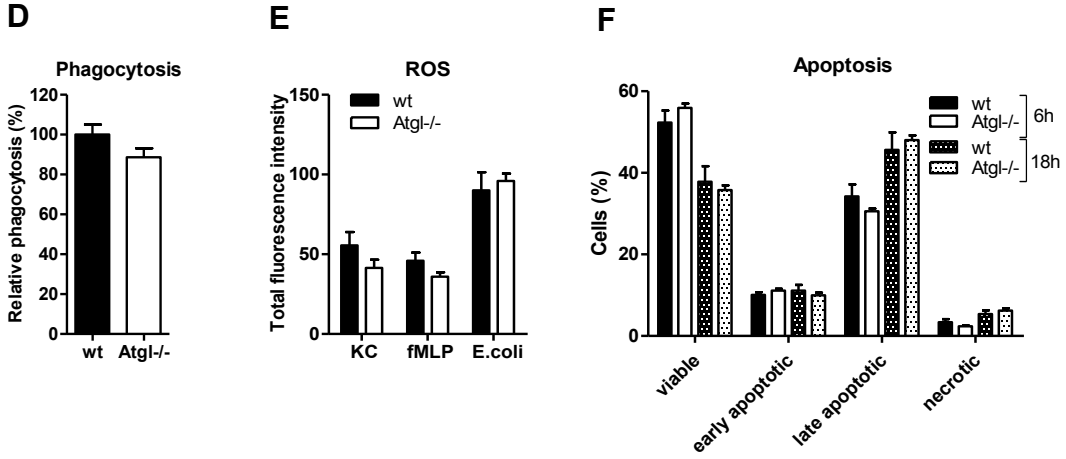

Figure 22: Ca^{2+} flux and chemotaxis are increased in Atgl-/- neutrophils

Activity of neutrophils from wt and Atgl-/- mice was tested *in vitro* by (A) Ca^{2+} flux and (B) chemotaxis assays in response to fMLP and KC. (n=5). (C) Agonist-induced CD11b surface expression of wt and Atgl-/- neutrophils was analyzed. Data are shown as -fold change relative to vehicle-treated control cells + SEM (n=6-12). (D) Phagocytosis of fluorescein-conjugated *E.coli* particles by wt and Atgl-/- neutrophils. Phagocytosis of wt cells was arbitrarily set to 100%. Data are presented as mean values (n=9-10) + SEM. (E) ROS staining after incubation of neutrophils for 20 min with KC (20 ng/ml), fMLP (1 µM) and during 1 h exposure to *E.coli* particles. Data are shown as geometric means of fluorescence intensity + SEM (n=5). (F) Apoptosis of wt and Atgl-/- neutrophils after 6 h and 18 h of culture. Quantifications of the total amount of annexin V-positive (early apoptotic), annexin V/propidium iodide-positive (late apoptotic), and propidium iodide -positive (necrotic) cells are shown as means (n=5) + SEM. $*p < 0.05$; $**p \leq 0.01$; $***p \leq 0.001$

3.2.3 Similar but less pronounced phenotype in myeloid-specific Atgl-/- mice

To elucidate whether the alterations observed in functional assays are caused by systemic or specific ATGL deficiency in neutrophils, I also assessed the functional properties of neutrophils from myeloid-specific Atgl-/- mice. Ca^{2+} flux assays with neutrophils isolated from myeloid-specific Atgl-/- mice using fMLP and KC as agonists showed a comparable response as wt cells (Fig. 23A). Chemotaxis was increased in response to fMLP but comparable to wt cells after KC stimulation (Fig. 23B). Similar to neutrophils from global Atgl-/-, I found no alterations in phagocytosis (Fig. 23C) and ROS formation (Fig. 23D). Together, these observations indicate a similar, yet less pronounced phenotype in neutrophils from myeloid-specific versus global Atgl-/- mice.

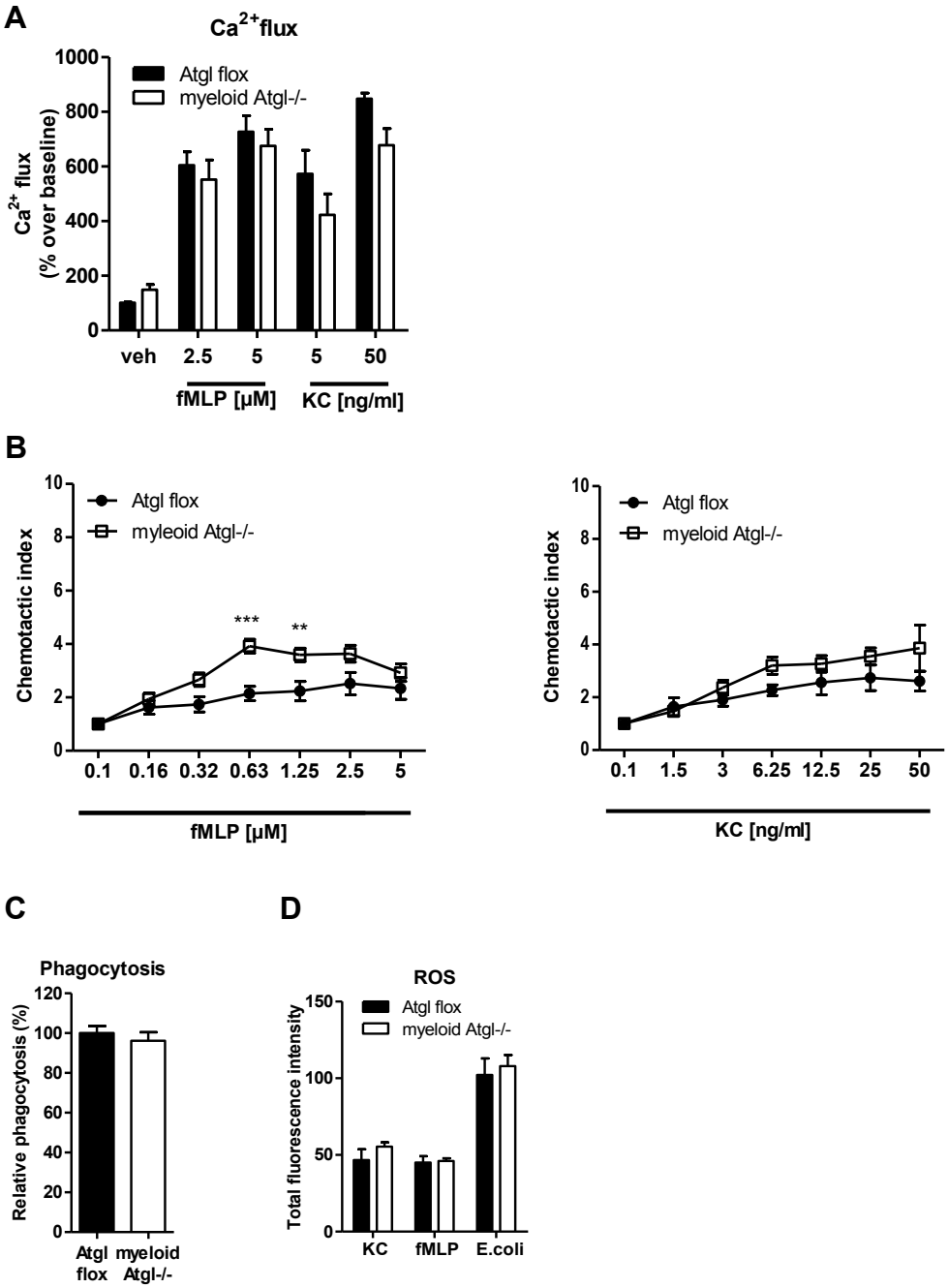

Figure 23: Unchanged Ca^{2+} flux and moderately increased chemotaxis in neutrophils from myeloid-specific Atgl-/- mice. Activity of neutrophils from Atgl flox and myeloid-specific Atgl-/- mice was tested *in vitro* by (A) Ca^{2+} flux and (B) chemotaxis assays in response to fMLP and KC. (n=5). Data are shown as -fold change relative to vehicle-treated control cells ± SEM (n=5). (C) Phagocytosis and (D) ROS measurements were performed as described above. (n=5). **p ≤ 0.01; ***p ≤ 0.001

3.2.4 Altered plasma cytokine concentrations in global and myeloid-specific Atgl-/- mice

To evaluate whether an altered release of inflammatory mediators causes the observed pro-inflammatory as well as the distinct phenotypes of global and myeloid-specific Atgl-/- mice, I determined plasma cytokine levels (Fig. 24). Therefore, cytokine arrays allowing for the detection of 32 cytokines were performed with pooled plasma samples. Quantification of the arrays revealed a similar cytokine profile between global and myeloid-specific Atgl-/- mice. Increased levels of the cytokines IL-5, IL-6, IL-9, MCP-5, MIP-1α, MIP-2, and MIP-3β were observed in both mouse models lacking ATGL. The cytokines, which were highest in both genotypes, were MIP-1α with an increase of 2.1-fold and 2.3-fold and MIP-2 with an increase of 1.6-fold and 2.3-fold in plasma from global and myeloid-specific Atgl-/- mice, respectively. Surprisingly, other well-established pro-inflammatory cytokines such as TNFα, KC or MCP-1 showed reduced concentrations in plasma from both genotypes. Interferon-γ (IFN-γ) was found to be reduced in myeloid-specific but not global Atgl-/- mice. Increased levels of MCP-5 (7-fold) were observed in plasma from myeloid-specific Atgl-/- mice and, to a lesser extent, in global Atgl-/- mice (1.4-fold). Further, the classical anti-inflammatory IL-4 was detected in reduced levels in plasma from both global and myeloid-specific Atgl-/- compared to wt mice.

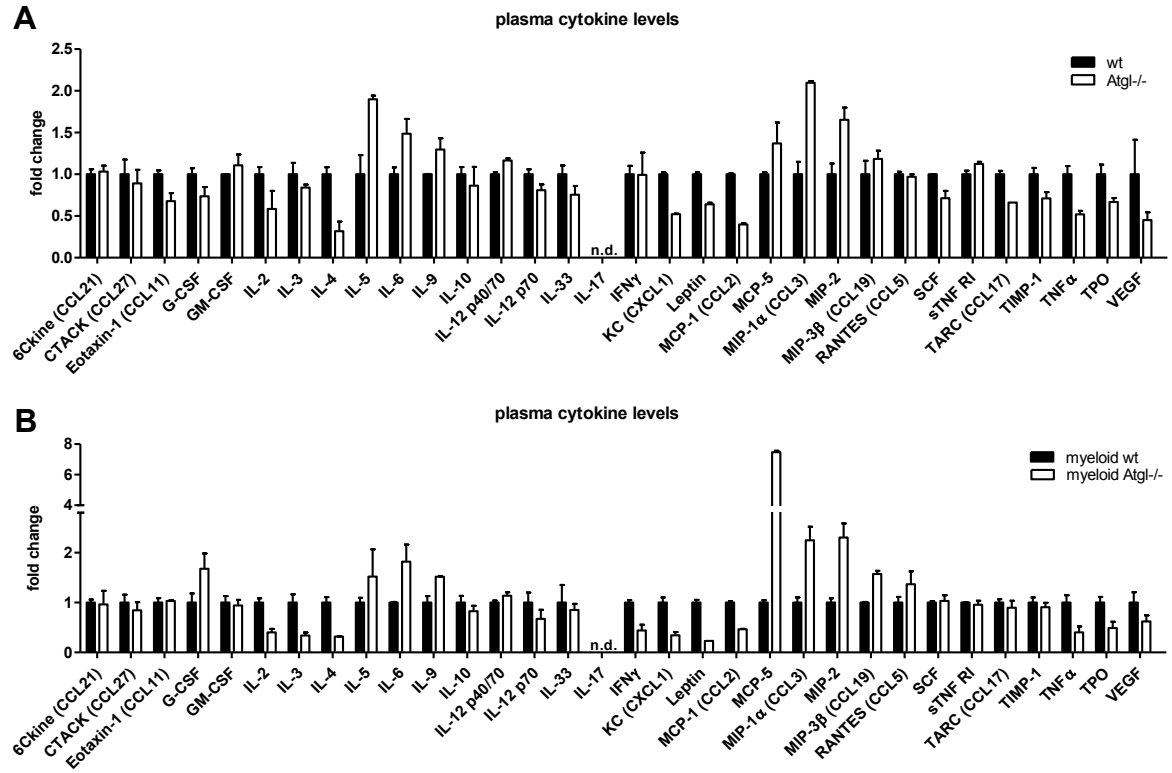

Figure 24: Plasma cytokine levels in global and myeloid-specific Atgl-/- mice

Plasma cytokine levels in (A) global and (B) myeloid-specific Atgl-/- mice were determined by plasma cytokine arrays. Plasma samples (pooled in an equal amount from 6 individual mice of each group) were incubated with membranes spotted in duplicates with antibodies against 32 cytokines (n=2). The intensity of each spot on the arrays was quantified and the data are shown as fold change to ctrl mice + SEM. n.d., not detectable

Taken together, a similar plasma cytokine profile was observed in global and myeloid-specific Atgl-/- mice showing an increased release of distinct pro-inflammatory cytokines in the absence of ATGL, predominantly of macrophage inflammatory proteins (MIPs). LDs in inflammatory cells were shown to be induced when exposed to distinct cytokines *in vivo* and *in vitro* (see Table 1). So far, the capability for MIP-1 and -2 to induce LDs in immune cells has never been investigated. Hence, our next aim was to reveal whether MIP-1 and -2 are able to trigger the formation of LDs in neutrophils, which, in the case of ATGL deficiency, cannot be catabolized and therefore results in the observed lipid accumulation. To elucidate this under conditions regardless of potential systemic effects caused by ATGL deficiency, I used a pharmacological approach to inhibit ATGL in wt neutrophils. Recently, Atglistatin, a specific ATGL inhibitor was developed (122). Since

Atglistatin has never been tested on immune cells, I first determined its efficacy to inhibit ATGL in neutrophils.

3.2.5 Atglistatin inhibits ATGL in neutrophils

By using thioglycolate-elicited neutrophils collected from wt mice one day after injection, I determined whether Atglistatin effectively inhibited ATGL in these cells. First, I induced LD formation by loading wt neutrophils with 300 µM OA (18:1) after which the cells were cultured in starvation medium in the absence and presence of Atglistatin. After 4 h and 6 h of starvation, I quantified LDs and observed an increased LD content in the presence of Atglistatin (Fig. 25A). These results indicate that the inhibitor blocks FA mobilization, which consequently results in TG accumulation. The combined use of Atglistatin and the HSL inhibitor Hi 76-0079 tended to further promote accumulation of LDs in neutrophils. Similar results were observed after loading neutrophils with 300 µM AA (20:4) (Fig. 25B). Together, these observations indicate that Atglistatin effectively inhibits ATGL in neutrophils.

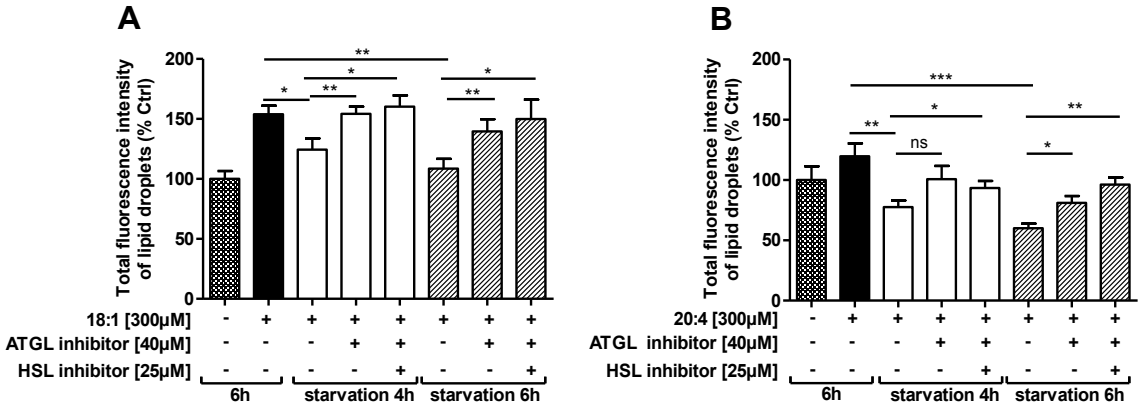

Figure 25: Neutrophil LD catabolism is blocked by the ATGL inhibitor Atglistatin

Wt neutrophils collected from peritoneal lavages one day post thioglycolate injection were incubated in culture medium supplemented with 300 µM (A) OA (18:1) or (B) AA (20:4) for 6 h, after which the medium was replaced by serum-free DMEM containing ATGL or ATGL/HSL inhibitors. After 4 h and 6 h of starvation, LDs were quantified by flow cytometry. Fluorescence intensities are expressed as percentages of untreated control cells + SEM (n=6-7). *$p < 0.05$; **$p \leq 0.01$; ***$p \leq 0.001$

3.2.6 Absent LD induction by MIP-1 and -2 in pharmacologically inhibited neutrophils

In order to assess whether elevated MIP-1 and MIP-2 plasma cytokine levels are causative for the observed LD accumulation in Atgl-/- neutrophils, I tested the ability of these cytokines to induce LD generation in neutrophils. Therefore, I cultured neutrophils from wt mice *ex vivo* in the absence and presence of Atglistatin and recombinant MIP-1 and MIP-2 (Fig. 26). Atglistatin-mediated ATGL inhibition resulted in a significantly elevated abundance of LDs when compared to neutrophils cultured without inhibitor. After 5 h of treatment with either MIP-1 or MIP-2, there was no increase in LD content in neutrophils, neither in the presence nor in the absence of Atglistatin treatment. This finding indicates that these cytokines are not able to induce LD formation in neutrophils.

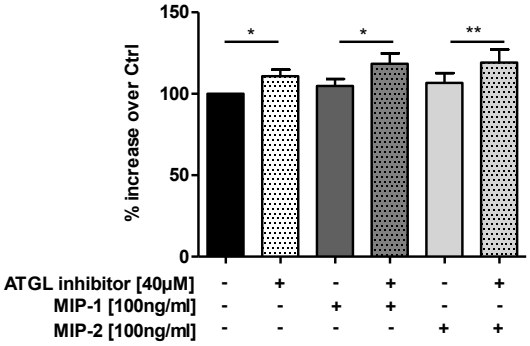

Figure 26: Determination of LD content in neutrophils after *in vitro* exposure to MIP-1 and MIP-2

Wt neutrophils collected from peritoneal lavages one day post thioglycolate injection were pre-incubated in culture medium for 2 h in the absence or presence of Atglistatin, after which recombinant MIP-1 and MIP-2 were added. After 5 h of incubation LDs were quantified by flow cytometry. Fluorescence intensities are expressed as percentages of untreated control cells + SEM (n=13). *$p < 0.05$; **$p \leq 0.01$

3.2.7 Reduced release of lipid mediators from neutrophils after ATGL inhibition

A key function of inflammatory cells (including neutrophils) is the generation of lipid mediators. Hence, our aim was to investigate and compare lipid mediator release in the absence of ATGL. Using thioglycolate-elicited wt neutrophils after Atglistatin-mediated ATGL inhibition, we studied the release of PUFAs and lipid mediators. As Appendix Table 1 and Fig. 27 show, Atglistatin treatment resulted in reduced release of 18:2 and 20:3 by 58%, 22:6 trended to be decreased, whereas 20:5 levels were unchanged. Concentrations

of 20:4 were below detection limit after ATGL inhibition. Lipid mediators derived from all three major enzymatic pathways, the COX, LOX and CYP450 pathway, were present in the media after 1 h *ex vivo* culture of thioglycolate-elicited peritoneal neutrophils. Upon ATGL inhibition, predominantly 20:4-derived metabolites were less abundant compared with media from cells without inhibitor (Fig. 27 and Appendix Table 1). Reduced metabolites included the COX-derived TxB2, prostaglandins (D2, E2, J2, 6-keto PGF1a), and 12(S)-HHT, the LOX-derived LTB4, LTE4, and 5-oxo ETE, the COX/CYP-derived 11-HETE, and the LOX/CYP-derived 15(S)-HETE, 5-HETE, and 14,15-EET. The effect of ATGL inhibition was not restricted to eicosanoids arising from 20:4. We also observed significantly reduced levels of the 20:3-derived PGD1 and 20:5-derived 5(S)-HEPE lipid mediators.

In addition, we investigated lipid mediator release from thioglycolate-elicited neutrophils after ATGL inhibition when exposed to the Ca^{2+} ionophore A23187 as additional stimulus. Neutrophil activation by A23187 was associated with even more reduced concentrations of 18:2 and 22:6 in the medium, whereas levels of 20:3, 20:4 and 20:5 released from thioglycolate- and A23187-stimulated cells were comparable (Fig. 27). A23187 treatment resulted in increased release of LOX-derived lipid mediators, in particular LTE4 (3-fold), LTB4 (7-fold), and 5-HETE (20-fold) when compared with thioglycolate-stimulated wt neutrophils (Fig. 27 and Appendix Table 1). This observation is in line with previous reports describing A23187 as a stimulus predominantly targeting the 5-LOX pathway (123). ATGL inhibition showed a similar reduction in lipid mediator release in A23187- and thioglycolate-only stimulated cells.

Together, these results point out that ATGL is required for the liberation of FAs from LD-associated TGs and thereby regulates the substrate availability for lipid mediator generation in neutrophils.

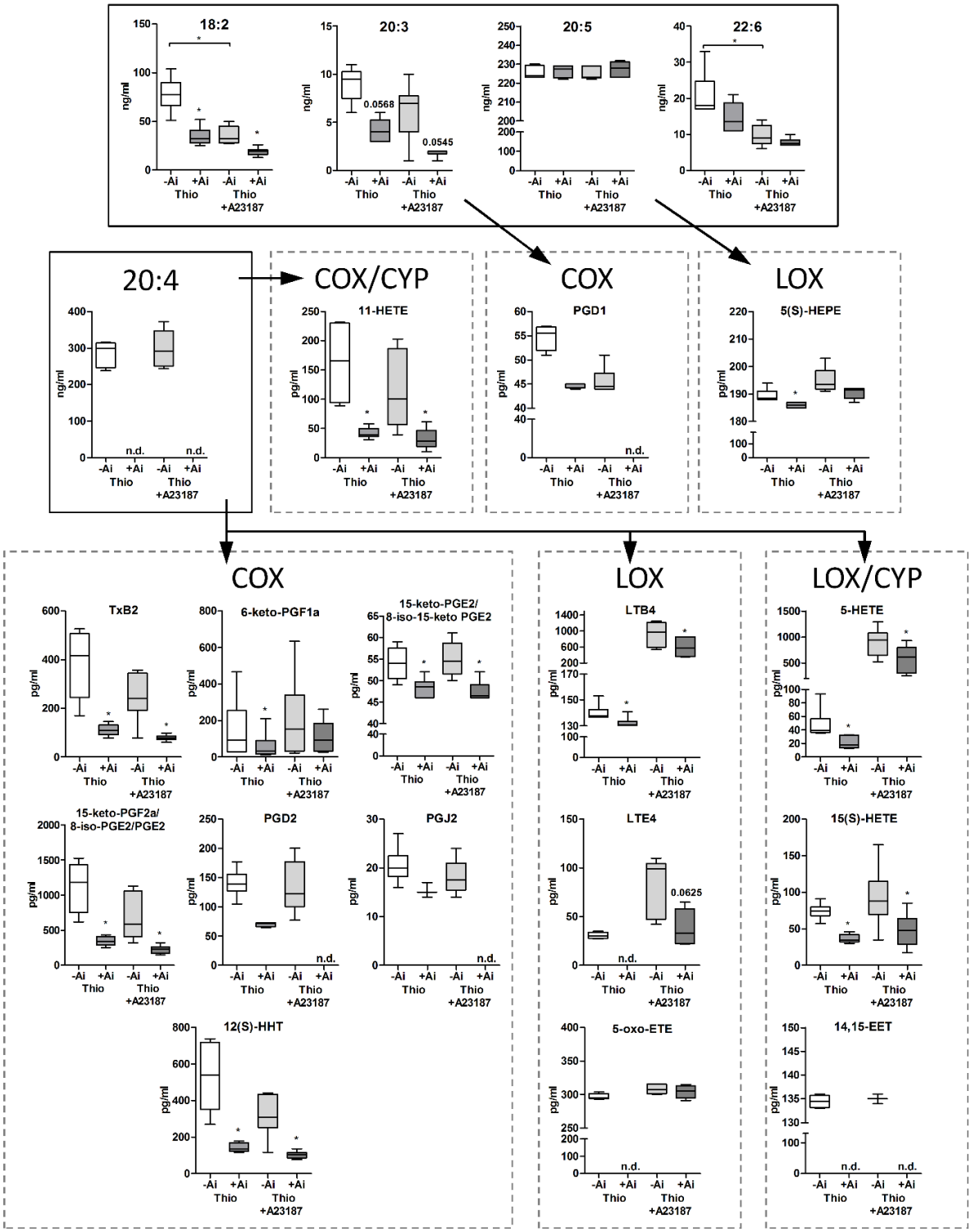

Figure 27: Reduced lipid mediator release upon pharmacological ATGL inhibition

Neutrophils were cultured for 6 h in medium in the absence or presence of the ATGL inhibitor Atglistatin (Ai). Media were collected from thioglycolate-elicited (Thio) and additionally activated neutrophils (0.5 µM A23187, 1 h). PUFA and lipid mediator concentrations were measured by LC-MS/MS analysis and are presented as median and range (n=6). n.d., not detectable. *$p < 0.05$

3.2.8 Reduced concentrations of lipid mediators in peritoneal exudates from Atgl-/- mice

To substantiate our *in vitro* findings and to test the *in vivo* impact of ATGL deficiency, we examined cell-free lavage fluids of one day thioglycolate-elicited peritoneal lavages from wt and global Atgl-/- mice with respect to lipid mediator concentrations. PUFAs in the lavage fluids of global Atgl-/- mice showed reduced concentrations of 18:2, 18:3, 20:5, and 22:6, whereas 20:3 and 20:4 levels were comparable between wt and Atgl-/- lavages (Fig. 28A). The lipid mediator profile revealed the presence of metabolites arising from all three major enzymatic pathways (Fig. 28B). The amount of the COX-derived TxB2 (the stable metabolite of TxA2), 6-keto-PGF1α, 12(S)-HHT, the LOX-derived Tetranor-12(S)-HETE and 5-HETE and the CYP-derived 8,9-DHET were significantly reduced in peritoneal exudates from Atgl-/- compared to wt mice. Among these, TxB2 and 5-HETE are mediators typically released from neutrophils under inflammatory conditions. Several detectable mediators such as LTB4, PGE2, various hydroxyeicosatetraenoic acids (11-HETE, 15(S)-HETE, 18-HETE) and dihydroxyeicosatrienoic acids (DHETs), the diol metabolites of EETs, showed a trend for reduced levels, which, however, did not reach statistical significance.

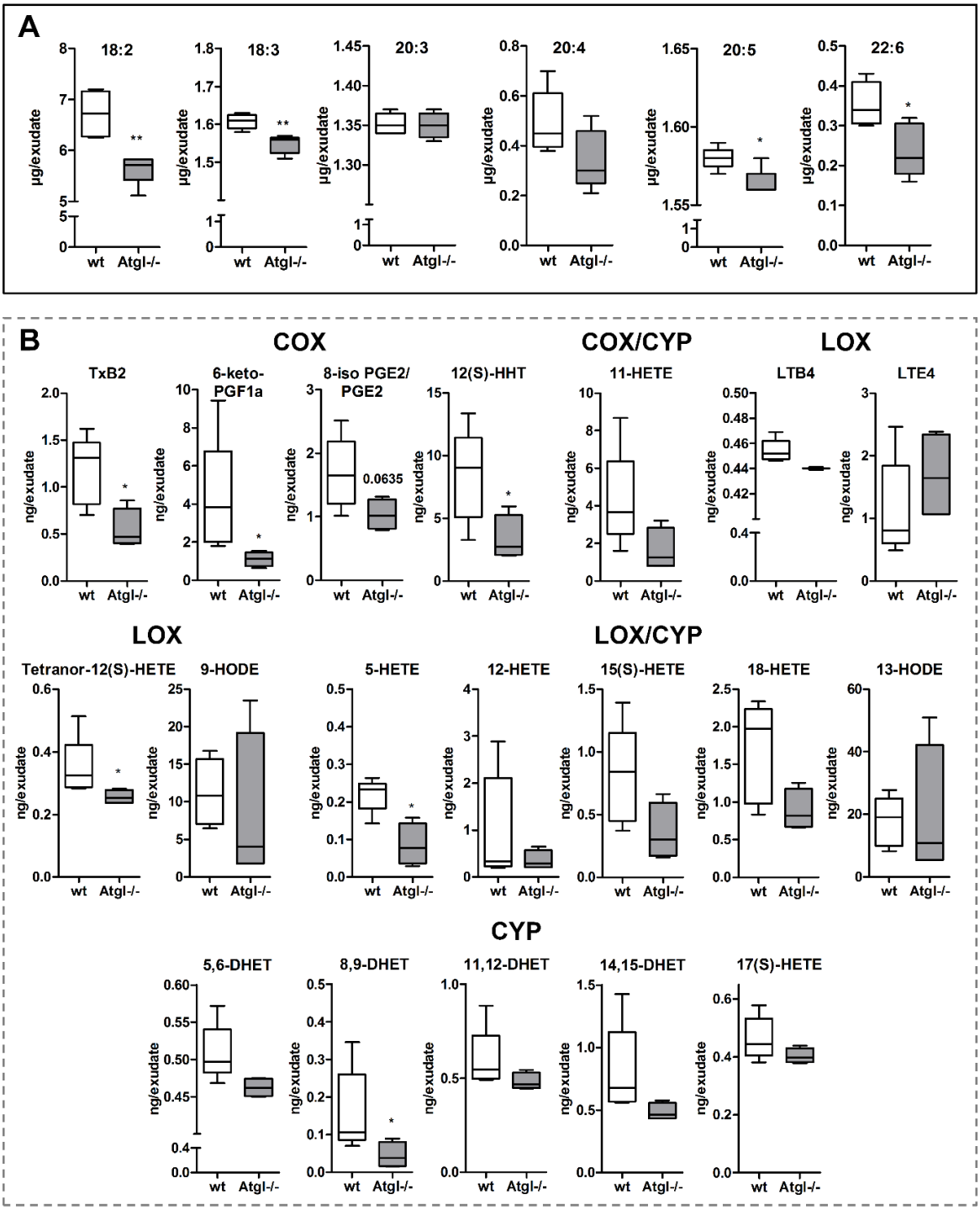

Figure 28: Reduced lipid mediator concentrations in peritoneal lavages from Atgl-/- mice

Cell-free fluids of peritoneal lavages from wt and Atgl-/- mice one day post thioglycolate injection were collected. (A) PUFA and (B) lipid mediator concentrations were measured by LC-MS/MS. Data are shown as median and range (n=4-5). *$p < 0.05$, **$p \leq 0.01$

3.2.9 Atgl-/- neutrophils accumulate TG-associated 18:1, 18:2, and 20:4

Concomitant with a reduced lipid mediator release in the absence of ATGL, I observed an accumulation of FAs in intracellular TGs of peritoneal cells from Atgl-/- mice. As Fig. 29 shows, lipid parameters of peritoneal cells isolated from mice one day after thioglycolate injection showed a 2.6-fold TG accumulation in Atgl-/- cells. TC, FC, and CE concentrations were unaffected (Fig. 29A). Using LC-ESI/MS analysis, we found that the relative FA composition of the most abundant TG species (abundance > 3% of total TGs) ranging from C_{50}-C_{56} differed significantly between wt and Atgl-/- cells (Fig. 29B). In neutrophils from Atgl-/- mice, TG species with more than 4 double bonds including predominantly 18:1, 18:2, 20:3, and 20:4 showed an increased relative abundance, whereas TG species with up to three double bonds containing mostly 16:0, 18:0, and 18:1 were decreased. Absolute concentrations of the most abundant PL species PC were unchanged (inset Fig. 29C). The relative PC composition was changed to an increase in 36:2 and a reduction in 34:1 in Atgl-/- neutrophils (Fig. 29C). No alterations were observed in PE concentrations between wt and Atgl-/- neutrophils, neither in absolute (inset) nor relative amounts (Fig. 29D).

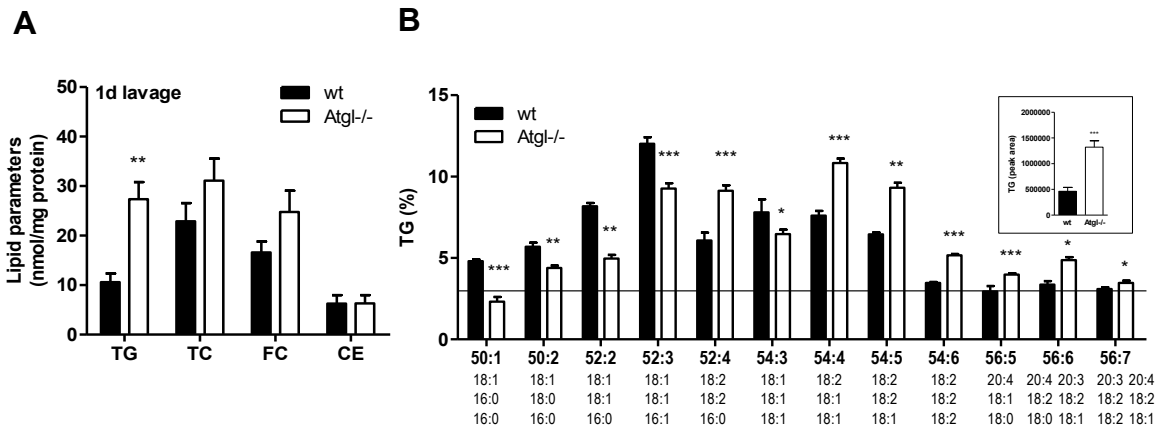

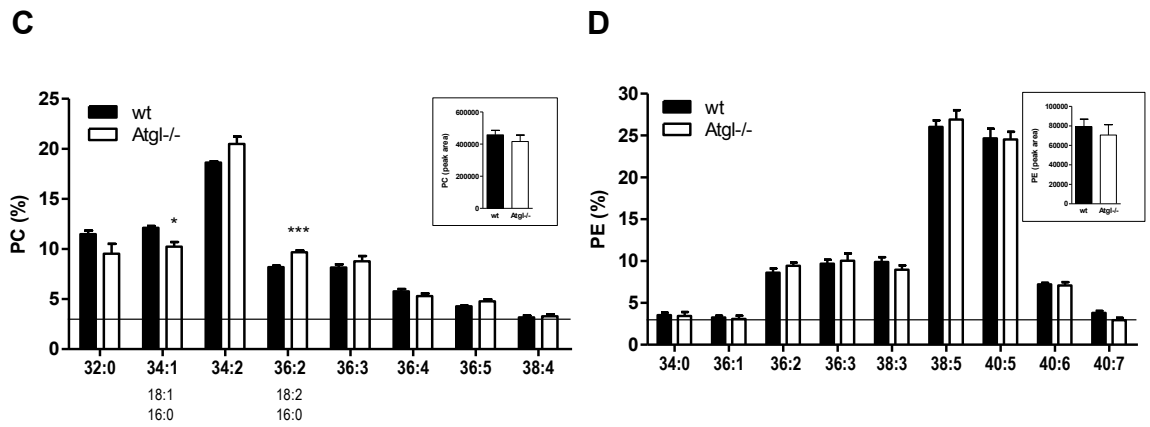

Figure 29: Atgl-/- neutrophils accumulate TG-associated 18:1, 18:2, and 20:4

Lipids of peritoneal lavage cells one day post thioglycolate injection were extracted and concentrations of TG, TC, FC, and CE were determined by enzymatic assays. Data are shown as means + SEM (n=5). FA composition of the most abundant (B) TG, (C) PC, and (D) PE species (abundance > 3%) were determined by LC/ESI-MS. Data are presented as means + SEM of absolute (inset) and relative values (n=4-5). *$p < 0.05$; **$p \leq 0.01$; ***$p \leq 0.001$

Summarized, the absence of ATGL in neutrophils resulted in a highly increased accumulation of FAs in TGs, whereas PLs remained mostly unaffected by ATGL deficiency. Thereby, our data provide strong evidence that ATGL acts as a TG hydrolase and is crucially involved in the hydrolysis of TG-rich LDs to provide eicosanoid precursors in neutrophils.

3.2.10 Reduced mRNA expression of eicosanoid-generating enzymes

Next, I evaluated mRNA expressions for the major enzymes involved in eicosanoid generation by quantitative PCR analysis in flow-sorted neutrophils derived from thioglycolate-induced lavages (Fig. 30). Compared to wt neutrophils, I observed unchanged transcript levels of cPLA2 and COX-1, whereas expression of COX-2, ALOX5 and ALOX12 were significantly reduced and ALOX15 and CYP2j showed a trend to reduced mRNA levels.

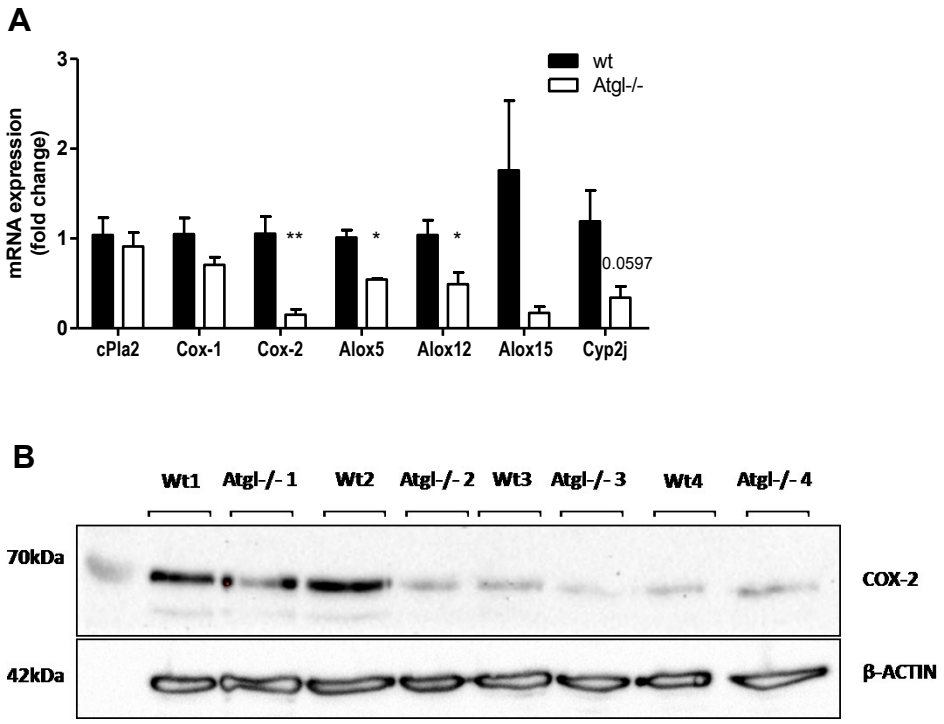

Figure 30: Reduced mRNA expression of eicosanoid-generating enzymes

(A) mRNA expression of eicosanoid-generating enzymes were determined by quantitative real-time PCR in flow-sorted wt and Atgl-/- neutrophils and are shown as –fold change to wt cells (n=4) (*$p < 0.05$; **$p \leq 0.01$). (B) Protein levels of COX-2 in isolated neutrophils were analyzed by Western blotting. Fifty µg of total protein lysate per lane were separated by 10% SDS-PAGE under reducing conditions. β-ACTIN was used as a loading control.

To substantiate the findings from gene expression analysis at the protein level, I analyzed the protein expression of COX-2, which is the COX isoform induced under inflammatory conditions (124), by Western blotting. The 70 kDa immunoreactive band representing COX-2 was clearly present in wt and Atgl-/- neutrophils. However, COX-2 expression showed considerable variations between different wt mice, which made it difficult to compare the expression levels between wt and Atgl-/- cells. Thus, a conclusion whether COX-2 enzymes are indeed downregulated in Atgl-/- neutrophils cannot be drawn from these results and requires further confirmation. An increase in sample size for mRNA expression analysis as well as the determination of additional eicosanoid-generating enzymes on protein levels might clarify this issue.

3.2.11 Increased clearance of bacteria in Atgl-/- mice after *E.coli* infection

Eicosanoids play a vital role in the regulation of inflammatory and infectious diseases as they are critical determinants for the initiation and resolution of the inflammatory response (reviewed in (90)). Based on the findings that ATGL deficiency results in reduced eicosanoid generation and release, we tested the hypothesis that this alteration has an impact on the modulation of an inflammatory response.

To this end, an experimental bacterial model was applied to wt and Atgl-/- mice, where *E.coli* were injected intraperitoneally and the clearance of bacteria in the peritoneum, blood, and liver was determined. To evaluate the optimal time point for sample collection, wt mice were injected with 2.2 x 10^4 CFU *E.coli* per mouse and the mortality rate after the bacterial challenge was assessed. As shown in Fig. 31A, most mice died within 30 to 60 h after the injection. Based on these findings, 18 h was defined as appropriate time point to investigate and compare bacterial burden between wt and Atgl-/- mice. Interestingly, bacterial growth of *E.coli* was significantly reduced Atgl-/- in peritoneal lavage, peripheral blood as well as liver when compared to wt mice (Fig. 31B).

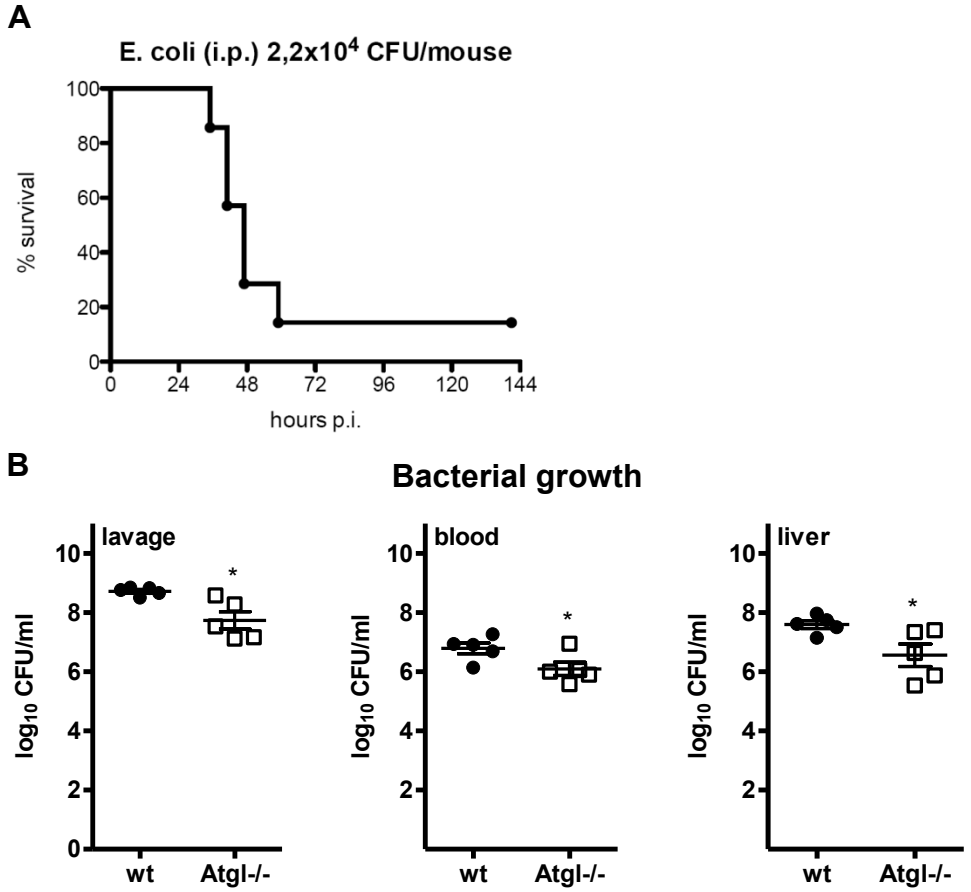

Figure 31: Atgl-/- mice show increased bacterial clearance after *E.coli* infection

(A) Mortality rate was determined in wt mice after an i.p. injection of 2.2 x 10^4 CFU *E.coli* per mouse. (B) 18 h after intraperitoneal infection of wt and Atgl-/- mice with 2 x 10^4 CFU *E.coli*, mice were sacrificed and bacterial growth in peritoneal lavage, blood, and liver homogenates was quantified. Data are shown as means ± SEM (n=5). *$p < 0.05$

Together, these results indicate that *E.coli*, after being inoculated into the peritoneum, are more effectively cleared in Atgl-/- mice, which further results in a reduced systemic bacterial dissemination to the blood and the liver. In the light of these preliminary observations, this would indicate that ATGL deficiency is associated with an improved performance in response to bacterial infections. Future research is necessary to ascertain the underlying mechanism(s) and key player(s) accounting for this beneficial effect on immune surveillance and host defense.

3.2.12 Discussion

The objective of this study was to test the hypothesis that ATGL plays a role in leukocyte LD metabolism and immune cell function. Neutrophils from Atgl-/- mice showed enhanced immune responses *in vitro*, which were more prominent in cells from global compared with myeloid-specific Atgl-/- mice. Certain pro-inflammatory cytokines, including MIPs and MCP-5, were found to be elevated in plasma of mice lacking ATGL. MIP-2, the IL-8 homologue in the mouse, is known to mediate pro-inflammatory and chemotactic effects, predominantly in neutrophils (125) and MIP-1α was shown to induce Ca^{2+} release in neutrophils (126). In human neutrophils, pro-inflammatory mediators, such as IL-8 and TNF, have been reported to prime cellular responses (127). Further exposure of primed neutrophils to a second stimulus elicits a faster and higher response compared to resting, unprimed cells. Based on this consideration together with our observations of elevated plasma cytokines in Atgl-/- mice, I suggest this as a possible mechanism to explain the observed pro-inflammatory response in Atgl-/- neutrophils. Whether MIPs are putative factors mediating neutrophil priming, however, remains to be proven.

LDs have a dual function within cells by controlling lipid storage, thereby protecting cells from lipotoxicity, and by serving as energy fuel upon starvation. In contrast to many other cell types, in which ATGL-mediated lipolysis represents an important biochemical mechanism to generate FAs as energy substrates, most lymphoid and myeloid cells (including neutrophils) derive their energy exclusively from glycolysis (128). In accordance, we did not observe alterations in cell viability or any limitations in highly energy demanding processes such as migration and phagocytosis in Atgl-/- neutrophils. Of note, the absence of ATGL was associated with an elevated Ca^{2+} mobilization and increased chemotaxis of neutrophils towards chemoattractants, indicating a pro-inflammatory phenotype of these cells. This phenotype was more pronounced in cells from global compared with myeloid-specific Atgl-/- mice, indicating that these alterations are likely boosted by secondary effects due to systemic ATGL deficiency. A causative reason for this might be additional factors provoked by the severe phenotype of global ATGL deficiency, including perivascular oxidative stress and endothelial dysfunction (129), ER stress, and mitochondrial dysfunction in various tissues (130) with the most dramatic

phenotype in cardiac muscle resulting in lethal cardiomyopathy within a few months after birth (102).

According to the current dogma, phospholipases, particularly cPLA2α, are assigned a central role in stimulus-dependent 20:4 mobilization from PLs during eicosanoid generation. Subcellular eicosanoid-generating compartments include membranes of the ER, phagosome, nuclear envelope, and LD but not the plasma membrane (75). In a recent study, the TG-rich core of LDs in human mast cells has been identified as an additional substrate reservoir for eicosanoid precursors with ATGL being critically involved in the release of these FAs (98). Our observations further support and extend this study showing that ATGL inhibition leads to an accumulation of TG-rich cytoplasmic LDs in neutrophils, monocytes, and macrophages and results in a reduced production of lipid mediators from neutrophils. A central question arising from the mast cell study was whether ATGL provides substrates for lipid mediator synthesis either by its TG hydrolase activity (131) or its putative phospholipase activity (132). Further it remained to be determined whether ATGL-mediated 20:4 release provides substrates directly for eicosanoid generation or indirectly by replenishing 20:4 in glycerophospholipids for the subsequent release by cPLA2α. Our lipidomics data clearly show a pronounced increase of 18:1, 18:2, and 20:4 in the TG fraction in the absence of ATGL and no accumulation of linoleyl- or arachidonyl-containing PC or PE, demonstrating that ATGL acts as a TG hydrolase and directly liberates FAs. We conclude that FA mobilization and release is a critical process and Atgl-/- neutrophils try to compensate for defective lipolysis by increased FA uptake from extracellular sources.

A key observation of this study is that genetic and pharmacological ATGL inhibition in neutrophils, both *in vivo* and *in vitro*, leads to a marked accumulation of neutral lipids in cytoplasmic LDs and, concomitantly, to a reduced production of some but not all lipid mediators. Lipid mediator generation is regulated in a highly time-dependent manner at various levels, e.g. through the availability of enzymes and substrates as well as the site of mediator generation within different cellular compartments (75). Our results indicate that lipid mediators, which remain unaffected by ATGL inhibition, are derived from non-LD compartments, whereas mediators with a reduced release upon ATGL inhibition are specifically generated from the TG-LD pool in an ATGL-dependent manner.

Recently, a comprehensive work describing the cellular and molecular events, including lipid mediator generation in mice with thioglycolate-induced peritonitis, has been published (133). This study revealed that in this model the inflammatory response after 24 h is characterized by high levels of 20:4-derived pro-inflammatory eicosanoids, such as PGD2, LTB4, PGE2, 5-HETE, and TxB2. This time point correlates with a high infiltration of the peritoneal cavity with neutrophils, rendering 24 h as a suitable time point to investigate neutrophil-mediated lipid mediator release. In accordance, we detected a release of these eicosanoids from lavages collected from one day thioglycolate-stimulated mice, which were reduced in Atgl-/- mice.

Clinical reports from patients with mutations in the ATGL gene describe the prevalence of Jordans' anomaly in all reported cases of NLSD. In these patients, Jordans' anomaly affects various immune cells, predominantly granulocytes (113, 114). In some case reports of NLSDM, an increased prevalence of reoccurring infections was observed (134). Unfortunately, it is not elusive whether these immune defects can be linked to Jordans' anomaly and whether eicosanoid production by blood leukocytes is altered in these patients. Surprisingly, we observed that Atgl-/- mice display an improved resistance to bacterial sepsis. Whether this improved host response is mediated by the pro-inflammatory neutrophils of Atgl-/- mice and whether altered eicosanoid generation is associated with this outcome requires more detailed analysis.

In general, a direct correlation between LD number and eicosanoid release was described in human and murine leukocytes (85). Thus, the increased presence of LDs in neutrophils from humans and mice with Jordans' anomaly should result in an increased potential of these cells to generate lipid mediators. Due to inhibited lipid mobilization from LDs in Atgl-/- conditions, however, the release of lipid mediators is partly inhibited, further underlining the important role of ATGL in the regulation of eicosanoid generation.

4 Conclusions and Perspectives

Elevated plasma FA levels in the circulation, due to increased breakdown of fat, can lead to the pathogenesis of insulin resistance, type 2 diabetes and the metabolic syndrome. ATGL, which is the rate-limiting enzyme in the degradation of lipid stores, determines the concentration of circulating FFAs. The observations that mice with genetic deletion of ATGL are resistant to diet-induced diabetes and cancer-associated weight loss (termed as cancer cachexia) suggest ATGL as a potential target for medical intervention. Thus, a specific ATGL inhibitor Atglistatin was developed and is under intensive investigations to prevent metabolic diseases, especially type 2 diabetes and cancer-associated cachexia.

In comparison to adipocytes and hepatocytes, immune cells contain less TGs stored in LDs indicating that the function of lipid stores in these cells is distinct from systemic TG metabolism, which mostly relates to storage and supply of energy. In our study, we provided profound evidence that TG-hydrolyzing enzymes regulate lipolysis of the lipid stores in various immune cells and thereby mediate intracellular pathways of lipid signaling and regulate metabolism and function of immune cells.

In the context of inflammatory cells, most knowledge about the TG hydrolases investigated here (MGL, HSL, ATGL, and LAL) is derived from studies in macrophages and during the pathogenesis of macrophage foam cell formation and atherosclerosis. MGL, based on its role to inactivate the endocannabinoid 2-AG, is expected to influence the inflammatory and atherosclerotic phenotype. The consequences of MGL deficiency on macrophage functions and atherosclerotic plaque formation are currently under investigation. HSL is implicated to play a role as CE hydrolase in macrophages. HSL deficiency in mice was reported to accelerate atherosclerotic plaque formation (135). However, another study revealed that macrophage-specific overexpression of HSL in mice increases atherogenesis via increased ACAT-1-mediated re-esterification of cholesterol resulting in CE accumulation in macrophages (49). Intensive investigations from our research group have unveiled a considerably altered phenotype of Atgl-/- macrophages. Loss of ATGL in macrophages leads to reduced TG hydrolase activity and intracellular LD accumulation. Summarized, Atgl-/- macrophages exhibit severely restrained energy substrate availabilities, which further result in phagocytosis defects (48), impaired

macrophage migration (136), ER stress, apoptosis, and mitochondrial dysfunction (137, 138). Further, ATGL deficiency in myeloid cells on the atherosclerotic LDLR-/- background resulted in an atheroprotective phenotype with reduced macrophage content of the plaque (139). In agreement with these observations, an anti-inflammatory M2-like phenotype was described for Atgl-/- macrophages. In contrast to macrophages, I observed that Atgl-/- neutrophils are associated (as evident by elevated Ca^{2+} signaling and increased chemotaxis) with a pro-inflammatory phenotype. Currently, the exact molecular mechanisms accounting for this phenotype are unclear.

Previous research showed an important role of LAL in immune cells, predominantly with regard to immune cell development and function (119). Substantial evidence from human and mouse studies revealed a reduced LAL activity as an underlying mechanism of macrophage foam cell formation and atherogenesis, and, hence, LAL supplementation for the prevention and treatment of atherosclerosis was suggested (140).

In summary, the determination of lipase expression profiles in distinct immune cells (including neutrophils, monocytes, eosinophils, and lymphocytes) presented in this work provides a basis for further studies addressing the contribution of lipolytic enzymes in LD catabolism of cells of the innate or adaptive immune system other than macrophages.

A key observation of this study is that the release of lipid mediators from neutrophils is dependent on liberation of FAs as precursor molecules from the TG-rich pool of LDs by ATGL. Considering that eicosanoids are not only generated from LDs but other subcellular compartments, the described impact of ATGL deficiency might mainly apply to cells and conditions, where a certain content of LDs is present. Notably, eicosanoid-synthesizing LDs are not restricted to immune cells such as neutrophils but were also found in many other immunomodulatory, endothelial, and epithelial cells under pathological conditions as well as neoplastic cells and tissues (reviewed in (76)). Therefore, it is reasonable to speculate that ATGL regulates FA availability and, consequently, the release of lipid mediators also in these cells.

Eicosanoids are key signaling molecules during the inflammatory response and promote the resolution and termination of inflammation. Moreover, eicosanoids have been assigned important functions to control cell activation, migration, proliferation, and apoptosis (2). Their dysregulation in any dimension might have pathologic consequences,

such as chronic inflammation, failure of pathogen clearance, and both local and distal tissue damage (141, 142). The physiological significance of our findings that ATGL deficiency is associated with reduced eicosanoid generation remains to be determined. Preliminary results indicate that Atgl-/- mice exhibit an improved clinical outcome in response to sepsis. Yet, the underlying mechanism(s) for the unexpected phenotype remains elusive and requires further clarification. In addition, analysis of immune cells of NLSD patients would provide further insight into the consequences of defective ATGL activity on immune cell functions.

Mechanisms to regulate eicosanoid production are attractive targets for anti-inflammatory therapy. The inhibition of LD formation, e.g. by aspirin and non-steroidal anti-inflammatory drugs (NSAIDs), has been implicated and tested in different model systems (reviewed in (76)). Given the protective role of LDs against lipotoxicity, however, the safety of this strategy raises questions. Our findings provide a new strategy to regulate the release of LD-derived lipid mediators by inhibiting the catabolism rather than the generation of LDs. We suggest that the ATGL-specific inhibitor Atglistatin is a promising compound for pharmacological intervention in this context.

The knowledge on the utilization of TG-associated acylglycerides as a source for eicosanoid precursors is far from complete. The observations reported here opened the perspective of further candidate lipases to be involved in the release of eicosanoid precursors by lipolysis, including enzymes such as HSL, MGL, and LAL. The contribution of these lipases to the mobilization of AA, EPA, and DHA for lipid mediator generation remains to be determined.

In summary, the present work strengthens the hypothesis that “lipolysis meets inflammation” with ATGL and possibly other lipid hydrolases participating in inflammatory signaling processes (143). Our findings provide an important basis for future experiments exploring the role of ATGL-mediated lipid mediator release in the context of inflammatory and neoplastic diseases. Further, we suggest that medical interventions to block ATGL should be undertaken with consideration of the potential effects of ATGL inhibition on immune cells, which are important regulators in health and disease.

PART II: THE ROLE OF TG HYDROLASES IN PLATELET FUNCTION

1 Introduction

1.1 Platelet physiology

Platelets are anucleated cell fragments derived from megakaryocytes, which reside in the bone marrow. Apart from their well-established, classical role in thrombosis and hemostasis platelets have important immunoregulatory functions. Platelet activation with consequent degranulation results in the liberation of numerous mediators stored in platelet granules. These mediators include pro- and anti-inflammatory as well as pro-angiogenic factors and microparticles, which can either be displayed on the platelet surface or released into the circulation, where they exert distinct biological activities. Thereby, platelets can recruit leukocytes and progenitor cells to sites of vascular injury and inflammation. Platelets are suggested as critical components of the immune system and therefore are implicated in the etiology of various diseases, such as autoimmune diseases, diabetes, atherothrombosis, and cardiovascular disease (144, 145).

Under physiological conditions, platelets circulate freely in the blood without interacting with each other or the vascular endothelium. Endothelial injury leads to the exposure of subendothelial extracellular matrix proteins and triggers platelet activation via a multi-step process (Fig. 32A). Platelet tethering and adhesion to the endothelial wall is mediated through multiple interactions between platelet membrane receptors (integrins) and various ligands in the damaged endothelium, most notably von Willebrand factor (vWF), fibrinogen, and collagen. Platelet adhesion to collagen occurs directly via binding of the platelet integrin complex GPIb-V-IX to vWF, which binds to collagen, and indirectly via binding of GPVI to collagen. Platelet activation is further amplified by soluble agonists such as ADP, thromboxane A2 (TxA2) or thrombin, which mediate their action via G-protein coupled receptors. The main platelet activation pathways are depicted in Fig. 32B. Intracellular signaling events result in the degranulation of α-granules and dense bodies. α-granules contain a vast array of proteins, ranging from adhesion molecules and coagulation factors to chemokines and cytokines, whereas dense bodies contain

predominantly small molecules, such as ADP and serotonin. Altogether these events provide a stimulus for the conformational change of the platelet αIIbβ3 integrin (GPIIb/IIIa receptor), which, in its activated form, can bind fibrinogen and vWF and thereby further triggers platelet aggregation and the formation of a stable thrombus (146, 147).

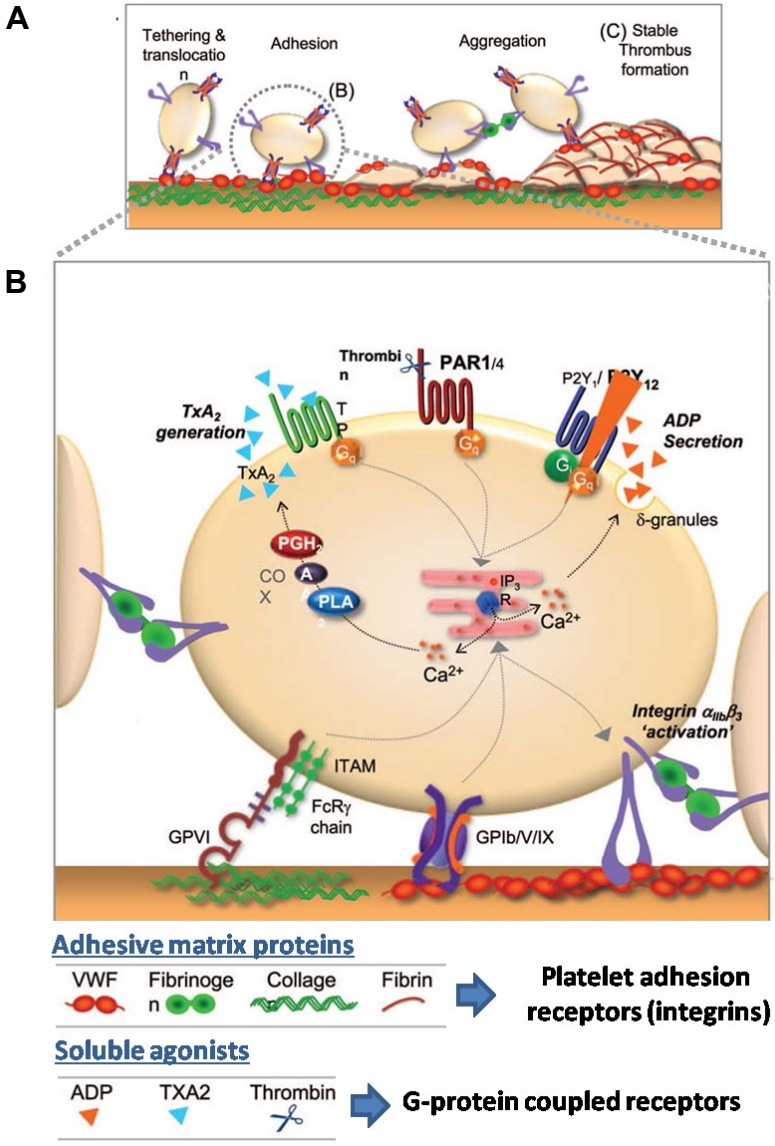

Figure 32: Platelet activation and thrombus formation

(A) Platelet activation is a sequential procedure. Endothelial damage initiates the recruitment and tethering of platelets from the blood. This is followed by platelet adhesion, activation, and secretion of soluble mediators, both for autocrine and paracrine activation. Platelet aggregation results in the formation of a thrombus. (B) Main platelet activation pathways. Platelet activation is mediated via various soluble agonists (ADP, TxA2, and thrombin) or adhesive matrix proteins (vWF, fibrinogen, and collagen). (modified from (147))

1.2 Platelet-lipoprotein interaction

Numerous studies support an active interplay between circulating platelets and plasma lipoproteins, which influences the functional properties of platelets (148, 149). Dyslipidemic conditions are characterized with altered platelet activity and thrombogenic potential. In patients, hypercholesterolemia is associated with increased platelet activity, such as hyperaggregability (150, 151), and the administration of lipid-lowering drugs reverses this prothrombotic phenotype (149). Patients with Tangier disease, a disorder characterized by the virtual absence of high-density lipoproteins (HDL), show defective activation in response to platelet agonists (152). The underlying mechanisms how lipoproteins influence platelet reactivity are listed in Table 8.

Table 8: Effects of native LDL, oxidized LDL and HDL on platelets

native LDL
Binding and activation of platelets
Increased platelet sensitivity to platelet-activating agents
Compositional changes in membrane phospholipids
Lipid exchange and transfer to other cells
Lipid peroxidation mediated by platelet ROS
oxLDL
Binding to platelets via SR-B, CD36, LOX-1
Induction of platelet hyperreactivity, shape change and aggregation
Cholesterol efflux from platelets to macrophages
Induction of foam cell formation in oxLDL-treated platelet co-culture
Foam cell formation after platelet phagocytosis by macrophages
HDL
Desensitization of platelets
Anti-atherosclerotic effects

(adapted from (144))

Lipoprotein-platelet interactions result in lipid exchange, thereby altering platelet dynamics and function (153). Various lipoprotein receptors (e.g. LRP-8, ApoER2) as well as scavenger receptors (e.g. CD36, SR-B1, LOX-1) have been described on the surface of platelets mediating the binding of lipoprotein particles (reviewed in (154)). Three major mechanisms are implicated for the lipid transfer from the plasma compartment to the platelets: (i) internalization of lipoprotein particles into the cells (e.g. by endocytosis or trapping in the open canalicular system (OCS)), (ii) total (specific and unspecific) binding

of lipoproteins to the platelet surface, and (iii) selective uptake of phospholipids (PL) by cellular membranes. Holoparticle uptake of LDL into platelets via endocytosis is considered as rather unlikely (155). However, the uptake and trapping of plasma components within the OCS seem to be possible (153).

1.3 Lipid signaling in platelets

Lipids are essential building blocks for biomembranes and represent storage molecules for fatty acids (FAs), cholesterol, and retinol. In common with all mammalian cells, the major structural lipids are PLs. During activation, bioactive lipids (e.g. 1,2-diacylglycerol (DG), FAs, eicosanoids, phosphatidylinositides, lysophospholipids) are formed. Platelets also contain appreciable amounts of neutral lipids, including triacylglycerol (TG) and cholesteryl ester (CE) (156). The sterol composition in platelets has been shown to have a direct role in fluidity, organization, and physiologic activities of platelet membranes (157). Unesterified (free) FAs (FFAs) act as powerful signaling molecules, which regulate numerous cellular processes. Their availability is regulated by the action of lipases via the hydrolysis of intracellular lipid stores.

In addition to cytokines and chemokines, platelets generate lipid-derived inflammatory mediators. The adhesion of platelets to leukocytes and the endothelium results in transcellular metabolism of eicosanoids, leading to the local synthesis of leukotrienes, platelet-activating factor (PAF), and TxA2. PAF is a potent platelet agonist and pro-inflammatory mediator, which regulates firm neutrophil adhesion on the surface of immobilized spread platelets.

1.4 Role of phospholipases in platelets

Agonist-induced platelet activation involves different signaling pathways leading to the activation of phospholipases, which produce important second messengers. An initial reaction during platelet activation involves the hydrolysis of phosphoinositide (PI) by phospholipase C (PLC). PLC transforms phosphatidylinositol-4,5-bisphosphate (PIP_2) to inositol triphosphate (IP_3) and DG, resulting in mobilization of Ca^{2+} from intracellular stores and protein kinase C (PKC) activation, respectively. DG can also be generated via a direct pathway through the hydrolysis of phosphatidylethanolamine (PE),

phosphatidylserine (PS) or phosphatidylcholine (PC). From these PLs, phospholipase D (PLD) releases phosphatidic acid (PA), which is further processed by phosphatidic acid phosphatase (PP) to generate DG. Phospholipase A2 (PLA2) mediates its function via a direct release of FFAs predominantly from PC but also PE and PS, thereby providing arachidonic acid (AA), which is a precursor for the generation of the lipid mediator TxA2 (Fig. 33).

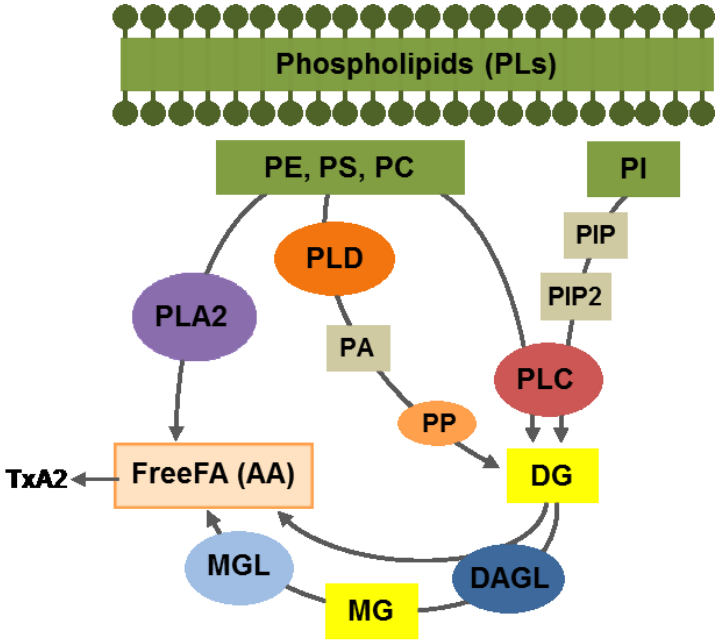

Figure 33: Lipid signaling in platelets

The signaling pathways are discussed in the text. Phosphatidylethanolamine, PE; phosphatidylserine, PS; phosphatidylcholine, PC; phosphatidylinositol, PI; phosphatidylinositol-4-phosphate, PIP; phosphatidylinositol 4,5-bisphosphate, PIP2; phospholipase C, PLC; phospholipase A2, PLA2; phospholipase D, PLD; phosphatidic acid, PA; phosphatidic acid phosphatase, PP; diacylglycerol, DG; diacylglycerol lipase, DAGL; monoacylglycerol, MG; monoacylglycerol lipase, MGL; fatty acid, FA.

The significance of PL signaling in platelets is supported by studies of platelet function in various knock-out (-/-) mouse models. Platelets from PLCβ-/-mice were shown to be unresponsive to ADP, TxA2 or thrombin and, hence, failed to normally spread after adhesion and to form stable thrombi (158). In studies of PLCγ2-/- platelets, an impaired activation has been observed to vWF through its GPIb-V-IX receptor, to collagen, and to GPVI- and integrin-specific ligands (159). Studies in PLD-/- mice revealed that the PLD1 isoform is required for proper integrin activation in response to weak agonist signals. Consequently, mice lacking PLD1 were protected against arterial thrombosis and ischemic

stroke (160). Interestingly, the single loss of PLD2, the second isoform, has no effect on platelet activation, whereas the combined deficiency of both PLD isoforms results in a defect in α-granule release and protection from ferric chloride-induced thrombosis (161).

The cytosolic phospholipase (cPLA)2α is one of the enzymes involved in AA release and TxA2 generation during the activation of platelets. *In vivo* studies using cPLA2α-/- mice revealed increased bleeding times and protection from thromboembolism. Platelet aggregation *in vitro*, however, was only fractionally decreased since small amounts of TxA2 were produced by redundant phospholipases, which sufficiently preserve aggregation. Similarly, Moriyama et al. demonstrated that at early stage of stimulation AA is released from PI via the PLC/DAGL/MGL pathway (162).

1.5 Role of neutral lipid hydrolases in platelets

Following its release from PLs, DG has an important role as signaling lipid itself by activating PKC. In addition, DG can also generate alternative signaling molecules through its lipolytic degradation (Fig. 33). DAGL cleaves the sn-1 acyl chain of DG and the resulting 2-acyl monoacylglycerol (MG) is hydrolyzed at the sn-2 position by monoacylglycerol lipase (MGL) producing glycerol and FFA. Since PI contains a high level of AA at the sn-2 position (132), the predominantly released FA by MGL is AA. Hence, the DAGL/MGL pathway is considered to be critically involved in provision of AA from membrane phospholipids.

Studies from guinea pig platelets revealed an important role for DAGL in platelet function since its pharmacological inhibition resulted in a reduced release of AA and its metabolites from thrombin-stimulated platelets, which ultimately resulted in inhibited platelet aggregation (163). Using Dagl-/- mice, it was further shown that DAGL-mediated lipolysis regulates the availability of the bioactive signaling lipid 2-arachidonoyl glycerol (2-AG) in the brain. 2-AG acts as an endogenous ligand for cannabinoid receptors (CBR) and is critical for the regulation of retrograde synaptic plasticity and adult neurogenesis (164). A recent study addressed the role of endocannabinoids during platelet activation (165). Therein, 2-AG was shown to promote platelet aggregation in blood as well as shape change, aggregation and ATP secretion in platelet-rich plasma (PRP). Platelet activation was inhibited by the selective MGL inhibitor JZL184, indicating that the platelet-stimulating phenotype was mediated by the MGL-triggered release of AA and its oxidative

metabolite TxA2 and not through an involvement of the CBR signaling pathway. Platelet function in mice with MGL deficiency has so far not been characterized. Whether the underlying mechanism in Mgl-/- platelets is the same as described for the pharmacological inhibition resulting in reduced AA concentrations and concomitantly reduced release of pro-thrombotic lipid mediators from platelets has not been investigated. Although, MGL was discovered in 1964 (166), Mgl-/- mice have been generated only recently. MGL deficiency in mice impairs lipolysis and attenuates diet-induced insulin resistance (106). Defective degradation of 2-AG, however, does not provoke cannabinomimetic effects on feeding behavior, lipogenesis, and energy expenditure, which may be explained by desensitization of the CBR1 (106, 167, 168).

DG and MG can also be derived from extracellular sources via the breakdown of lipoproteins by lipoprotein lipase or from lipolysis of intracellular triglyceride (TG)-rich lipid stores. Lipolysis is the sequential breakdown of TGs stored in cytosolic lipid droplets (LDs). The first and rate-limiting step is mediated by adipose triglyceride lipase (ATGL) generating DG and FA. Hormone-sensitive lipase (HSL) degrades DG to release the second FA and monoacylglycerol (MG). Finally, MG is hydrolyzed by MGL to release another FA and glycerol (Fig. 2).

The importance of lipolysis in various tissues and cell types became evident since ATGL results in a severe phenotype both in humans and mice with the most dramatic phenotype in the heart resulting in cardiac myopathy (reviewed in (37)). Studies from our group revealed that loss of ATGL in macrophages leads to TG-rich LD accumulation and phagocytosis defects (48), impaired macrophage migration (136), ER stress and apoptosis leading to mitochondrial dysfunction (137, 138). ATGL deficiency in myeloid cells on the atherosclerotic low-density lipoprotein receptor (LDLR)-/- background resulted in reduced plaque formation compared with LDLR-/- mice after Western-type diet feeding (139).

ATGL specifically generates sn-1,3 and (in the presence of its co-activator CGI-58) sn-1,3 and sn-2,3 DG (67). In addition to its TG hydrolase activity, ATGL is reported to exhibit DG acyltransferase (generating TG and MG from two DG molecules) and phospholipase activities (132). To date, the role of ATGL in platelet function is not known.

1.6 Aims

In platelets, the presence of LDs and the role of their lipolytic machinery to degrade TG have not been investigated yet. According to genome-wide RNA-sequencing data from human and mouse platelets, ATGL and MGL are expressed in platelets (169). However, the role of lipolytic enzymes, such as ATGL, HSL, and MGL, in platelet function has never been addressed. Notably, studies from our group revealed that ATGL deficiency in LDLR-/- mice results in reduced plaque formation when compared with LDLR-/- mice after Western-type diet feeding (139). This atheroprotective phenotype was associated with decreased infiltration of less inflammatory macrophages into the arterial wall and increased macrophage apoptosis. The contribution of platelets in this context was not investigated.

In the present work, I investigated a potential function of TG-hydrolyzing enzymes in platelets. Utilizing lipase-deficient mice, I aimed (i) to characterize the morphology and lipid profile of platelets from mice genetically lacking ATGL and (ii) to investigate the effect of systemic ATGL, HSL, and MGL deficiency on platelet function and thrombosis.

2 Materials and Methods

2.1 Buffers, solutions, and equipment

Tyrode buffer pH 7.0

134 mM NaCl

0.34 mM Na_2HPO_4

2.9 mM KCl

12 mM $NaHCO_3$

20 mM Hepes

5 mM Glucose

0.35% BSA

10x PBS pH 7.4

1.4 M NaCl

25 mM KCl

81 mM Na_2HPO_4

15 mM KH_2PO_4

Reagent	**Company**
3,3'-dihexyloxacarbocyanine iodide	Sigma
Iloprost	Cayman
Agonists	
Collagen-type I	Chrono-Log
CRP-XL (cross-linked)	Provided by Richard Farndale
PMA	Sigma
PAR-4 agonist	Dynabyte
ADP	Chronopar, Sigma
Thrombin	Chronopar
TxA2 analog U46619	Chronopar
Antibodies	
CD41-APC	eBioscience
CD41-PE	eBioscience
CD62P-FITC (P-selectin)	BD Biosciences
CD41/61-PE (JON/A)	Emfret
GPVI-FITC	Emfret

Equipment	**Company**
Centrifuge 5471R	Eppendorf
Power supply Power Pac 300	Bio-Rad
Ultra Turrax	IKA works
Sonicator	B.Braun
Nano Drop Spectrophotometer	Peqlab
Thermal cycler C1000	Biorad
Anthos 2000	Anthos
Guava Easy Cyte 8	Merck Millipore
FACSCalibur	BD Biosciences

2.2 Platelet count

Blood samples were collected via retrobulbar plexus puncture using EDTA-coated capillary tubes and platelet counts were performed using an automated cell counter MS9-5V (Melet Schloesing, Cergy-Pontoise, France).

2.3 Platelet preparation

Platelets were isolated from mice and purified as described (169). In brief, whole blood was collected from retrobulbar plexus and anticoagulated with 3.8% sodium citrate. The blood was centrifuged for 20 min at 400 x *g* to obtain platelet-rich plasma (PRP). For washed platelets, the PRP was centrifuged (10 min, 500 x *g*) and platelet pellets were resuspended twice in Tyrode buffer. For platelets isolation, washed platelets were incubated in the presence of anti-Ter-119 and anti-CD45 beads (Miltenyi Biotec, Bergisch Gladbach, Germany) to remove residual red blood cells and leukocytes, respectively. After this depletion step, purified platelets were used for RNA extraction and Western blot analysis.

2.4 RNA isolation and cDNA synthesis

Total RNA from isolated platelets was extracted as described in Part I 2.6. Five hundred ng of total RNA were reverse transcribed using the High Capacity cDNA Reverse Transcription Kit (Applied Biosystems, Carlsbad, CA).

2.5 Reverse transcriptase-PCR

For PCR, specific oligonucleotide primers were designed and are listed in Table 9. PCR products were analyzed by agarose gel electrophoresis.

Table 9: Primer sequences for RT-PCR

Gene	Forward primer (5'-3')	Reverse Primer (5'-3')
CD41	TTCTTGGGTCCTAGTGCTGTT	CGCTTCCATGTTTGTCCTTATGA
CD45	ATATCGCGGTGTAAAACTCGTC	TAGGCTTAGGCGTTTCTGGAA
CD235a	GGTAACCCAAATCAGCATTCAGC	GGTGACGGCATTCCTCCAA
Atgl	GCCACTCACATCTACGGAGC	GACAGCCACGGATGGTGTTC
Hsl	GCTGGTGACACTCGCAGAAG	TGGCTGGTGTCTCTGTGTCC
Mgl	CGGACTTCCAAGTTTTTGTCAGA	GCAGCCACTAGGATGGAGATG

2.6 Western blot analysis

Western blot analysis was performed as described in Part I 2.10. White adipose tissue (WAT) protein lysates from wt and lipase-deficient mice were used as controls and were prepared as follows: Gonadal WAT was surgically removed and washed in ice-cold PBS containing 1 mM EDTA. Homogenization was performed on ice in lysis buffer A (0.25 M sucrose, 1 mM EDTA, 1 mM DTT, pH 7.0) using an ultra turrax. The infranatants were obtained after centrifugation at 20000 x *g* at 4°C for 60 min.

2.7 Electron microscopy

Electron microscopy was performed by Dr. Dagmar Kolb.

Transmission electron microscopy

Transmission electron microscopy of washed platelets was performed as described in Part I 2.9.

Scanning electron microscopy

Fifty µl of a washed platelet suspension were placed on alcian blue-coated cover slips and immediately fixed with 2.5% glutaraldehyde (w/vol) and 2% methanol-free formalin in 0.1 M cacodylate buffer for 15 min. Samples were rinsed in 0.1 M cacodylate buffer, then post-fixed for 15 min in 2% osmium tetroxide (w/vol), and rinsed again in cacodylate buffer. Samples were dehydrated in graded series of ethanol. Cover slips in super-dry ethanol were critical-point dried, mounted on aluminum pin and sputter-coated. Images were taken by a Zeiss scanning electron microscopy (DSM 950) (Carld Zeiss, Oberkochen, Germany) using a Digital image scanning system (Point Electronic, Halle, Germany).

2.8 Thin layer chromatography (TLC)

Lipids were extracted from isolated, purified platelets according to the method of Bligh and Dyer (170). Solvents were evaporated under a stream of nitrogen, and the lipids were dissolved in chloroform/methanol (2/1; vol/vol). Various lipid classes were separated by TLC on HPTLC Silica gel 60 (Merck, Darmstadt, Germany). Hexane/diethylether/acetic acid/H_2O (26/6/0.4/0.1; vol/vol) and chloroform/methanol/acetic acid/H_2O (10/3/1.6/0.7; vol/vol) were used as mobile phase for neutral lipids and PLs, respectively. The separated

lipids were visualized by exposing the Silica gels to 3% $CuSO_4$ and 8% H_2PO_4 and subsequent heating at 160°C. Appropriate lipid standards were purchased from Sigma.

2.9 *In vitro* thrombogenesis

Vena8Fluoro+ Biochips (Cellix, Dublin, Ireland) were coated with collagen (200 µg/ml) at 4°C overnight and thereafter blocked with BSA (10 µg/ml) for 30 min at RT followed by washing steps. Whole blood collected in 3.8% sodium citrate was incubated with 3, 3-dihexyloxacarbocyanine iodide (1 µM) in the dark for 10 min. To record inhibition of thrombus formation, whole blood was treated with Iloprost (10 µM) for 5 min before starting the perfusion. $CaCl_2$ at a final concentration of 1 mM was added 2 min before perfusion over the collagen-coated chip. Perfusion was carried out at a shear rate of 30 dynes/cm^2. Thrombus formation was recorded every 10 sec for 3 min by a Zeiss Axiovert 40 CFL microscope using a Hamamatsu ORCA-03G digital camera (Hamamatsu, Bridgewater, NJ) and Cellix VenaFlux software. Computerized image analysis was performed by DucoCell analysis software (Cellix) and the area covered by the thrombus was calculated. Data are expressed as percent of area covered in a control sample.

2.10 Flow cytometric analysis of P-selectin and αIIbβ3 expression

Fifty µl of blood were collected and diluted 1:20 in Tyrode buffer. Samples were stimulated with agonists at the indicated concentrations in the presence of a FITC-conjugated anti-mouse P-selectin antibody (BD Biosciences) or JON/A-PE antibody directed against the activated form of mouse integrin αIIbβ3 (Emfret Analytics, Würzburg, Germany). Stimulation was carried out at 37°C for 15 min. Samples were washed, fixed and analyzed by flow cytometry using a FACSCalibur (BD Biosciences).

2.11 GPVI staining

Diluted whole blood was incubated with FITC-labeled anti-GPVI (JAQ1, Emfret Analytics) at saturating concentrations in the absence and presence of collagen-related peptide (CRP; 1 µg, 10 µg) for 15 min at RT. Cells were fixed and analyzed directly by flow cytometry. CD41-APC (eBioscience) was used as a platelet-specific marker.

2.12 Fibrinogen ELISA

Blood samples were collected via retrobulbar plexus puncture and anticoagulated with 3.8% sodium citrate. Fibrinogen concentrations in plasma were assessed using commercial enzyme-linked immunosorbent assay (AssayPro, Winfield, MO).

2.13 Statistical analysis

Statistical analyses were performed using GraphPad Prism 5.0 software. The significance was determined by Student's unpaired *t*-test or ANOVA, followed by Bonferroni correction. Data are presented as mean values ± SEM. The following levels of statistical significance were used: *$p < 0.05$, ** $p \leq 0.01$, *** $p \leq 0.001$.

3 Results and Discussion

3.1 TG hydrolases are expressed in mouse platelets

The expression of lipases in purified platelets was analyzed by reverse transcriptase-PCR and Western blotting experiments. I detected mRNA expression of Mgl and Atgl and very low expression of Hsl (Fig. 34A, lane 1). Whole blood RNA from wt mice (lane 2), Atgl-/- mice (lane 3), and H_20 (nCtrl, lane 4) were used as controls. Further, platelets (pooled from 6 wt mice) were purified and protein lysates were separated by SDS-Page (Fig. 34B, lane 1). WAT protein lysates from wt (lane 2) and lipase-deficient mice (lanes 3-5) were used as controls. Western blot analysis confirmed the presence of MGL and ATGL and an absent expression of HSL in mouse platelets. To investigate the purity of our platelet preparations, platelet RNA was analyzed by reverse transcriptase-PCR using primers specific for platelets (CD41), erythrocytes (CD235a), and leukocytes (CD45) (Fig. 34C, lane 1). As positive control RNA from whole blood was used (lane 2). According to mRNA queries from a plateletomics database MGL and ATGL belong to the top percentage of expressed genes also in humans, whereas HSL is much lower expressed (Fig. 34D). These findings indicate similar expressions of lipases in platelets from mice and humans.

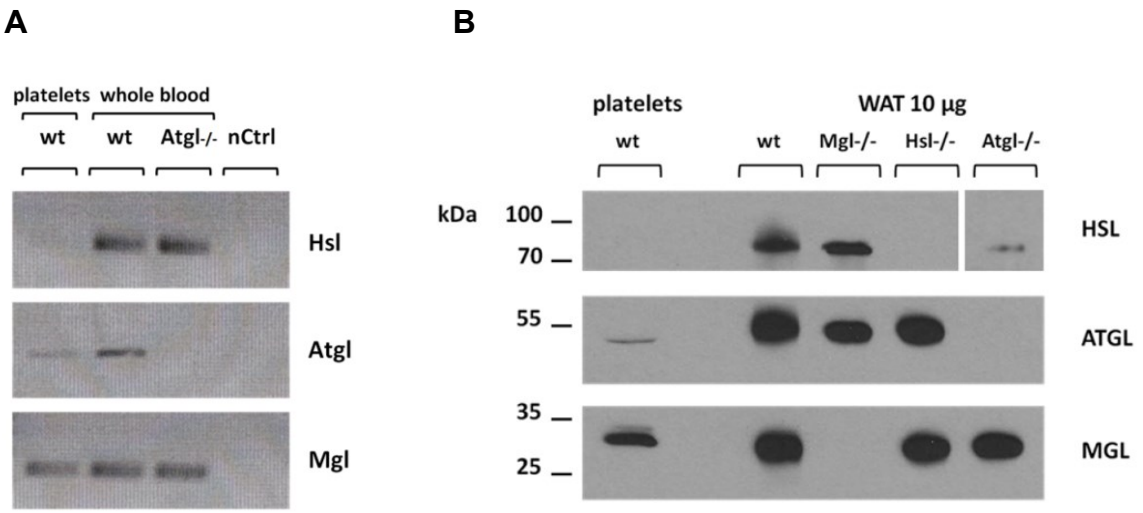

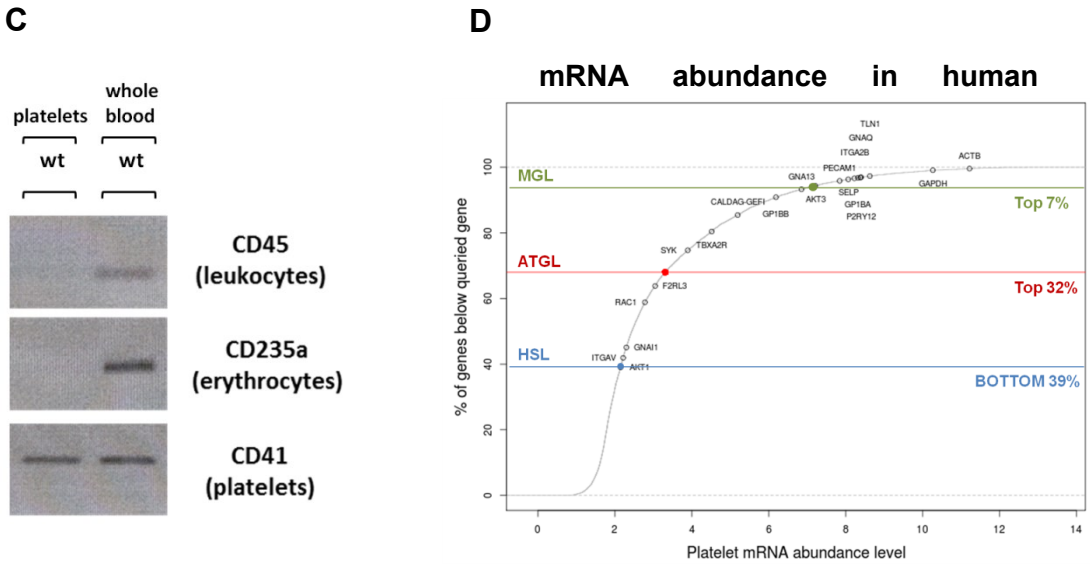

Figure 34: Lipases are expressed in mouse and human platelets

The expression of lipases was determined by (A) reverse transcriptase-PCR and (B) Western blot analysis. (C) To confirm the purity of platelets, platelet RNA was analyzed using primers specific for platelets, erythrocytes and leukocytes. (D) Data from the human plateletomics database http://www.plateletomics.org/plateletomics/ reveal expression of human MGL, ATGL, and HSL.

3.2 Unaltered morphology and spreading of Atgl-/- platelets

Platelets from wt and Atgl-/- mice were visualized using standard transmission electron microscopy (Fig. 35A), which revealed no significant morphological alterations. The two major organelles within platelets, α-granules (black arrows) and dense bodies (white arrows), as well as mitochondria and the open canalicular system are indicated. In contrast to macrophages lacking Atgl-/-, platelets from Atgl-/- mice look normal and show no indications of mitochondrial dysfunction or LD accumulation. In addition, the ability of platelets for adhesion and spreading was tested and visualized via scanning electron microscopy (Fig. 35B). We observed a similar spreading behavior between wt and Atgl-/- platelets.

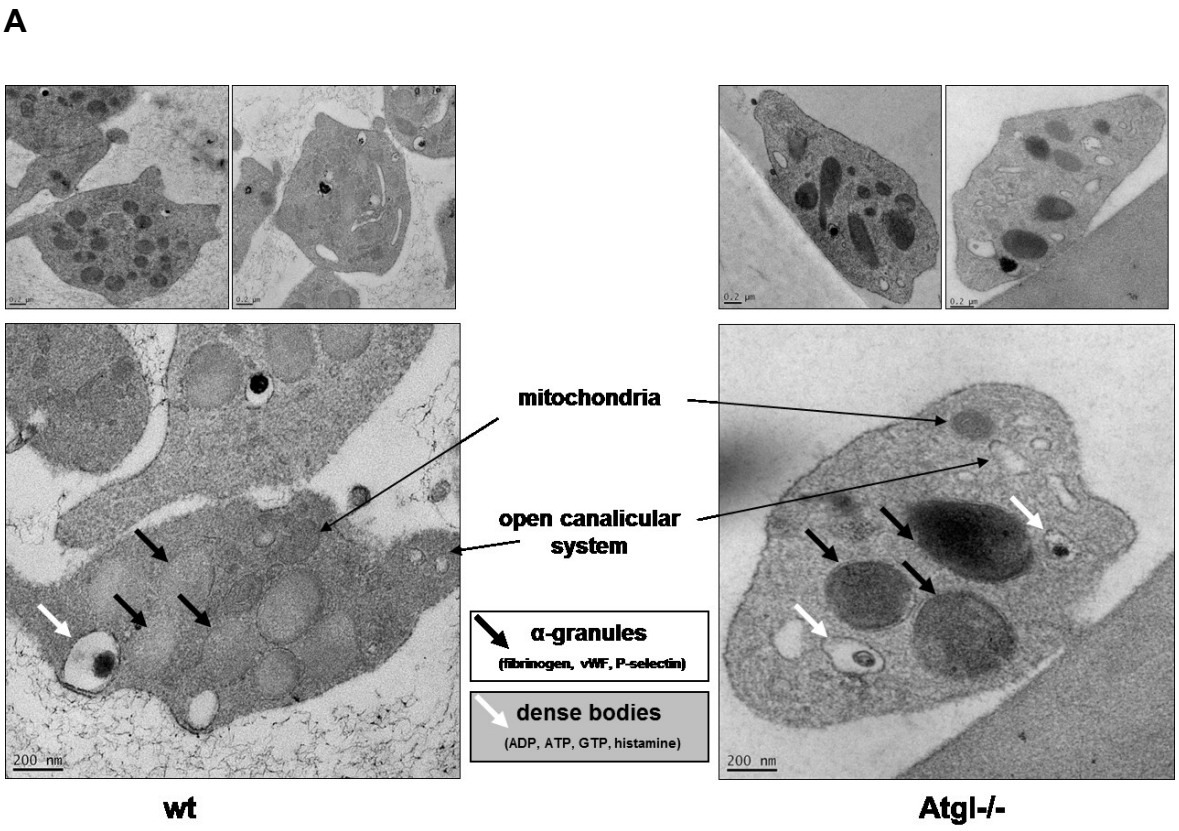

Figure 35: Unaltered morphology and spreading of Atgl-/- platelets

Platelets from wt and Atgl-/- mice were visualized by (A) standard transmission electron microscopy. (B) Spreading of platelets was visualized by scanning electron microscopy.

3.3 No evident lipid accumulation in Atgl-/- platelets

Neutral lipid and PL composition of purified platelets from wt and Atgl-/- mice were analyzed using TLC. Among neutral lipids, free cholesterol (FC) constitutes the most prominent class of lipids followed by FFA (Fig. 36A). Other detectable lipid species were TG, CE and a species close to the sample application that most likely resembles MG. PC and sphingomyelin could be determined as most abundant polar lipids in platelets (Fig. 36B). Impurities in the lipid extracts did not allow do make a statement on the content of PE and PS. A defined band close to the sample application most likely represents lysophosphatidylcholine (LysoPC). A marker for this species was not included in the standard lane.

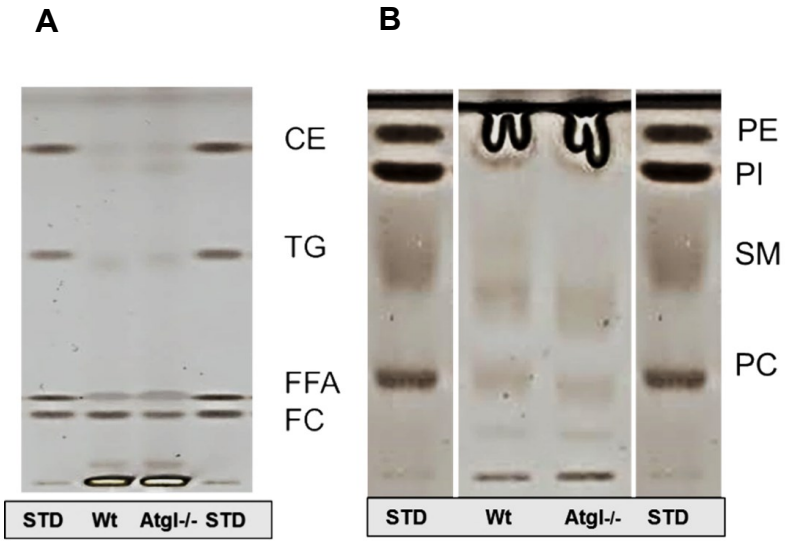

Figure 36: Lipid composition of platelets

Platelets (pooled from 6 mice) were isolated, lipids were extracted and separated by TLC. (A) Lipids were separated by hexane/diethylether/acetic acid/H2O (26/6/0.4/0.1; v/v/v/v): CE, cholesterol ester; TG, triglyceride; FFA, free fatty acid; FC, free cholesterol. (B) Phospholipids were separated by chloroform/methanol/acetic acid/H_2O (10/3/1.6/0.7; v/v/v/v) PE, phosphatidylethanolamine; PI, phosphatidylinositol; SM, sphingomyelin; PC, phosphatidylcholine; STD, standard

3.4 Reduced activation and shape change of Atgl-/- platelets in response to collagen

Blood from wt and Atgl-/- mice was incubated with the indicated agonists and platelet activation was measured by analysis of P-selectin expression (Fig. 37A) and integrin

αIIbβ3 activation (Fig. 37B), which are the two most commonly used markers for platelet activation. Blood from Atgl-/- mice showed reduced platelet activation in response to CRP, a synthetic peptide that mimics the structure of collagen and acts as a strong platelet agonist, but not to any other agonists tested including phorbol myristate acetate (PMA), protease-activated receptor 4 (PAR-4) agonist, ADP, thrombin and the TxA2 analog U46619. These results suggest that the reduced platelet activation is mediated selectively via the collagen receptor pathway.

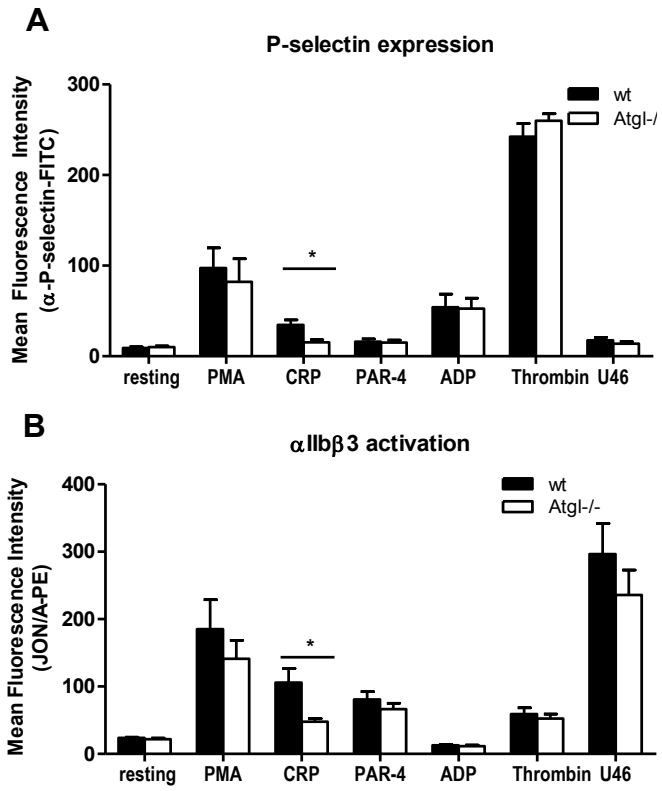

Figure 37: Reduced agonist-induced activation in response to CRP

Blood from wt and Atgl-/- mice was activated with various agonists in the presence of (A) FITC-conjugated anti-mouse P-selectin antibody or (B) JON/A-PE antibody directed against the activated form of mouse integrin αIIbβ3. Data are shown as geometric means of fluorescence intensity + SEM (n=4). (phorbol myristate acetate (PMA): 100 nmol/l; collagen-related peptide (CRP): 1 µg/ml; PAR-4: 600 µmol/l; ADP: 10 µmol/l; thrombin: 1U/ml; U46619: 3 µmol/l). *$p < 0.05$

Most platelet agonists can trigger shape change. During this process the discoid cells undergo cytoskeletal changes including the disassembly of a microtubule ring that results in an intermediate spherical shape. This is followed by actin polymerization and the formation of filopodia (171). These agonist-induced changes in platelet morphology can

be assessed by flow cytometry as changes in the forward scatter/side scatter properties of the cell (Fig. 38).

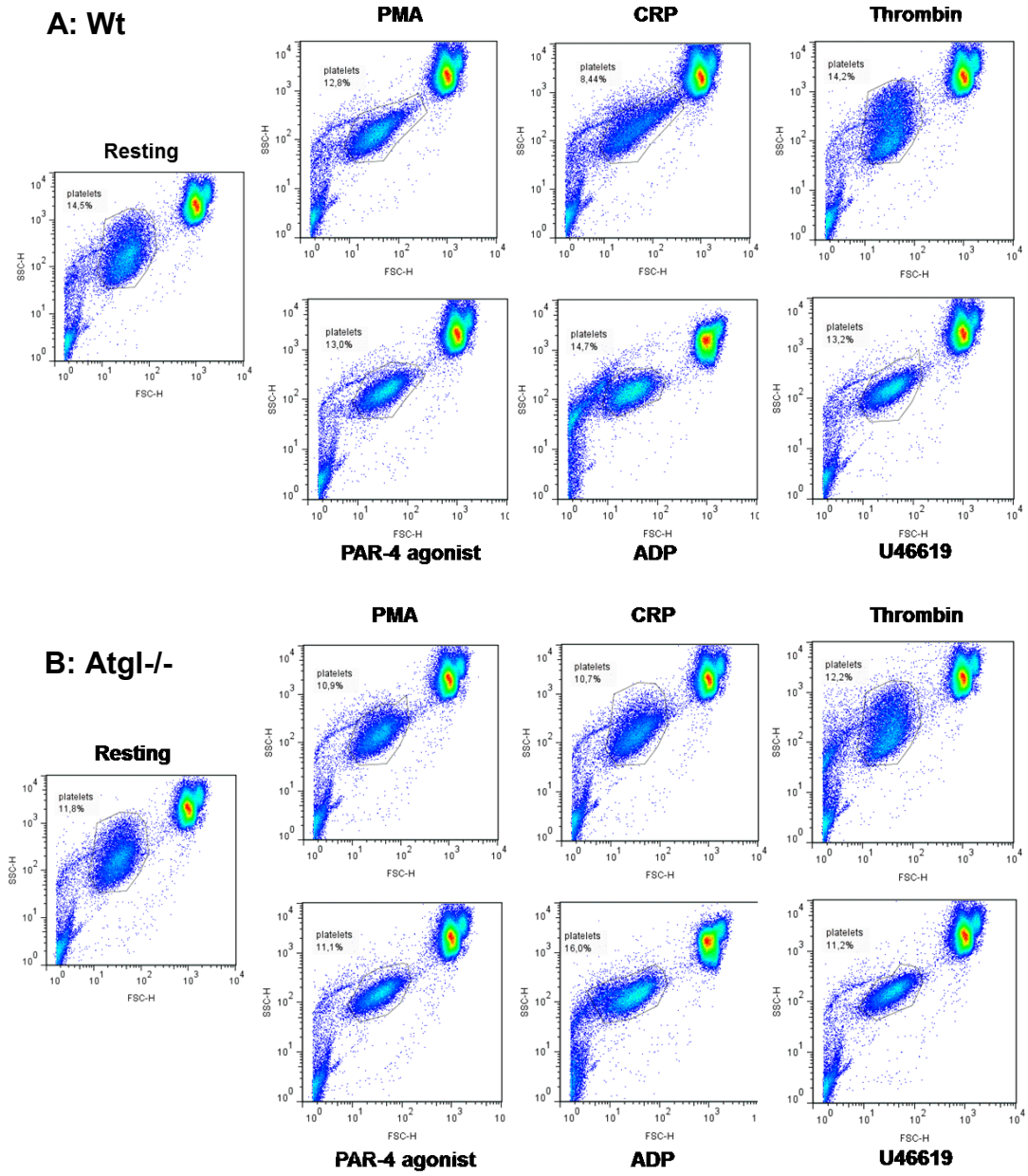

Figure 38: Reduced platelet shape change of Atgl-/- platelets in response to CRP

Platelet shape change was determined under resting and stimulated conditions by changes in the forward scatter (FSC)/side scatter (SSC) properties of (A) wt and (B) Atgl-/- cells. The figure depicts plots from one representative experiment, in which platelet shape change was induced with various agonists. (phorbol myristate acetate (PMA): 100 nmol/l; collagen-related peptide (CRP): 1 µg/ml; thrombin: 1U/ml; PAR-4: 600 µmol/l; ADP: 10 µmol/l; U46619: 3 µmol/l).

PMA, CRP, PAR-4 agonist, ADP, and U46619 induced a strong change in platelet forward-scatter/side-scatter, while the response to thrombin was rather weak (Fig. 38). Similar to earlier observations, Atgl-/- platelets showed an inhibited shape change after CRP activation (Fig. 38B), whereas the response to all other agonists tested, including PMA, thrombin, PAR-4 agonist, ADP, and U46619 was comparable to wt platelets (Fig. 38A).

3.5 Reduced *in vitro* thrombus formation in Atgl-/- mice

To study platelet reactivity, whole blood was perfused over collagen-coated channels and thrombus formation was recorded by fluorescence microscopy. A schematic picture of this method is shown in Fig. 39A. Fig. 39B depicts fluorescence images from wt (upper panel) and Atgl-/- blood (lower panel) after 1-3 min of perfusion with a markedly reduced thrombus formation in Atgl-/- mice. Thrombus-covered area was calculated by computerized image analysis and revealed a statistically significant difference in surface coverage in Atgl-/- blood between 2 to 3 min of perfusion (Fig. 39C). Iloprost, a structural analogue of PGI2, was used as a control as it is known to inhibit thrombus formation.

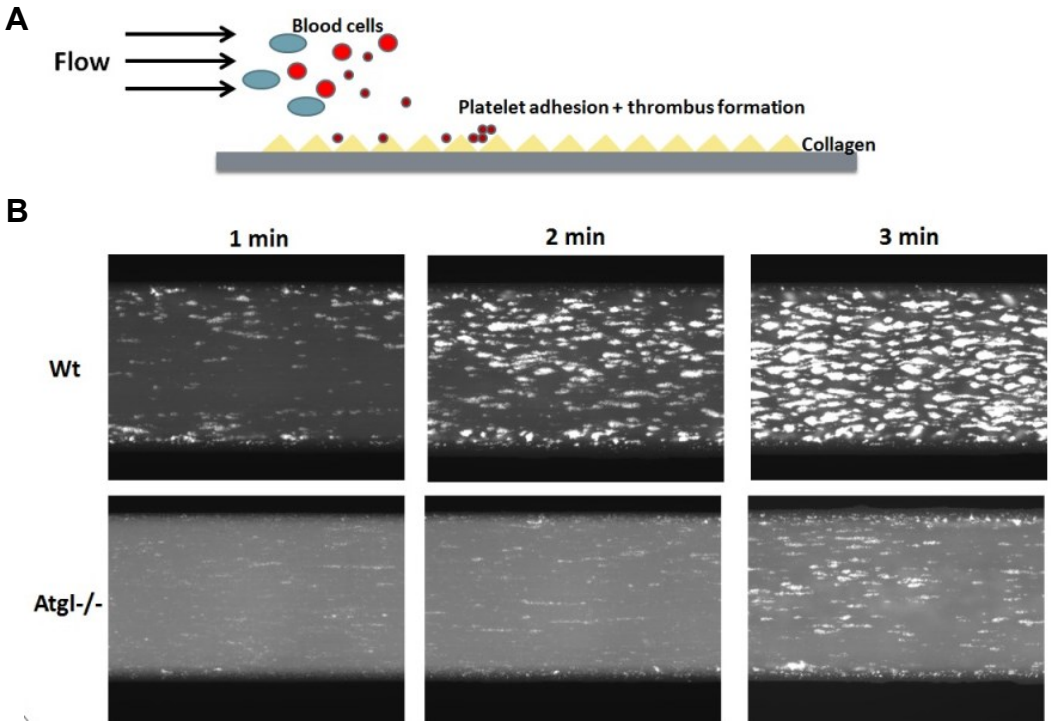

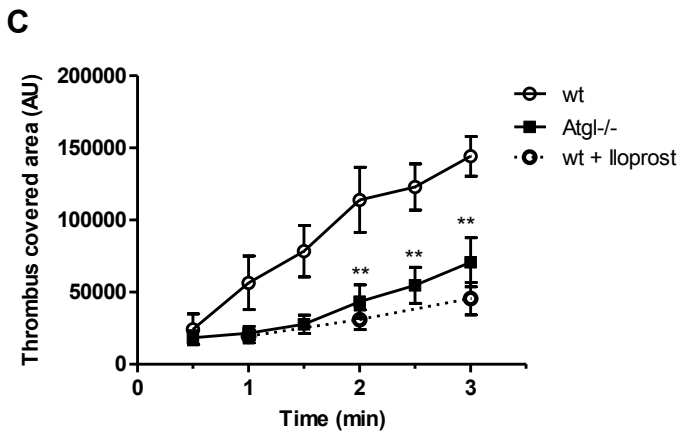

Figure 39: Reduced *in vitro* thrombus formation in Atgl-/- mice

(A) Platelet reactivity was tested by *in vitro* thrombus formation assay, in which platelets in whole blood were stained and perfused over collagen-coated channels. (B) Thrombus formation after 1-3 min of perfusion was recorded by fluorescence microscopy. (C) Thrombus-covered area was calculated by computerized image analysis. Iloprost, which causes an inhibition of thrombus formation in wt blood, was used as control. Data are shown in arbitrary units (AU) (mean ± SEM) (n=10 per group). **p ≤ 0.01

3.6 Unchanged platelet counts between wt and Atgl-/- mice

To exclude the possibility that the observed reduction in thrombus formation is caused by a reduced number of platelets, I determined platelet counts. This measurement revealed unaltered platelet counts between wt and Atgl-/- mice in both male and female mice (Fig. 40).

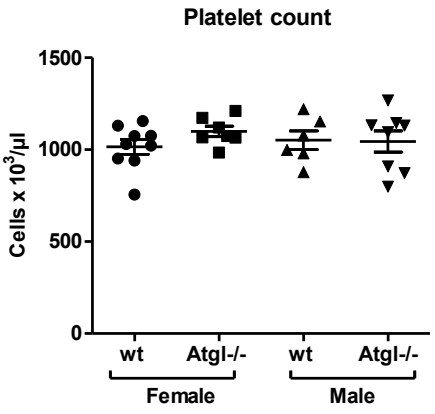

Figure 40: Unchanged platelet numbers in wt and Atgl-/- mice

Platelet counts from whole blood were performed using an automated cell counter. Data represent mean values ± SEM (n=6-9).

3.7 No difference in collagen receptor expression

Based on the observation of reduced platelet activation in response to collagen and CRP, I determined the expression level of the collagen receptor of wt platelets compared to Atgl-/- platelets, both in resting and CRP-stimulated cells (Fig. 41). The surface expression of GPVI, the collagen receptor in platelets, was comparable between both genotypes under the tested conditions. As reported earlier, various agonists induce shedding of the platelet collagen receptor (172). This receptor shedding was observed in wt and Atgl-/- platelets in response to CRP (1 µg, 10 µg) and was similar between wt and Atgl-/- platelets (Fig. 41).

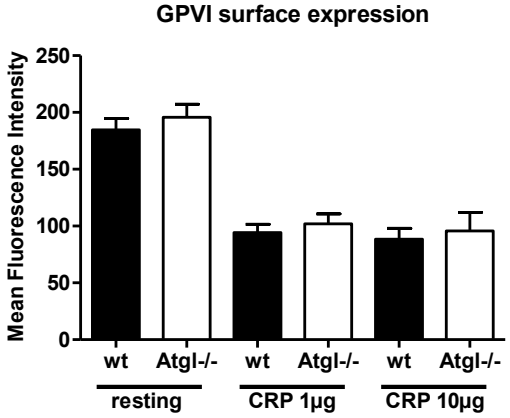

Figure 41: Unchanged GPVI expression in wt compared to Atgl-/- platelets

Whole blood (resting and CRP-stimulated) was stained with a FITC-conjugated anti-GPVI antibody and platelets were analyzed by flow cytometry. Data are shown as geometric mean of fluorescence intensity + SEM (n=5).

3.8 Unaltered plasma fibrinogen levels

Fibrinogen plays a pivotal role in the hemostatic balance by binding to platelets to support platelet aggregation and, hence, has a role in wound healing. Fibrinogen is synthesized by hepatocytes before it is secreted into the plasma. Since ATGL deficiency is associated with severe hepatosteatosis (102, 173), I investigated the capacity of the liver to produce fibrinogen. Plasma fibrinogen levels of fed and fasted wt and Atgl-/- mice were comparable. Therefore, alterations in fibrinogen levels can be excluded as possible cause for reduced *in vitro* thrombosis of Atgl-/- mice.

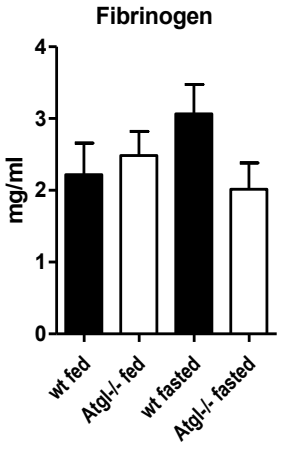

Figure 42: Unaltered plasma fibrinogen levels

Fibrinogen concentrations (mg/ml) in plasma in fed and 6 h fasted mice were determined by ELISA. Data represent mean values (n=6) + SEM.

3.9 *In vitro* thrombus formation in Hsl-/- and Mgl-/- mice

Thrombus formation under arterial flow conditions was also measured in whole blood from Hsl-/- and Mgl-/- mice. In comparison with blood from wt mice, blood from Mgl-/- mice showed significantly reduced thrombus formation as evident by reduced thrombus-covered area (Fig. 43). Blood from Hsl-/- mice revealed a comparable ability to form thrombi when perfused over collagen-coated surface. Interestingly, the thrombus formation in blood from Hsl-/- mice reached a steady state after 2 min of perfusion, while in blood from wt mice thrombus formation was still ongoing.

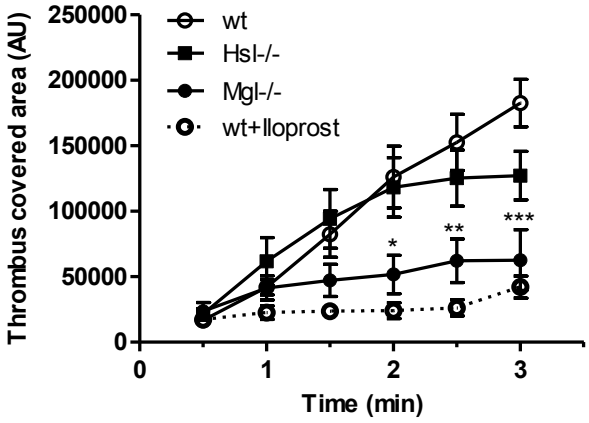

Figure 43: Thrombus formation is unchanged in Hsl-/- and reduced in Mgl-/- mice

Platelet reactivity was tested by *in vitro* thrombus formation assay, in which platelets in whole blood were stained, perfused over collagen-coated channels and thrombus formation was recorded after 1-3 min of perfusion by fluorescence microscopy. Iloprost was used as an inhibitor of thrombus formation in wt blood. Thrombus-covered area was calculated by computerized image analysis and is shown in arbitrary units (AU) (mean ± SEM) (n=4-10). *$p < 0.05$; **$p \leq 0.01$; ***$p \leq 0.001$

3.10 Discussion

In most cell types, lipolysis represents an important biochemical mechanism to generate FFAs, which are further used as energy substrates, precursors for lipid and membrane synthesis, and ligands for various signaling processes. Platelets derive their energy mostly from glycolysis. However, they contain mitochondria, are capable of *de novo* FA and phospholipid synthesis (174, 175) but the importance of FA β-oxidation for energy production is unclear (176).

Based on our observations, murine platelets express ATGL and MGL but lack HSL. According to genome-wide RNA-sequencing data from humans, MGL and ATGL are expressed in platelets (169). Unlike typical lipid-storing cells (e.g. adipocytes or macrophages), lipids in platelets are primarily membrane components. The plasma membrane of platelets is composed of a bilayer of PLs, which represent 75% of total platelet lipids. Neutral lipids constitute approximately 25% of total platelet lipids, with FC as predominant species (177). Lipid analysis by TLC revealed the presence of TGs in murine platelets. However, electron microscopy did not show evidence for the presence of LDs, neither in wt nor in Atgl-/- platelets. The present TGs in platelets could be derived from TG-rich plasma lipoproteins, such as VLDL and LDL that are trapped in the OCS. The fact that ATGL requires LD association to act as a TG hydrolase together with the absence of (TG-rich) LDs in platelets indicate an alternative function for ATGL in this type of cell. As reported earlier, ATGL has been assigned a functional role as phospholipase or transacylase (132). Rearrangement of FAs in PLs is an important process during platelet activation and several acyltransferases for the acylation of lysophospholipids have been detected in platelets (178, 179). The physiological relevance of these alternative enzyme functions for ATGL in platelets as well as other cells remains to be determined.

The lipid composition of membranes defines membrane-mediated platelet activities such as membrane fluidity, eicosanoid generation, and signaling pathways and can be influenced by various factors. A beneficial effect of statins as inhibitors of platelet aggregation is well described (148, 149). One of the suggested mechanisms is that statins influence platelet activity by lowering cholesterol content in the platelet plasma membrane (180). Similarly, changes in plasma lipoproteins have an important effect on platelet function. Whole body ATGL deficiency is accompanied by systemic changes of

lipid metabolism resulting in altered lipoprotein profiles: Plasma cholesterol, FFA as well as TG concentrations are markedly reduced and plasma lipid profiles show reduced VLDL, LDL, and HDL fractions (102). Hence, one causative explanation for the observed alterations in platelet function might be the dyslipidemia caused by a systemic lack of ATGL. To address this question, a more sensitive approach, such as mass spectrometry, is necessary to determine alterations in the lipid composition of Atgl-/- platelets. In addition, further analysis including platelet-specific Atgl-/- and Mgl-/- mice would help to clarify whether platelet-specific or systemic ATGL and MGL deficiency are causative for the observed alterations in platelet activity.

Our studies reveal decreased platelet activation associated with reduced granule release, integrin signaling, and thrombus formation in the absence of ATGL. Platelet number was not changed between wt and Atgl-/- animals, excluding the possibility that an altered abundance of platelets is the reason for this reduced thrombotic phenotype. Interestingly, the observed alterations in the activation in Atgl-/- platelets selectively affected one pathway. While stimulation with agonists such as ADP, thrombin, and TxA2 resulted in comparable platelet activation, collagen or CRP were not able to stimulate Atgl-/- platelets to the same extent as wt platelets. This finding indicates that the observed phenotype is specifically limited to the collagen GPVI receptor signaling pathway. However, surface expression levels of GPVI were comparable between wt and Atgl-/- platelets, suggesting a modulation of the intracellular signaling pathway downstream of GPVI.

A similar reduction in thrombus formation was also observed in Mgl-/- mice. These findings are in agreement with previously reported inhibitor studies showing a reduced activity of platelets lacking functional MGL (165). As underlying mechanism, a decreased cleavage of 2-AG resulting in reduced AA levels and a concomitant reduced generation and release of the pro-thrombotic lipid mediator TxA2 was reported. These observations, together with the findings derived from Atgl-/- neutrophil studies (Part I), implicate ATGL and MGL as key enzymes to regulate eicosanoid signaling. Whether a reduced generation of pro-thrombotic eicosanoids, either from platelets or other cells, is causative for the diminished thrombogenesis observed in the absence of these enzymes requires further evaluation.

In summary, my results indicate that the lipases ATGL and MGL are expressed in platelets. Additional research is necessary to fully ascertain the underlying mechanism(s) and whether the altered thrombogenic phenotype is caused by the platelet-specific or the systemic lack of these enzymes.

Table 1: Release of lipid mediators from peritoneal neutrophils

Wt neutrophils from peritoneal lavages one day post thioglycolate injection were cultured for 6 h in medium in the absence or presence of Atglistatin. Media were collected from non-activated and activated cells (0.5 µM A23187, 1 h). Data are shown as median (pg/ml) and range (n=6).

		Thioglycolate-stimulated				Thioglycolate +A23187-stimulated			
Pathway	**Lipid mediator**	**-Atglistatin**		**+Atglistatin**		**-Atglistatin**		**+Atglistatin**	
		median	range	median	range	median	range	media	range
COX-AA	6-keto-PGF1a	95	(29 - 467)	35*	(12 - 211)	152	(22 - 634)	94	(26 - 262)
COX-EPA	TxB3	3681	(2820 - 3961)	3159	(3002 - 3521)	2079	(1713 - 2525)	3142	(1940 - 3332)
COX-AA	TxB2	416	(170 - 527)	111*	(79 - 145)	241	(79 - 357)	77*	(61 - 99)
COX-AA	PGF2a	116	(58 - 145)	70	(54 - 74)	82	(65 - 105)	57	(53 - 61)
ROS, COX-AA	15-keto-PGF2a/ 8-iso-PGE2/ PGE2	1184	(617 - 1524)	343*	(252 - 434)	585	(319 - 1127)	230*	(147 - 320)
ROS, COX-AA	8-iso-PGE2/ PGE2	795	(364 - 1021)	190*	(132 - 227)	423	(194 - 704)	108*	(32 - 169)
COX-AA	PGD2	140	(105 - 177)	72	(65 - 73)	123	(77 - 201)	n.d.	
COX-DHGLA	PGD1	56	(51 - 57)	45	(44 - 45)	45	(44 - 51)	n.d.	
COX, ROS-AA	15-keto-PGE2/ 8-iso-15-keto PGE2	54	(49 - 59)	49*	(46 - 52)	55	(50 - 61)	47*	(46 - 52)
LOX-AA	LTE4	30	(27 - 35)	n.d.		99	(42 - 110)	33	(22 - 65)
COX-AA	PGJ2	20	(16 - 27)	15	(14 - 17)	18	(14 - 24)	n.d.	
LOX-AA	5(S).15(S)-DiHETE	n.d.		n.d.		78	(56 - 81)	62*	(57 - 68)
LOX-AA	LTB4	138	(137 - 153)	131*	(130 - 141)	971	(538 - 1252)	577*	(351 - 858)
LOX-AA	12-oxo-LTB4	n.d.		n.d.		195	(174 - 210)	172	(165 - 173)
LOX-AA	Tetranor-12(S)-HETE	58	(57 - 58)	60	(58 - 60)	58	(57 - 58)	58	(58 - 58)
COX-AA	12(S)-HHT	541	(269 - 739)	136*	(117 - 178)	311	(117 - 442)	104*	(77 - 135)
LOX-AA	5(S).6(S)-DiHETE	n.d.		n.d.		238	(185 - 284)	214	(160 - 274)
CYP-AA	5,6-DHET	168	(167 - 168)	167	(166 - 168)	167	(166 - 167)	167	(166 - 168)
CYP, LOX-AA	(±)18-HETE	41	(32 - 61)	41	(22 - 50)	22	(9 - 22)	24	(10 - 43)
LOX-EPA	12(S)-HEPE	n.d.		n.d.		142	(138 - 145)	140	(139 - 148)
CYP-AA	17(S)-HETE	154	(152 - 156)	152	(152 - 153)	151	(151 - 151)	152	(151 - 152)
LOX-EPA	5(S)-HEPE	189	(188 - 194)	186*	(185 - 187)	194	(191 - 203)	192	(187 - 192)
CYP, LOX-LA	(±)13-HODE	176	(47 - 885)	153	(90 - 216)	284	(120 - 615)	214	(59 - 345)
LOX-LA	(±)9-HODE	234	(104 - 805)	72	(27 - 107)	231	(72 - 428)	156	(59 - 204)
LOX, CYP-AA	15(S)-HETE	75	(57 - 91)	34*	(30 - 46)	88	(35 - 165)	48*	(17 - 85)
CYP, COX-AA	11-HETE	166	(89 - 232)	39*	(31 - 58)	101	(39 - 203)	28*	(10 - 61)
CYP, LOX-AA	8(S)-HETE	280	(244 - 303)	254	(230 - 267)	327	(267 - 407)	298	(222 - 393)
CYP, LOX-AA	12-HETE	15	(10 - 20)	19	(13 - 28)	72	(15 - 103)	51	(8 - 107)
LOX-AA	12-oxo-ETE	212	(210 - 213)	212	(210 - 212)	215	(211 - 220)	212	(212 - 216)
CYP, LOX-AA	5-HETE	40	(36 - 93)	18*	(13 - 33)	942	(519 - 1292)	613*	(257 - 929)
CYP-AA	(±)14,15-EET	135	(133 - 136)	n.d.		135	(134 - 136)	n.d.	
LOX-AA	5-oxo-ETE	295	(293 - 304)	n.d.		308	(300 - 316)	305	(291 - 315)
CYP-AA	(±)8,9-EET	509	(504 - 517)	500	(499 - 505)	502	(497 - 503)	498	(496 - 499)

n.d., not detected; presence vs. absence of Atglistatin, *$p < 0.05$

Fig. S1: Gating strategy of peripheral blood cells

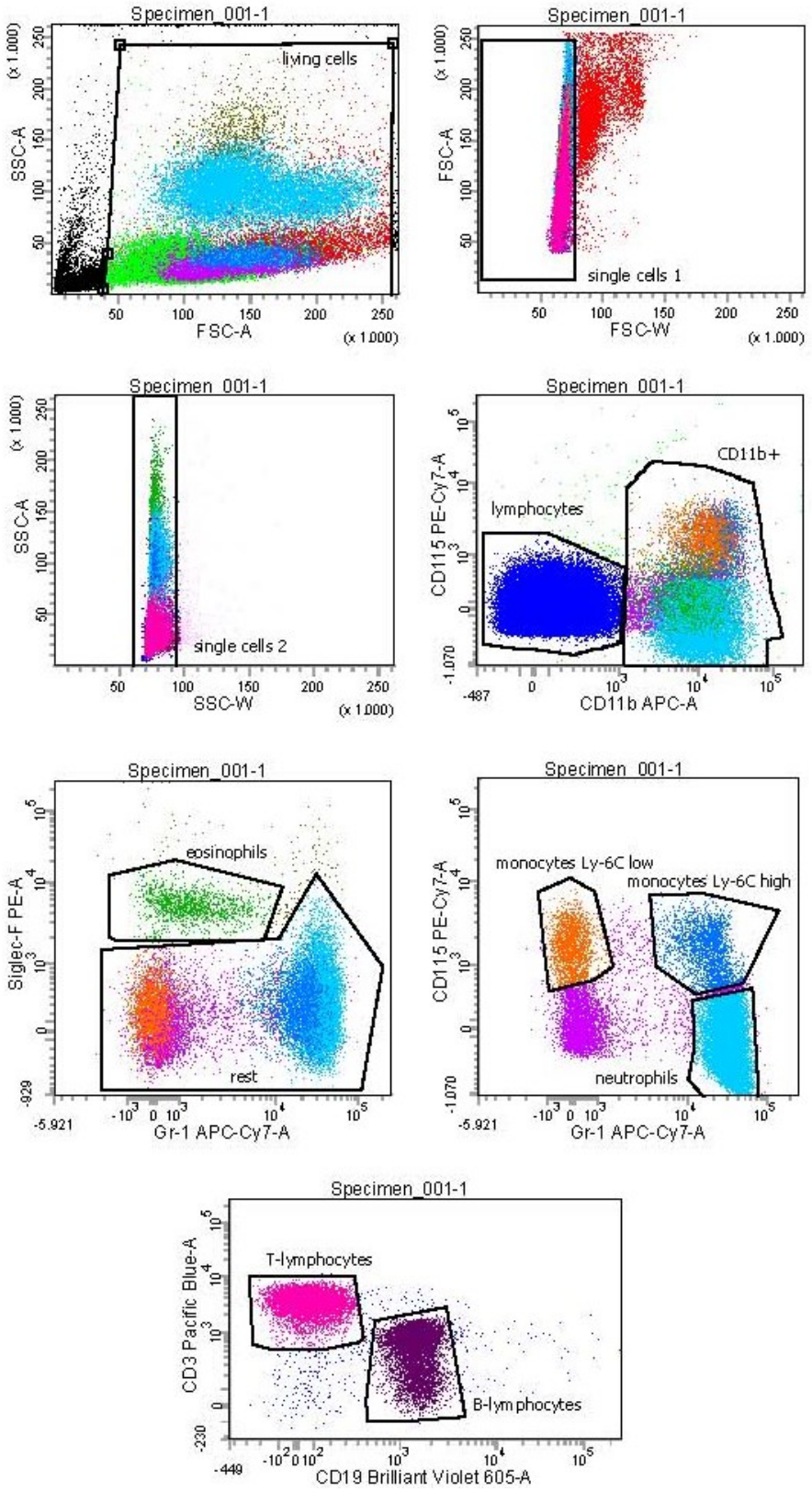

Fig. S2: Gating strategy of peritoneal lavage

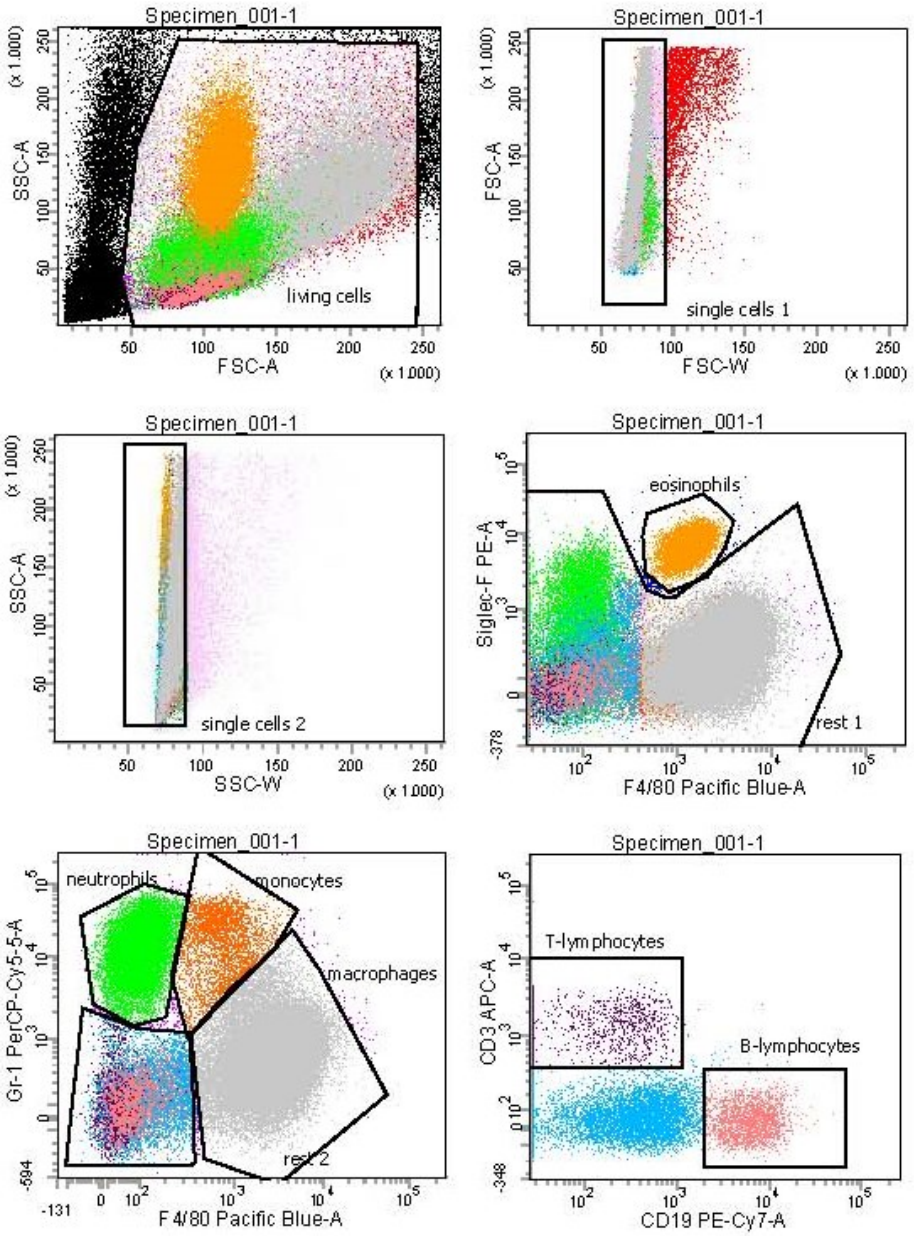

Fig. S3: Gating strategy of bone marrow

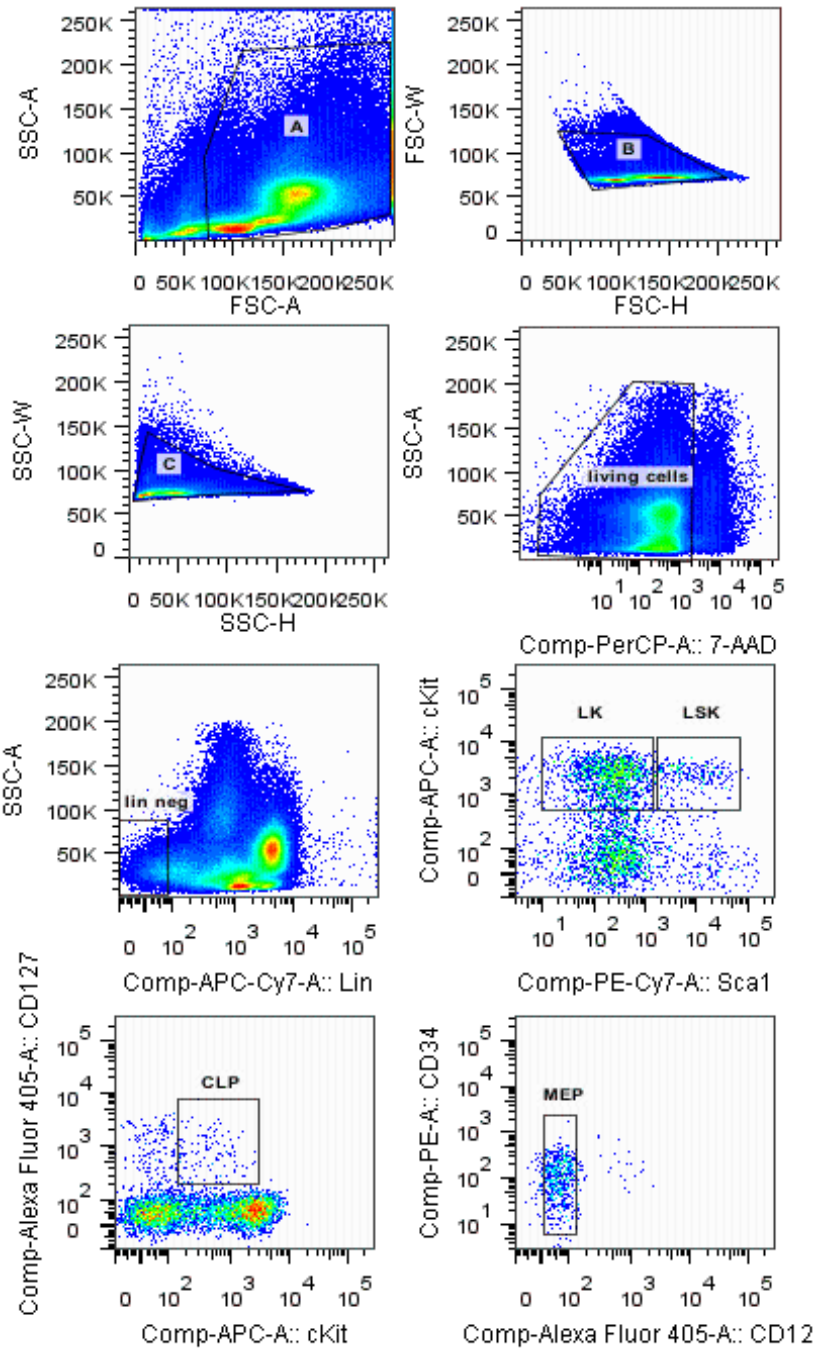

Fig. S4: Gating strategy of bone marrow

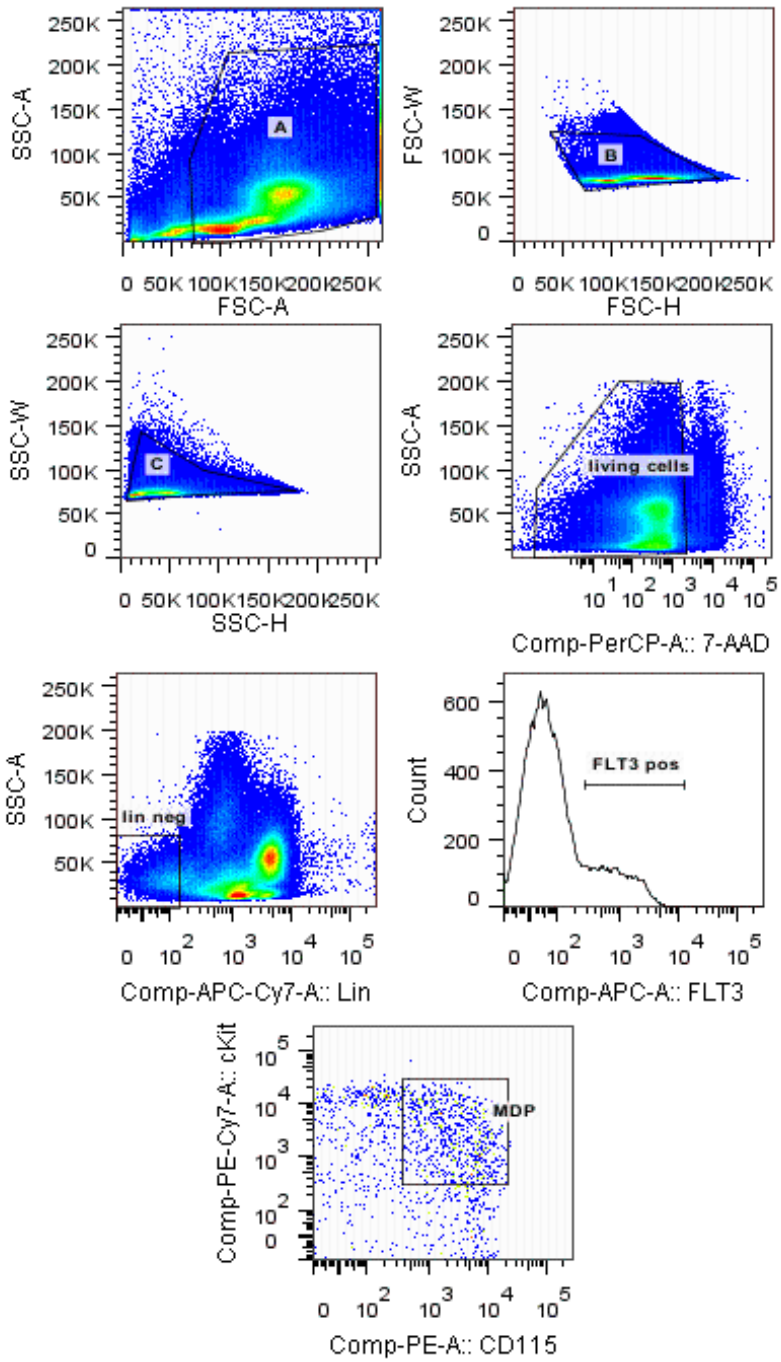

Fig. S5: Gating strategy of bone marrow

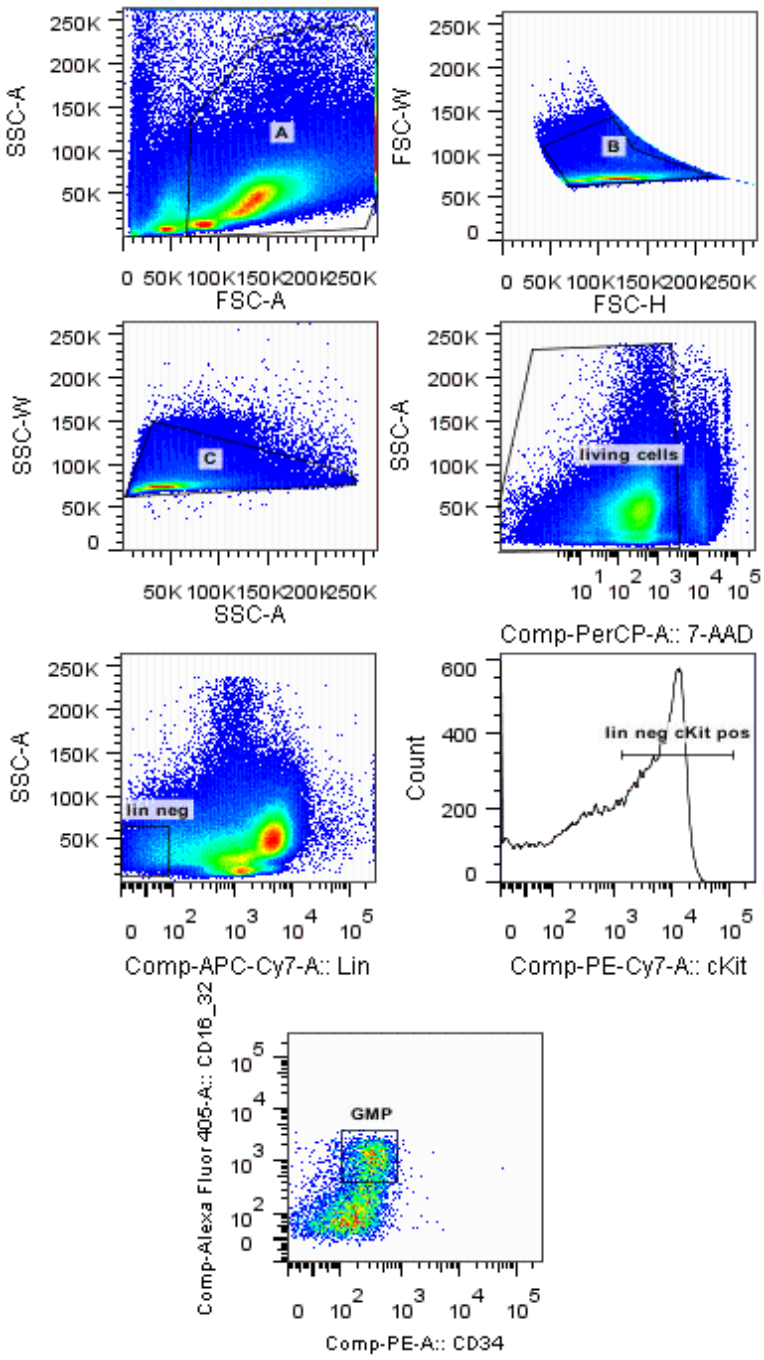

REFERENCES

1. Ibarguren M, Lopez DJ, Escriba PV. (2014) The effect of natural and synthetic fatty acids on membrane structure, microdomain organization, cellular functions and human health. *Biochim Biophys Acta*. 1838 (6):1518-28.

2. Wymann MP, Schneiter R. (2008) Lipid signalling in disease. *Nat Rev Mol Cell Biol*. 9 (2):162-76.

3. Fessler MB, Parks JS. (2011) Intracellular lipid flux and membrane microdomains as organizing principles in inflammatory cell signaling. *J Immunol*. 187 (4):1529-35.

4. Murphy AJ, Woollard KJ, Suhartoyo A, Stirzaker RA, Shaw J, Sviridov D, et al. (2011) Neutrophil activation is attenuated by high-density lipoprotein and apolipoprotein A-I in in vitro and in vivo models of inflammation. *Arterioscler Thromb Vasc Biol*. 31 (6):1333-41.

5. Pearce EL, Pearce EJ. (2013) Metabolic pathways in immune cell activation and quiescence. *Immunity*. 38 (4):633-43.

6. Dvorak AM, Dvorak HF, Peters SP, Shulman ES, MacGlashan DW, Jr., Pyne K, et al. (1983) Lipid bodies: cytoplasmic organelles important to arachidonate metabolism in macrophages and mast cells. *J Immunol*. 131 (6):2965-76.

7. Melo RC, Weller PF. (2014) Unraveling the complexity of lipid body organelles in human eosinophils. *J Leukoc Biol*. 96 (5):703-12.

8. Bozza PT, Bandeira-Melo C. (2005) Mechanisms of leukocyte lipid body formation and function in inflammation. *Mem Inst Oswaldo Cruz*. 100 Suppl 1:113-20.

9. Weller PF, Ackerman SJ, Nicholson-Weller A, Dvorak AM. (1989) Cytoplasmic lipid bodies of human neutrophilic leukocytes. *Am J Pathol*. 135 (5):947-59.

10. Weller PF, Ryeom SW, Picard ST, Ackerman SJ, Dvorak AM. (1991) Cytoplasmic lipid bodies of neutrophils: formation induced by cis-unsaturated fatty acids and mediated by protein kinase C. *J Cell Biol*. 113 (1):137-46.

11. Bozza PT, Payne JL, Goulet JL, Weller PF. (1996) Mechanisms of platelet-activating factor-induced lipid body formation: requisite roles for 5-lipoxygenase and de novo protein synthesis in the compartmentalization of neutrophil lipids. *J Exp Med*. 183 (4):1515-25.

12. Wilfling F, Haas JT, Walther TC, Farese RV, Jr. (2014) Lipid droplet biogenesis. *Curr Opin Cell Biol*. 29:39-45.

13. Long AP, Manneschmidt AK, VerBrugge B, Dortch MR, Minkin SC, Prater KE, et al. (2012) Lipid droplet de novo formation and fission are linked to the cell cycle in fission yeast. *Traffic*. 13 (5):705-14.

14. Murphy DJ. (2001) The biogenesis and functions of lipid bodies in animals, plants and microorganisms. *Prog Lipid Res*. 40 (5):325-438.

15. Walther TC, Farese RV, Jr. (2012) Lipid droplets and cellular lipid metabolism. *Annu Rev Biochem*. 81:687-714.

16. Kuerschner L, Moessinger C, Thiele C. (2008) Imaging of lipid biosynthesis: how a neutral lipid enters lipid droplets. *Traffic*. 9 (3):338-52.

17. McFie PJ, Banman SL, Kary S, Stone SJ. (2011) Murine diacylglycerol acyltransferase-2 (DGAT2) can catalyze triacylglycerol synthesis and promote lipid droplet formation independent of its localization to the endoplasmic reticulum. *J Biol Chem*. 286 (32):28235-46.

18. Fujimoto T, Ohsaki Y, Cheng J, Suzuki M, Shinohara Y. (2008) Lipid droplets: a classic organelle with new outfits. *Histochem Cell Biol*. 130 (2):263-79.

19. Tan JS, Seow CJ, Goh VJ, Silver DL. (2014) Recent advances in understanding proteins involved in lipid droplet formation, growth and fusion. *J Genet Genomics*. 41 (5):251-9.

20. Hashemi HF, Goodman JM. (2015) The life cycle of lipid droplets. *Curr Opin Cell Biol*. 33:119-24.

21. D'Avila H, Maya-Monteiro CM, Bozza PT. (2008) Lipid bodies in innate immune response to bacterial and parasite infections. *Int Immunopharmacol*. 8 (10):1308-15.

22. Bozza PT, Magalhaes KG, Weller PF. (2009) Leukocyte lipid bodies - Biogenesis and functions in inflammation. *Biochim Biophys Acta*. 1791 (6):540-51.

23. Dichlberger A, Schlager S, Lappalainen J, Kakela R, Hattula K, Butcher SJ, et al. (2011) Lipid body formation during maturation of human mast cells. *J Lipid Res*. 52 (12):2198-208.

24. Melo RC, D'Avila H, Wan HC, Bozza PT, Dvorak AM, Weller PF. (2011) Lipid bodies in inflammatory cells: structure, function, and current imaging techniques. *J Histochem Cytochem*. 59 (5):540-56.

25. Pacheco P, Bozza FA, Gomes RN, Bozza M, Weller PF, Castro-Faria-Neto HC, et al. (2002) Lipopolysaccharide-induced leukocyte lipid body formation in vivo: innate immunity elicited intracellular Loci involved in eicosanoid metabolism. *J Immunol*. 169 (11):6498-506.

26. Melo RC, Dvorak AM. (2012) Lipid body-phagosome interaction in macrophages during infectious diseases: host defense or pathogen survival strategy? *PLoS Pathog*. 8 (7):e1002729.

27. Meester I, Rosas-Taraco AG, Solís-Soto JM, Salinas-Carmona MC. (2011) The roles of lipid droplets in human infectious disease. *Medicina Universitaria*. 13 (53):207–16.

28. Saka HA, Valdivia R. (2012) Emerging roles for lipid droplets in immunity and host-pathogen interactions. *Annu Rev Cell Dev Biol*. 28:411-37.

29. Lutas EM, Zucker-Franklin D. (1977) Formation of lipid inclusions in normal human leukocytes. *Blood*. 49 (2):309-20.

30. Triggiani M, Oriente A, de Crescenzo G, Rossi G, Marone G. (1995) Biochemical functions of a pool of arachidonic acid associated with triglycerides in human inflammatory cells. *Int Arch Allergy Immunol*. 107 (1-3):261-3.

31. Blaner WS, O'Byrne SM, Wongsiriroj N, Kluwe J, D'Ambrosio DM, Jiang H, et al. (2009) Hepatic stellate cell lipid droplets: a specialized lipid droplet for retinoid storage. *Biochim Biophys Acta*. 1791 (6):467-73.

32. Bartz R, Li WH, Venables B, Zehmer JK, Roth MR, Welti R, et al. (2007) Lipidomics reveals that adiposomes store ether lipids and mediate phospholipid traffic. *J Lipid Res*. 48 (4):837-47.

33. Tauchi-Sato K, Ozeki S, Houjou T, Taguchi R, Fujimoto T. (2002) The surface of lipid droplets is a phospholipid monolayer with a unique Fatty Acid composition. *J Biol Chem*. 277 (46):44507-12.

34. Triggiani M, Oriente A, Seeds MC, Bass DA, Marone G, Chilton FH. (1995) Migration of human inflammatory cells into the lung results in the remodeling of arachidonic acid into a triglyceride pool. *J Exp Med*. 182 (5):1181-90.

35. Wolins NE, Quaynor BK, Skinner JR, Schoenfish MJ, Tzekov A, Bickel PE. (2005) S3-12, Adipophilin, and TIP47 package lipid in adipocytes. *J Biol Chem*. 280 (19):19146-55.

36. Brasaemle DL. (2007) Thematic review series: adipocyte biology. The perilipin family of structural lipid droplet proteins: stabilization of lipid droplets and control of lipolysis. *J Lipid Res*. 48 (12):2547-59.

37. Lass A, Zimmermann R, Oberer M, Zechner R. (2011) Lipolysis - a highly regulated multi-enzyme complex mediates the catabolism of cellular fat stores. *Prog Lipid Res*. 50 (1):14-27.

38. Wang H, Bell M, Sreenivasan U, Hu H, Liu J, Dalen K, et al. (2011) Unique regulation of adipose triglyceride lipase (ATGL) by perilipin 5, a lipid droplet-associated protein. *J Biol Chem*. 286 (18):15707-15.

39. Larigauderie G, Furman C, Jaye M, Lasselin C, Copin C, Fruchart JC, et al. (2004) Adipophilin enhances lipid accumulation and prevents lipid efflux from THP-1 macrophages: potential role in atherogenesis. *Arterioscler Thromb Vasc Biol*. 24 (3):504-10.

40. Wolins NE, Skinner JR, Schoenfish MJ, Tzekov A, Bensch KG, Bickel PE. (2003) Adipocyte protein S3-12 coats nascent lipid droplets. *J Biol Chem*. 278 (39):37713-21.

41. Ohsaki Y, Suzuki M, Fujimoto T. (2014) Open questions in lipid droplet biology. *Chem Biol*. 21 (1):86-96.

42. Zehmer JK, Bartz R, Liu P, Anderson RG. (2008) Identification of a novel N-terminal hydrophobic sequence that targets proteins to lipid droplets. *J Cell Sci*. 121 (Pt 11):1852-60.

43. Robenek H, Lorkowski S, Schnoor M, Troyer D. (2005) Spatial integration of TIP47 and adipophilin in macrophage lipid bodies. *J Biol Chem*. 280 (7):5789-94.

44. Robenek H, Robenek MJ, Troyer D. (2005) PAT family proteins pervade lipid droplet cores. *J Lipid Res*. 46 (6):1331-8.

45. Robenek MJ, Severs NJ, Schlattmann K, Plenz G, Zimmer KP, Troyer D, et al. (2004) Lipids partition caveolin-1 from ER membranes into lipid droplets: updating the model of lipid droplet biogenesis. *FASEB J*. 18 (7):866-8.

46. Hodges BD, Wu CC. (2010) Proteomic insights into an expanded cellular role for cytoplasmic lipid droplets. *J Lipid Res*. 51 (2):262-73.

47. Bozza PT, Yu W, Weller PF. (1997) Mechanisms of formation and function of eosinophil lipid bodies: inducible intracellular sites involved in arachidonic acid metabolism. *Mem Inst Oswaldo Cruz*. 92 Suppl 2:135-40.

48. Chandak PG, Radovic B, Aflaki E, Kolb D, Buchebner M, Frohlich E, et al. (2010) Efficient phagocytosis requires triacylglycerol hydrolysis by adipose triglyceride lipase. *J Biol Chem*. 285 (26):20192-201.

49. Escary JL, Choy HA, Reue K, Schotz MC. (1998) Hormone-sensitive lipase overexpression increases cholesteryl ester hydrolysis in macrophage foam cells. *Arterioscler Thromb Vasc Biol*. 18 (6):991-8.

50. Buchebner M, Pfeifer T, Rathke N, Chandak PG, Lass A, Schreiber R, et al. (2010) Cholesteryl ester hydrolase activity is abolished in HSL-/- macrophages but unchanged in macrophages lacking KIAA1363. *J Lipid Res*. 51 (10):2896-908.

51. Fredrikson G, Tornqvist H, Belfrage P. (1986) Hormone-sensitive lipase and monoacylglycerol lipase are both required for complete degradation of adipocyte triacylglycerol. *Biochim Biophys Acta*. 876 (2):288-93.

52. Yeaman SJ. (1990) Hormone-sensitive lipase--a multipurpose enzyme in lipid metabolism. *Biochim Biophys Acta*. 1052 (1):128-32.

53. Xie S, Borazjani A, Hatfield MJ, Edwards CC, Potter PM, Ross MK. (2010) Inactivation of lipid glyceryl ester metabolism in human THP1 monocytes/macrophages by activated organophosphorus insecticides: role of carboxylesterases 1 and 2. *Chem Res Toxicol*. 23 (12):1890-904.

54. Dinh TP, Carpenter D, Leslie FM, Freund TF, Katona I, Sensi SL, et al. (2002) Brain monoglyceride lipase participating in endocannabinoid inactivation. *Proc Natl Acad Sci U S A*. 99 (16):10819-24.

55. Singh R, Cuervo AM. (2012) Lipophagy: connecting autophagy and lipid metabolism. *Int J Cell Biol*. 2012:282041.

56. Singh R, Kaushik S, Wang Y, Xiang Y, Novak I, Komatsu M, et al. (2009) Autophagy regulates lipid metabolism. *Nature*. 458 (7242):1131-5.

57. Singh R, Xiang Y, Wang Y, Baikati K, Cuervo AM, Luu YK, et al. (2009) Autophagy regulates adipose mass and differentiation in mice. *J Clin Invest*. 119 (11):3329-39.

58. Liu K, Czaja MJ. (2013) Regulation of lipid stores and metabolism by lipophagy. *Cell Death Differ*. 20 (1):3-11.

59. Kaushik S, Rodriguez-Navarro JA, Arias E, Kiffin R, Sahu S, Schwartz GJ, et al. (2011) Autophagy in hypothalamic AgRP neurons regulates food intake and energy balance. *Cell Metab*. 14 (2):173-83.

60. Rambold AS, Cohen S, Lippincott-Schwartz J. (2015) Fatty acid trafficking in starved cells: regulation by lipid droplet lipolysis, autophagy, and mitochondrial fusion dynamics. *Dev Cell*. 32 (6):678-92.

61. Ma Y, Galluzzi L, Zitvogel L, Kroemer G. (2013) Autophagy and cellular immune responses. *Immunity*. 39 (2):211-27.

62. Ouimet M, Franklin V, Mak E, Liao X, Tabas I, Marcel YL. (2011) Autophagy regulates cholesterol efflux from macrophage foam cells via lysosomal acid lipase. *Cell Metab*. 13 (6):655-67.

63. Goeritzer M, Vujic N, Schlager S, Chandak PG, Korbelius M, Gottschalk B, et al. (2015) Active autophagy but not lipophagy in macrophages with defective lipolysis. *Biochim Biophys Acta*.in press.

64. Thiam AR, Farese RV, Jr., Walther TC. (2013) The biophysics and cell biology of lipid droplets. *Nat Rev Mol Cell Biol*. 14 (12):775-86.

65. Resh MD. (1999) Fatty acylation of proteins: new insights into membrane targeting of myristoylated and palmitoylated proteins. *Biochim Biophys Acta*. 1451 (1):1-16.

66. Choudhary C, Weinert BT, Nishida Y, Verdin E, Mann M. (2014) The growing landscape of lysine acetylation links metabolism and cell signalling. *Nat Rev Mol Cell Biol*. 15 (8):536-50.

67. Eichmann TO, Kumari M, Haas JT, Farese RV, Jr., Zimmermann R, Lass A, et al. (2012) Studies on the substrate and stereo/regioselectivity of adipose triglyceride lipase, hormone-sensitive lipase, and diacylglycerol-O-acyltransferases. *J Biol Chem*. 287 (49):41446-57.

68. Zechner R. (2015) FAT FLUX: enzymes, regulators, and pathophysiology of intracellular lipolysis. *EMBO Mol Med*. 7 (4):359-62.

69. Welte MA. (2007) Proteins under new management: lipid droplets deliver. *Trends Cell Biol*. 17 (8):363-9.

70. Herker E, Ott M. (2011) Unique ties between hepatitis C virus replication and intracellular lipids. *Trends Endocrinol Metab*. 22 (6):241-8.

71. Herker E, Ott M. (2012) Emerging role of lipid droplets in host/pathogen interactions. *J Biol Chem*. 287 (4):2280-7.

72. Harris C, Herker E, Farese RV, Jr., Ott M. (2011) Hepatitis C virus core protein decreases lipid droplet turnover: a mechanism for core-induced steatosis. *J Biol Chem*. 286 (49):42615-25.

73. Cocchiaro JL, Valdivia RH. (2009) New insights into Chlamydia intracellular survival mechanisms. *Cell Microbiol*. 11 (11):1571-8.

74. Bougneres L, Helft J, Tiwari S, Vargas P, Chang BH, Chan L, et al. (2009) A role for lipid bodies in the cross-presentation of phagocytosed antigens by MHC class I in dendritic cells. *Immunity*. 31 (2):232-44.

75. Bozza PT, Bakker-Abreu I, Navarro-Xavier RA, Bandeira-Melo C. (2011) Lipid body function in eicosanoid synthesis: an update. *Prostaglandins Leukot Essent Fatty Acids*. 85 (5):205-13.

76. Bozza PT, Viola JP. (2010) Lipid droplets in inflammation and cancer. *Prostaglandins Leukot Essent Fatty Acids*. 82 (4-6):243-50.

77. Balaban S, Lee LS, Schreuder M, Hoy AJ. (2015) Obesity and Cancer Progression: Is There a Role of Fatty Acid Metabolism? *Biomed Res Int*. 2015:274585.

78. Jordans GH. (1953) The familial occurrence of fat containing vacuoles in the leukocytes diagnosed in two brothers suffering from dystrophia musculorum progressiva (ERB.). *Acta Med Scand*. 145 (6):419-23.

79. Lefevre C, Jobard F, Caux F, Bouadjar B, Karaduman A, Heilig R, et al. (2001) Mutations in CGI-58, the gene encoding a new protein of the esterase/lipase/thioesterase subfamily, in Chanarin-Dorfman syndrome. *Am J Hum Genet*. 69 (5):1002-12.

80. Fischer J, Lefevre C, Morava E, Mussini JM, Laforet P, Negre-Salvayre A, et al. (2007) The gene encoding adipose triglyceride lipase (PNPLA2) is mutated in neutral lipid storage disease with myopathy. *Nat Genet*. 39 (1):28-30.

81. Igal RA, Rhoads JM, Coleman RA. (1997) Neutral lipid storage disease with fatty liver and cholestasis. *J Pediatr Gastroenterol Nutr*. 25 (5):541-7.

82. Wolf R, Zaritzky A, Pollak S. (1988) Value of looking at leukocytes in every case of ichthyosis. *Dermatologica*. 177 (4):237-40.

83. Bernstein DL, Hulkova H, Bialer MG, Desnick RJ. (2013) Cholesteryl ester storage disease: review of the findings in 135 reported patients with an underdiagnosed disease. *J Hepatol*. 58 (6):1230-43.

84. Grabowski GA, Charnas L, Du H. Lysosomal acid lipase deficiencies: the Wolman disease/cholesteryl ester storage disease spectrum. 2012. In: The Online Metabolic and Molecular Bases of Inherited Disease [Internet]. New York, NY, USA: The McGraw-Hill Companies, Inc.

85. Bozza PT, Payne JL, Morham SG, Langenbach R, Smithies O, Weller PF. (1996) Leukocyte lipid body formation and eicosanoid generation: cyclooxygenase-independent inhibition by aspirin. *Proc Natl Acad Sci U S A*. 93 (20):11091-6.

86. Finstad HS, Kolset SO, Holme JA, Wiger R, Farrants AK, Blomhoff R, et al. (1994) Effect of n-3 and n-6 fatty acids on proliferation and differentiation of promyelocytic leukemic HL-60 cells. *Blood*. 84 (11):3799-809.

87. Weller PF, Monahan-Earley RA, Dvorak HF, Dvorak AM. (1991) Cytoplasmic lipid bodies of human eosinophils. Subcellular isolation and analysis of arachidonate incorporation. *Am J Pathol*. 138 (1):141-8.

88. Yu W, Bozza PT, Tzizik DM, Gray JP, Cassara J, Dvorak AM, et al. (1998) Co-compartmentalization of MAP kinases and cytosolic phospholipase A2 at cytoplasmic arachidonate-rich lipid bodies. *Am J Pathol*. 152 (3):759-69.

89. Chilton FH, Murphy RC. (1986) Remodeling of arachidonate-containing phosphoglycerides within the human neutrophil. *J Biol Chem*. 261 (17):7771-7.

90. Buckley CD, Gilroy DW, Serhan CN, Stockinger B, Tak PP. (2013) The resolution of inflammation. *Nat Rev Immunol*. 13 (1):59-66.

91. Kortz L, Dorow J, Ceglarek U. (2014) Liquid chromatography-tandem mass spectrometry for the analysis of eicosanoids and related lipids in human biological matrices: a review. *J Chromatogr B Analyt Technol Biomed Life Sci*. 964:1-11.

92. Irvine RF. (1982) How is the level of free arachidonic acid controlled in mammalian cells? *Biochem J*. 204 (1):3-16.

93. eAstudillo AM, Balgoma D, Balboa MA, Balsinde J. (2012) Dynamics of arachidonic acid mobilization by inflammatory cells. *Biochim Biophys Acta*. 1821 (2):249-56.

94. Mounier CM, Ghomashchi F, Lindsay MR, James S, Singer AG, Parton RG, et al. (2004) Arachidonic acid release from mammalian cells transfected with human groups IIA and X secreted phospholipase A(2) occurs predominantly during the secretory process and with the involvement of cytosolic phospholipase A(2)-alpha. *J Biol Chem*. 279 (24):25024-38.

95. Dichlberger A, Kovanen PT, Schneider WJ. (2013) Mast cells: from lipid droplets to lipid mediators. *Clin Sci (Lond)*. 125 (3):121-30.

96. Triggiani M, Oriente A, Marone G. (1994) Differential roles for triglyceride and phospholipid pools of arachidonic acid in human lung macrophages. *J Immunol*. 152 (3):1394-403.

97. Johnson MM, Vaughn B, Triggiani M, Swan DD, Fonteh AN, Chilton FH. (1999) Role of arachidonyl triglycerides within lipid bodies in eicosanoid formation by human polymorphonuclear cells. *Am J Respir Cell Mol Biol*. 21 (2):253-8.

98. Dichlberger A, Schlager S, Maaninka K, Schneider WJ, Kovanen PT. (2014) Adipose triglyceride lipase regulates eicosanoid production in activated human mast cells. *J Lipid Res*. 55 (12):2471-8.

99. Dichlberger A, Schlager S, Kovanen PT, Schneider WJ. (2015) Lipid droplets in activated mast cells – a significant source of triglyceride-derived arachidonic acid for eicosanoid production. *Eur J Pharmacol*. submitted.

100. Papackova Z, Cahova M. (2015) Fatty acid signaling: the new function of intracellular lipases. *Int J Mol Sci*. 16 (2):3831-55.

101. Radovic B, Aflaki E, Kratky D. (2012) Adipose triglyceride lipase in immune response, inflammation, and atherosclerosis. *Biol Chem*. 393 (9):1005-11.

102. Haemmerle G, Lass A, Zimmermann R, Gorkiewicz G, Meyer C, Rozman J, et al. (2006) Defective lipolysis and altered energy metabolism in mice lacking adipose triglyceride lipase. *Science*. 312 (5774):734-7.

103. Obrowsky S, Chandak PG, Patankar JV, Povoden S, Schlager S, Kershaw EE, et al. (2013) Adipose triglyceride lipase is a TG hydrolase of the small intestine and regulates intestinal PPARalpha signaling. *J Lipid Res*. 54 (2):425-35.

104. Zierler KA, Jaeger D, Pollak NM, Eder S, Rechberger GN, Radner FP, et al. (2013) Functional cardiac lipolysis in mice critically depends on comparative gene identification-58. *J Biol Chem*. 288 (14):9892-904.

105. Haemmerle G, Zimmermann R, Hayn M, Theussl C, Waeg G, Wagner E, et al. (2002) Hormone-sensitive lipase deficiency in mice causes diglyceride accumulation in adipose tissue, muscle, and testis. *J Biol Chem*. 277 (7):4806-15.

106. Taschler U, Radner FP, Heier C, Schreiber R, Schweiger M, Schoiswohl G, et al. (2011) Monoglyceride lipase deficiency in mice impairs lipolysis and attenuates diet-induced insulin resistance. *J Biol Chem*. 286 (20):17467-77.

107. Du H, Duanmu M, Witte D, Grabowski GA. (1998) Targeted disruption of the mouse lysosomal acid lipase gene: long-term survival with massive cholesteryl ester and triglyceride storage. *Hum Mol Genet*. 7 (9):1347-54.

108. Boxio R, Bossenmeyer-Pourie C, Steinckwich N, Dournon C, Nusse O. (2004) Mouse bone marrow contains large numbers of functionally competent neutrophils. *J Leukoc Biol*. 75 (4):604-11.

109. Knittelfelder OL, Weberhofer BP, Eichmann TO, Kohlwein SD, Rechberger GN. (2014) A versatile ultra-high performance LC-MS method for lipid profiling. *J Chromatogr B Analyt Technol Biomed Life Sci*. 951-952:119-28.

110. Kortz L, Dorow J, Becker S, Thiery J, Ceglarek U. (2013) Fast liquid chromatography-quadrupole linear ion trap-mass spectrometry analysis of polyunsaturated fatty acids and eicosanoids in human plasma. *J Chromatogr B Analyt Technol Biomed Life Sci*. 927:209-13.

111. Crabtree M, Pileggi R, Bhattacharyya I, Caudle R, Perez F, Riley J, et al. (2008) RAGE mRNA expression and its correlation with nuclear factor kappa beta mRNA expression in inflamed human periradicular tissues. *J Endod*. 34 (6):689-92.

112. Hirano K, Ikeda Y, Zaima N, Sakata Y, Matsumiya G. (2008) Triglyceride deposit cardiomyovasculopathy. *N Engl J Med*. 359 (22):2396-8.

113. Reilich P, Horvath R, Krause S, Schramm N, Turnbull DM, Trenell M, et al. (2011) The phenotypic spectrum of neutral lipid storage myopathy due to mutations in the PNPLA2 gene. *J Neurol*. 258 (11):1987-97.

114. Missaglia S, Tasca E, Angelini C, Moro L, Tavian D. (2015) Novel missense mutations in PNPLA2 causing late onset and clinical heterogeneity of neutral lipid storage disease with myopathy in three siblings. *Mol Genet Metab*. in press.

115. Kupiecki FP. (1966) Partial purification of monoglyceride lipase from adipose tissue. *J Lipid Res*. 7 (2):230-5.

116. Du H, Witte DP, Grabowski GA. (1996) Tissue and cellular specific expression of murine lysosomal acid lipase mRNA and protein. *J Lipid Res*. 37 (5):937-49.

117. Du H, Heur M, Duanmu M, Grabowski GA, Hui DY, Witte DP, et al. (2001) Lysosomal acid lipase-deficient mice: depletion of white and brown fat, severe hepatosplenomegaly, and shortened life span. *J Lipid Res*. 42 (4):489-500.

118. Crocker AC, Vawter GF, Neuhauser EB, Rosowsky A. (1965) Wolman's Disease: Three New Patients with a Recently Described Lipidosis. *Pediatrics*. 35:627-40.

119. Qu P, Yan C, Blum JS, Kapur R, Du H. (2011) Myeloid-specific expression of human lysosomal acid lipase corrects malformation and malfunction of myeloid-derived suppressor cells in lal-/- mice. *J Immunol*. 187 (7):3854-66.

120. Haemmerle G, Moustafa T, Woelkart G, Buttner S, Schmidt A, van de Weijer T, et al. (2011) ATGL-mediated fat catabolism regulates cardiac mitochondrial function via PPAR-alpha and PGC-1. *Nat Med*. 17 (9):1076-85.

121. Ong KT, Mashek MT, Bu SY, Greenberg AS, Mashek DG. (2011) Adipose triglyceride lipase is a major hepatic lipase that regulates triacylglycerol turnover and fatty acid signaling and partitioning. *Hepatology*. 53 (1):116-26.

122. Mayer N, Schweiger M, Romauch M, Grabner GF, Eichmann TO, Fuchs E, et al. (2013) Development of small-molecule inhibitors targeting adipose triglyceride lipase. *Nat Chem Biol*. 9 (12):785-7.

123. Gijon MA, Zarini S, Murphy RC. (2007) Biosynthesis of eicosanoids and transcellular metabolism of leukotrienes in murine bone marrow cells. *J Lipid Res*. 48 (3):716-25.

124. Dubois RN, Abramson SB, Crofford L, Gupta RA, Simon LS, Van De Putte LB, et al. (1998) Cyclooxygenase in biology and disease. *FASEB J*. 12 (12):1063-73.

125. Appelberg R. (1992) Interferon-gamma (IFN-gamma) and macrophage inflammatory proteins (MIP)-1 and -2 are involved in the regulation of the T cell-dependent chronic peritoneal neutrophilia of mice infected with mycobacteria. *Clin Exp Immunol*. 89 (2):269-73.

126. McColl SR, Hachicha M, Levasseur S, Neote K, Schall TJ. (1993) Uncoupling of early signal transduction events from effector function in human peripheral blood neutrophils in response to recombinant macrophage inflammatory proteins-1 alpha and -1 beta. *J Immunol*. 150 (10):4550-60.

127. Elbim C, Bailly S, Chollet-Martin S, Hakim J, Gougerot-Pocidalo MA. (1994) Differential priming effects of proinflammatory cytokines on human neutrophil oxidative burst in response to bacterial N-formyl peptides. *Infect Immun*. 62 (6):2195-201.

128. Borregaard N, Herlin T. (1982) Energy metabolism of human neutrophils during phagocytosis. *J Clin Invest*. 70 (3):550-7.

129. Schrammel A, Mussbacher M, Wolkart G, Stessel H, Pail K, Winkler S, et al. (2014) Endothelial dysfunction in adipose triglyceride lipase deficiency. *Biochim Biophys Acta*. 1841 (6):906-17.

130. Kratky D, Obrowsky S, Kolb D, Radovic B. (2014) Pleiotropic regulation of mitochondrial function by adipose triglyceride lipase-mediated lipolysis. *Biochimie*. 96:106-12.

131. Zimmermann R, Strauss JG, Haemmerle G, Schoiswohl G, Birner-Gruenberger R, Riederer M, et al. (2004) Fat mobilization in adipose tissue is promoted by adipose triglyceride lipase. *Science*. 306 (5700):1383-6.

132. Jenkins CM, Mancuso DJ, Yan W, Sims HF, Gibson B, Gross RW. (2004) Identification, cloning, expression, and purification of three novel human calcium-independent phospholipase A2 family members possessing triacylglycerol lipase and acylglycerol transacylase activities. *J Biol Chem*. 279 (47):48968-75.

133. Lastrucci C, Baillif V, Behar A, Al Saati T, Dubourdeau M, Maridonneau-Parini I, et al. (2015) Molecular and cellular profiles of the resolution phase in a damage-associated molecular pattern (DAMP)-mediated peritonitis model and revelation of leukocyte persistence in peritoneal tissues. *FASEB J*. 29 (5):1914-29.

134. Janssen MC, van Engelen B, Kapusta L, Lammens M, van Dijk M, Fischer J, et al. (2013) Symptomatic lipid storage in carriers for the PNPLA2 gene. *Eur J Hum Genet*. 21 (8):807-15.

135. Sekiya M, Osuga J, Nagashima S, Ohshiro T, Igarashi M, Okazaki H, et al. (2009) Ablation of neutral cholesterol ester hydrolase 1 accelerates atherosclerosis. *Cell Metab*. 10 (3):219-28.

136. Aflaki E, Balenga NA, Luschnig-Schratl P, Wolinski H, Povoden S, Chandak PG, et al. (2011) Impaired Rho GTPase activation abrogates cell polarization and migration in macrophages with defective lipolysis. *Cell Mol Life Sci*. 68 (23):3933-47.

137. Aflaki E, Doddapattar P, Radovic B, Povoden S, Kolb D, Vujic N, et al. (2012) C16 ceramide is crucial for triacylglycerol-induced apoptosis in macrophages. *Cell Death Dis*. 3:e280.

138. Aflaki E, Radovic B, Chandak PG, Kolb D, Eisenberg T, Ring J, et al. (2011) Triacylglycerol accumulation activates the mitochondrial apoptosis pathway in macrophages. *J Biol Chem*. 286 (9):7418-28.

139. Lammers B, Chandak PG, Aflaki E, Van Puijvelde GH, Radovic B, Hildebrand RB, et al. (2011) Macrophage adipose triglyceride lipase deficiency attenuates atherosclerotic lesion development in low-density lipoprotein receptor knockout mice. *Arterioscler Thromb Vasc Biol*. 31 (1):67-73.

140. Du H, Schiavi S, Wan N, Levine M, Witte DP, Grabowski GA. (2004) Reduction of atherosclerotic plaques by lysosomal acid lipase supplementation. *Arterioscler Thromb Vasc Biol*. 24 (1):147-54.

141. Serhan CN. (2010) Novel lipid mediators and resolution mechanisms in acute inflammation: to resolve or not? *Am J Pathol*. 177 (4):1576-91.

142. Nathan C, Ding A. (2010) Nonresolving inflammation. *Cell*. 140 (6):871-82.

143. Schreiber R, Zechner R. (2014) Lipolysis meets inflammation: arachidonic acid mobilization from fat. *J Lipid Res*. 55 (12):2447-9.

144. Siegel-Axel D, Langer H, Lindemann S, Gawaz M. (2006) [Role of platelets in atherosclerosis and inflammation]. *Med Klin (Munich)*. 101 (6):467-75.

145. Weyrich A, Cipollone F, Mezzetti A, Zimmerman G. (2007) Platelets in atherothrombosis: new and evolving roles. *Curr Pharm Des*. 13 (16):1685-91.

146. Steinhubl SR, Moliterno DJ. (2005) The role of the platelet in the pathogenesis of atherothrombosis. *Am J Cardiovasc Drugs*. 5 (6):399-408.

147. Kaplan ZS, Jackson SP. (2011) The role of platelets in atherothrombosis. *Hematology Am Soc Hematol Educ Program*. 2011:51-61.

148. Ferroni P, Basili S, Santilli F, Davi G. (2006) Low-density lipoprotein-lowering medication and platelet function. *Pathophysiol Haemost Thromb*. 35 (3-4):346-54.

149. Milionis HJ, Elisaf MS, Mikhailidis DP. (1999) Platelet function and lipid-lowering interventions. *Platelets*. 10 (6):357-67.

150. Aviram M, Brook JG. (1987) Platelet activation by plasma lipoproteins. *Prog Cardiovasc Dis*. 30 (1):61-72.

151. Betteridge DJ, Cooper MB, Saggerson ED, Prichard BN, Tan KC, Ling E, et al. (1994) Platelet function in patients with hypercholesterolaemia. *Eur J Clin Invest*. 24 Suppl 1:30-3.

152. Nofer JR, Herminghaus G, Brodde M, Morgenstern E, Rust S, Engel T, et al. (2004) Impaired platelet activation in familial high density lipoprotein deficiency (Tangier disease). *J Biol Chem*. 279 (32):34032-7.

153. Engelmann B, Kogl C, Kulschar R, Schaipp B. (1996) Transfer of phosphatidylcholine, phosphatidylethanolamine and sphingomyelin from low- and high-density lipoprotein to human platelets. *Biochem J*. 315 (Pt 3):781-9.

154. Relou IA, Hackeng CM, Akkerman JW, Malle E. (2003) Low-density lipoprotein and its effect on human blood platelets. *Cell Mol Life Sci*. 60 (5):961-71.

155. Koller E, Koller F. (1992) Binding characteristics of homologous plasma lipoproteins to human platelets. *Methods Enzymol*. 215:383-98.

156. O'Donnell VB, Murphy RC, Watson SP. (2014) Platelet lipidomics: modern day perspective on lipid discovery and characterization in platelets. *Circ Res*. 114 (7):1185-203.

157. Shattil SJ, Anayagalindo R, Bennett J, Colman RW, Cooper RA. (1975) Platelet Hypersensitivity Induced by Cholesterol Incorporation. *Journal of Clinical Investigation*. 55 (3):636-43.

158. Lian L, Wang Y, Draznin J, Eslin D, Bennett JS, Poncz M, et al. (2005) The relative role of PLCbeta and PI3Kgamma in platelet activation. *Blood*. 106 (1):110-7.

159. Mangin P, Yuan Y, Goncalves I, Eckly A, Freund M, Cazenave JP, et al. (2003) Signaling role for phospholipase C gamma 2 in platelet glycoprotein Ib alpha calcium flux and cytoskeletal reorganization. Involvement of a pathway distinct from FcR gamma chain and Fc gamma RIIA. *J Biol Chem*. 278 (35):32880-91.

160. Elvers M, Stegner D, Hagedorn I, Kleinschnitz C, Braun A, Kuijpers ME, et al. (2010) Impaired alpha(IIb)beta(3) integrin activation and shear-dependent thrombus formation in mice lacking phospholipase D1. *Sci Signal*. 3 (103):ra1.

161. Thielmann I, Stegner D, Kraft P, Hagedorn I, Krohne G, Kleinschnitz C, et al. (2012) Redundant functions of phospholipases D1 and D2 in platelet alpha-granule release. *J Thromb Haemost*. 10 (11):2361-72.

162. Moriyama T, Wada K, Oki M, Matsuura T, Kito M. (1994) The mechanism of arachidonic acid release in collagen-activated human platelets. *Biosci Biotechnol Biochem*. 58 (1):93-8.

163. Amin D, Sutherland CA, Khandwala AS, Jamall IS, Kapoor AL. (1986) Inhibition of the effects of thrombin on guinea pig platelets by the diacylglycerol lipase inhibitor RHC 80267. *Thromb Res*. 44 (1):75-84.

164. Gao Y, Vasilyev DV, Goncalves MB, Howell FV, Hobbs C, Reisenberg M, et al. (2010) Loss of retrograde endocannabinoid signaling and reduced adult neurogenesis in diacylglycerol lipase knock-out mice. *J Neurosci*. 30 (6):2017-24.

165. Brantl SA, Khandoga AL, Siess W. (2014) Mechanism of platelet activation induced by endocannabinoids in blood and plasma. *Platelets*. 25 (3):151-61.

166. Vaughan M, Berger JE, Steinberg D. (1964) Hormone-Sensitive Lipase and Monoglyceride Lipase Activities in Adipose Tissue. *J Biol Chem*. 239:401-9.

167. Chanda PK, Gao Y, Mark L, Btesh J, Strassle BW, Lu P, et al. (2010) Monoacylglycerol lipase activity is a critical modulator of the tone and integrity of the endocannabinoid system. *Mol Pharmacol*. 78 (6):996-1003.

168. Schlosburg JE, Blankman JL, Long JZ, Nomura DK, Pan B, Kinsey SG, et al. (2010) Chronic monoacylglycerol lipase blockade causes functional antagonism of the endocannabinoid system. *Nat Neurosci*. 13 (9):1113-9.

169. Rowley JW, Oler AJ, Tolley ND, Hunter BN, Low EN, Nix DA, et al. (2011) Genome-wide RNA-seq analysis of human and mouse platelet transcriptomes. *Blood*. 118 (14):e101-11.

170. Bligh EG, Dyer WJ. (1959) A rapid method of total lipid extraction and purification. *Can J Biochem Physiol*. 37 (8):911-7.

171. Sanderson HM, Heptinstall S, Vickers J, Losche W. (1996) Studies on the effects of agonists and antagonists on platelet shape change and platelet aggregation in whole blood. *Blood Coagul Fibrinolysis*. 7 (2):245-8.

172. Gardiner EE, Arthur JF, Kahn ML, Berndt MC, Andrews RK. (2004) Regulation of platelet membrane levels of glycoprotein VI by a platelet-derived metalloproteinase. *Blood*. 104 (12):3611-7.

173. Wu JW, Wang SP, Alvarez F, Casavant S, Gauthier N, Abed L, et al. (2011) Deficiency of Liver Adipose Triglyceride Lipase in Mice Causes Progressive Hepatic Steatosis. *Hepatology*. 54 (1):122-32.

174. Lewis N, Majerus PW. (1969) Lipid metabolism in human platelets. II. De novo phospholipid synthesis and the effect of thrombin on the pattern of synthesis. *J Clin Invest*. 48 (11):2114-23.

175. Majerus PW, Smith MB, Clamon GH. (1969) Lipid metabolism in human platelets. I. Evidence for a complete fatty acid synthesizing system. *J Clin Invest*. 48 (1):156-64.

176. Guppy M, Abas L, Neylon C, Whisson ME, Whitham S, Pethick DW, et al. (1997) Fuel choices by human platelets in human plasma. *Eur J Biochem*. 244 (1):161-7.

177. Ruebsaamen K, Liebisch G, Boettcher A, Schmitz G. (2010) Lipidomic analysis of platelet senescence. *Transfusion*. 50 (8):1665-76.

178. Iritani N, Ikeda Y, Kajitani H. (1984) Selectivities of 1-acylglycerophosphorylcholine acyltransferase and acyl-CoA synthetase for n-3 polyunsaturated fatty acids in platelets and liver microsomes. *Biochim Biophys Acta*. 793 (3):416-22.

179. McKean ML, Smith JB, Silver MJ. (1982) Phospholipid biosynthesis in human platelets. Formation of phosphatidylcholine from 1-acyl lysophosphatidylcholine by acyl-CoA:1-acyl-sn-glycero-3-phosphocholine acyltransferase. *J Biol Chem*. 257 (19):11278-83.

180. Le Quan Sang KH, Levenson J, Megnien JL, Simon A, Devynck MA. (1995) Platelet cytosolic Ca2+ and membrane dynamics in patients with primary hypercholesterolemia. Effects of pravastatin. *Arterioscler Thromb Vasc Biol*. 15 (6):759-64.

SCIENTIFIC CV

STEFANIE SCHLAGER

Date of Birth	29.07.1983
Nationality	Austria
Current address	Wielandgasse 38/8 A-8010 Graz
Phone	+43-(0)6642707315
E-mail	schlager.stefanie@gmail.com

EDUCATION

since 03/2012 PhD Thesis (Doctoral College "Metabolic and Cardiovascular Disease") Institute of Molecular Biology and Biochemistry, Medical University Graz, Austria. *"The Role of Neutral Lipid Hydrolases in Immune Cell Function*" supervised by Univ. Prof. Dr. Dagmar Kratky.

2004 - 2009 Undergraduate Studies in Microbiology and Genetics - University of Vienna, Austria. Diploma Thesis: *"Mutational Analysis of Ligand-LDL-Receptor Interactions"* supervised by Univ. Prof. Dr. Wolfgang J. Schneider.

2001 - 2004 „Akademie für den medizinisch-technischen Laboratoriumsdienst" - Vienna General Hospital (AKH).

CAREER RELATED ACTIVITIES

2010 - 2012 Research Assistant at Wihuri Research Institute, Helsinki, Finland.

Project: *"Characterization of Lipid Droplets in Peripheral Blood-derived Human Mast Cells"* supervised by Dr. Andrea Dichlberger and Prof. DDr. Petri Kovanen.

2006 - 2010 Biomedical Technician - Department of Blood Group Serology and Transfusion Medicine, Vienna General Hospital (AKH).

2004 - 2006 Biomedical Technician - Department of Gynaecology, Division of Medical Genetics, Vienna General Hospital (AKH).

PUBLICATIONS

Original Articles

Schlager S, Goeritzer M, Jandl K, Frei R, Vujic N, Kolb D, Strohmaier H, Dorow J, Eichmann TO, Rosenberger A, Wölfler A, Lass A, Kershaw EE, Ceglarek U, Dichlberger A, Heinemann A, Kratky D. (2015). *Adipose triglyceride lipase acts on neutrophil lipid droplets to regulate substrate availability for lipid mediator synthesis*. J Leukocyte Biol: in press.

Goeritzer M*, Vujic N*, Schlager S, Chandak PG, Korbelius M, Gottschalk B, Leopold C, Obrowsky S, Rainer S, Doddapattar1 P, Aflaki E, Wegscheider M, Sachdev V, Graier WF, Kolb D, Radovic B, Kratky D. (2015). *Active autophagy but not lipophagy in macrophages with defective lipolysis.* Biochimica et Biophysica Acta (BBA)*:* in press, *equal contribution

Goeritzer M, Schlager S, Radovic B, Madreiter CT, Rainer S, Thomas G, Lord CC, Sacks J, Brown AL, Vujic N, Obrowsky S, Sachdev V, Kolb D, Chandak PG, Graier WF, Sattler W, Brown JM, Kratky D. (2014*). Deletion of CGI-58 or adipose triglyceride lipase differently affects macrophage function and atherosclerosis*. J Lipid Res 55: 2562-2575.

Dichlberger A, Schlager S, Maaninka K, Schneider WJ, Kovanen PT. (2014). *Adipose triglyceride lipase regulates eicosanoid production in activated human mast cells*. J Lipid Res 55: 2471-2478.

Obrowsky S, Chandak PG, Patankar JV, Povoden S, Schlager S, Kershaw EE, Bogner-Strauss JG, Hoefler G, Levak-Frank S, Kratky D. (2013). *Adipose triglyceride lipase is a TG hydrolase of the small intestine and regulates intestinal PPARalpha signaling*. J Lipid Res 54: 425-435.

Dichlberger A, Schlager S, Lappalainen J, Kakela R, Hattula K, Butcher SJ, Schneider WJ, Kovanen PT. (2011). *Lipid body formation during maturation of human mast cells*. J Lipid Res 52: 2198-2208.

Reviews

Dichlberger A, Schlager S, Kovanen PT, Schneider WJ. (2015). *Lipid droplets in activated mast cells – a significant source of triglyceride-derived arachidonic acid for eicosanoid production*. Eur J Pharmacol: submitted.

ORAL PRESENTATIONS

22nd Annual Meeting of the Austrian Atherosclerosis Society (AAS); May 2015; St. Gilgen, Austria; *ATGL Acts on Neutrophil Lipid Droplets to Generate Lipid Mediators*

Doctoral Day 2014 Medical University of Graz; December 2015; Graz, Austria; *Functional Consequences of Jordans' Anomaly Caused by Adipose Triglyceride Lipase (ATGL)-Deficiency* Award: Best Presentation Award

21st Annual Meeting of the Austrian Atherosclerosis Society (AAS); May 2014; St. Gilgen, Austria; *Adipose Triglyceride Lipase Regulates Eicosanoid Production in Activated Human Mast Cells*

21st Annual Meeting of the Austrian Atherosclerosis Society (AAS); May 2014; St. Gilgen, Austria; *ATGL-Deficient Mice Exhibit Jordans' Anomaly*

20th Annual Meeting of the Austrian Atherosclerosis Society (AAS); May 2013; St. Gilgen, Austria*; Platelet Function in Adipose Triglyceride Lipase-Deficient Mice*

19th Annual Meeting of the Austrian Atherosclerosis Society (AAS); May 2012; St. Gilgen, Austria; *Mast Cell Lipid Bodies as Arachidonic Acid Storage Site*

Annual Graduate Seminars (2012-2014) from the Doctoral College "Metabolic and Cardiovascular Disease"- Seggau Castle, Austria.

POSTERS

The Role of Metabolic Lipases in Inflammatory cells- Functional Consequences of Jordans' Anomaly Caused by Adipose Triglyceride Lipase (ATGL)-Deficiency.

FASEB Meeting "Lipid Droplets and Metabolic Consequences of Neutral Lipid Storage"; July 2014; Saxtons River, VT, US.

The Role of Metabolic Lipases in Inflammatory Cells- ATGL-Deficient Mice Exhibit Jordans' Anomaly.

Keystone Symposium *"Lipid Pathways in Biology and Disease";* March 2014; Dublin, Ireland.

The Role of Metabolic Lipases in Inflammatory Cells- Platelet Function in ATGL-Deficient Mice

GRC conference "Cell Biology of Megakaryocytes & Platelets"; March 2013; Galveston, TX, US.

Doctoral Day 2012 Medical University Graz; December 2012; Graz, Austria.

4th Annual Meeting of the Austrian Association of Molecular Life Sciences and Biotechnology (ÖGMBT); September 2012; Graz, Austria.